Bulletin No. 55

Geology of the basement beneath the Athabasca Basin in Alberta

J.A. Wilson

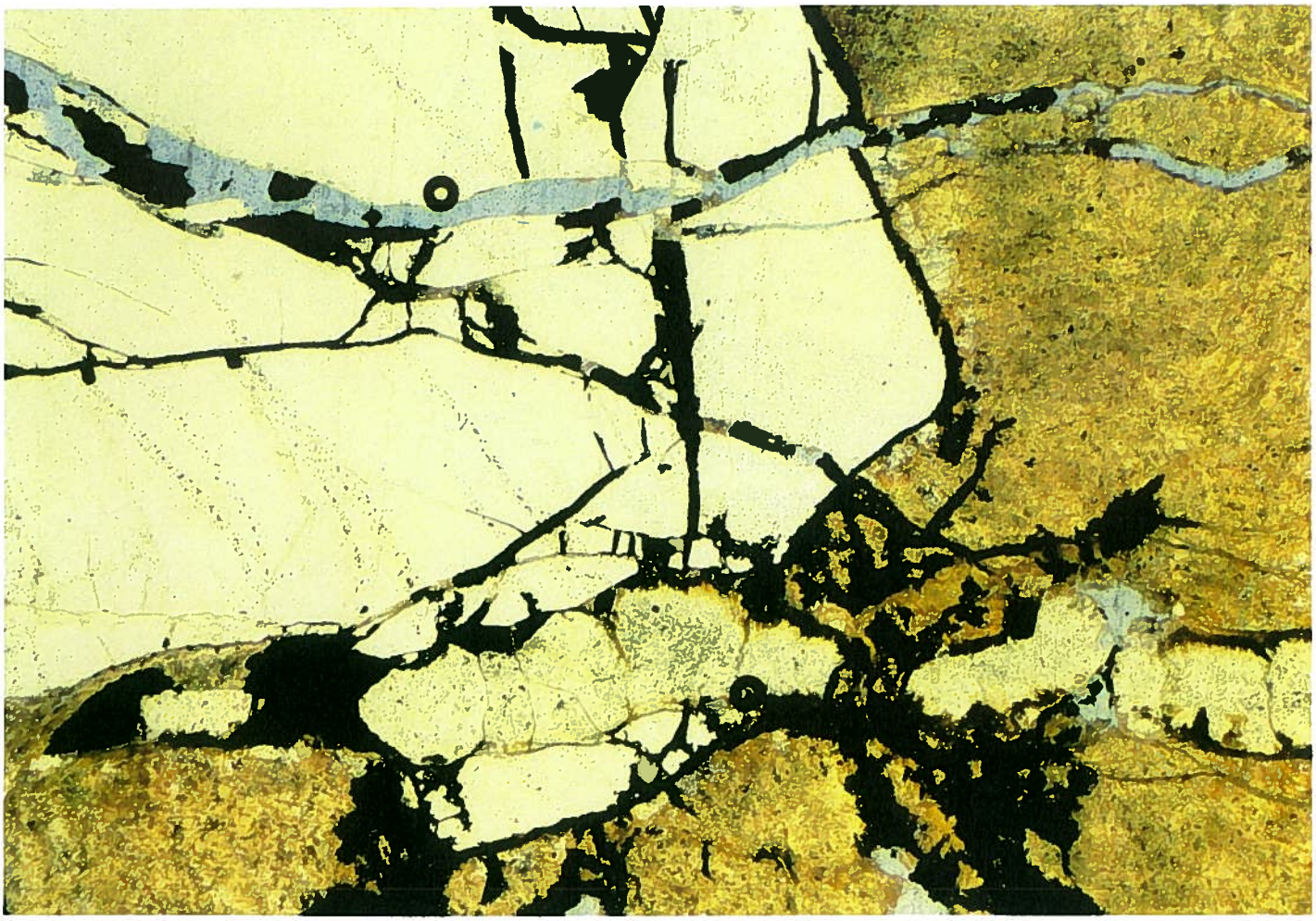

ALBERTA RESEARCH COUNCIL
Natural Resources Division
Alberta Geological Survey

Geology of the basement beneath the Athabasca Basin in Alberta

J.A. Wilson

Cover photo:
Pyrite outlining fractures in a quartz grain. The brown portion is a stained alkali feldspar and there is a carbonate-filled fracture near the bottom. From a zone of extensive hydrothermal alteration in the basement below Devonian carbonates. JAW84-074-65, plane polarized light. Width of view is approximately 3.5 mm.

GEOLOGICAL SURVEY DEPARTMENT, ALBERTA RESEARCH COUNCIL
EDMONTON, ALBERTA, CANADA 1986

Acknowledgments

This work was funded in part by Alberta Energy through its support of Alberta's mineral core storage program, and in part by the Alberta Research Council. Thin section preparation, X-ray diffraction, data entry and graph preparation work were done by M. Baaske, C. Kidston, S. Putz, L. Swenson and D. Boisvert. Their assistance is gratefully acknowledged.

Major and trace element analyses were done by Jack Nelson of the Research Council's chemistry department, and uranium values were obtained on the SLOWPOKE reactor at the University of Alberta. The manuscript was typed by S. Binda and H. Williams. Figures and maps were prepared by Research Council Graphic Services. Editing and Publishing Services produced the report.

The manuscript was critically read by my colleagues Willem Langenberg and Wylie Hamilton, and by Reg Olson of Trigg, Woollett Olson Consulting Ltd. Their helpful comments are greatly appreciated.

Copies of this report are available from:

Edmonton:
Alberta Research Council
Publications Sales
250 Karl Clark Road
Edmonton, Alberta
Canada

Phone (403)450-5111

Mailing address:
Alberta Research Council
Publications Sales
PO Box 8330
Postal Station F
Edmonton, Alberta
Canada T6H 5X2

Calgary:
Alberta Research Council
Publications Sales
3rd Floor
6815 - 8 Street NE
Calgary, Alberta
Canada T2E 7H7

Phone (403)297-2600

Table of contents

Tables

Figures

Appendices

Abstract

The unconformity beneath the Athabasca Basin in Alberta lies within 600 m of the surface for over 6000 km², or 75 percent of the basin area. The basement beneath the unconformity can be subdivided into four granitoid rock types recognized as part of the Wylie Lake pluton, and two mylonitic rock types derived partly from the granitoids and partly from a metasedimentary or metavolcanic parent.

A zoned saprolite is present regionally on the basement immediately beneath the unconformity. It represents a period of Helikian surficial weathering preserved by deposition of the Athabasca Group. The saprolite is crosscut by two types of widespread hydrothermal alteration, a thin bleached zone at the unconformity and a more widespread alteration associated with fracturing. Geochemical profiles of the saprolite and hydrothermal alteration types indicate that they are the products of leaching processes and would not be good mechanisms for concentrating economic minerals.

Locally, a fourth type of alteration, which may be associated with mylonitic rocks, shows enrichment in several potentially economic minerals (including uranium, nickel, zinc, lead and gold), and has a geochemical signature similar to the halos around some uranium ore deposits in Saskatchewan. This alteration is present beneath a considerable thickness of Athabasca Group sediments, but similar rock types and many of the conditions necessary for ore concentration are also present beneath the southern portion of the Athabasca Basin in Alberta, where the cover is thin.

Exploration in Alberta has utilized the Key Lake model for uranium ore concentration. However, there are many similarities to the geology at Cluff Lake, suggesting that a model incorporating these features may be more appropriate.

Introduction

This bulletin deals with the Precambrian Shield beneath Helikian and Phanerozoic cover in northeastern Alberta. It covers the same study area and is a companion publication to Wilson's (1985a) work on the Athabasca Group. The research was carried out in conjunction with Alberta's program to collect and preserve mineral exploration drill core, and was jointly funded by Alberta Energy and the Alberta Research Council. The drill core obtained during this study is housed in the Mineral Core Research Facility of Edmonton.

This work examines four aspects of the basement geology of northeastern Alberta.

1. The detailed mapping of the exposed Shield in the study area (Godfrey, 1970, 1980a, 1980b, 1984, in press; Godfrey and Langenberg, 1986, in press) has been extended beneath the cover on the basis of drill core and geophysical data. That mapping has been presented in Wilson (1985b) and is complementary to that done by Gilboy (1982, 1983) in Saskatchewan. Whole rock geochemical analyses for the various rock types are also presented.
2. A regionally developed, in-situ paleoweathering profile (saprolite) beneath the Athabasca Group is described and geochemically characterized.
3. Hydrothermal alteration of the basement is examined and geochemically compared to the saprolite.
4. The basement geology and its alteration products are related to the economic potential of the area; promising areas for further exploration are defined.

The study area, located in northeastern Alberta between 57°32′ and 59°26′N latitude, and 110° and 112°W longitude (figure 1), covers townships 99 to 120 and ranges 1 to 12, west of the 4th meridian. The area encompasses the Fort Chipewyan (NTS 74L) and parts of the Fitzgerald (NTS 74M) and Bitumount (NTS 74E) map sheets. The area borders Saskatchewan to the east and Wood Buffalo National Park to the west. The Northwest Territories lie close by to the north; to the south are the oil sand deposits of the Fort McMurray area. Access and physiography of the study area are outlined in Wilson (1985a).

Methods

Thin sections of 244 core samples of fresh and altered basement were studied. Thin sections of 20 standard reference outcrop samples from the Marguerite River outcrop area (Godfrey, 1970) were included in this study. Point counts (500 points) were done on selected fresh basement samples and on outcrop samples from the Marguerite River area.

One hundred and eighty-five basement samples were analyzed for major and trace elements. The bulk of the analyses were done by Alberta Research Council staff using atomic absorption spectroscopy. The $LiBO_2$ fusion procedure, as outlined in Yule and Swanson (1969), was used, except that 0.2 g of sample and 1 g of flux were used with a Claise Fluxer. This system has a reported accuracy of 0.1 percent (Yule and Swanson, 1969). Carbon values were obtained by infrared absorption using the LECO CR-12 system. The accuracy of this method is ± 1 percent with a sensitivity of 0.001 percent. Uranium values were determined by delayed neutron counting at the University of Alberta's SLOWPOKE reactor. The irradiation:decay:count scheme was 20:10:20 s, at a flux of 1×10^{12}n $cm^{-2}s^{-1}$, giving a sensitivity of 50.1 ± 1.1 cts μg^{-1} natural uranium (Duke, 1983).

The geochemical data for the fresh and altered basement samples are presented in the form of Dice diagrams (figure 2). Modified after Sokal (1965) and Jones (1974), these are plots of a variable (element or oxide concentration) against sample groupings (rock type or alteration type). The total range of variation is shown by the horizontal line, with the mean marked by a vertical line. The solid portion of the bar represents two standard errors of the mean (SEM) on each side of the mean, and the solid plus open bars are one standard deviation (SD) on either side of the mean. Where

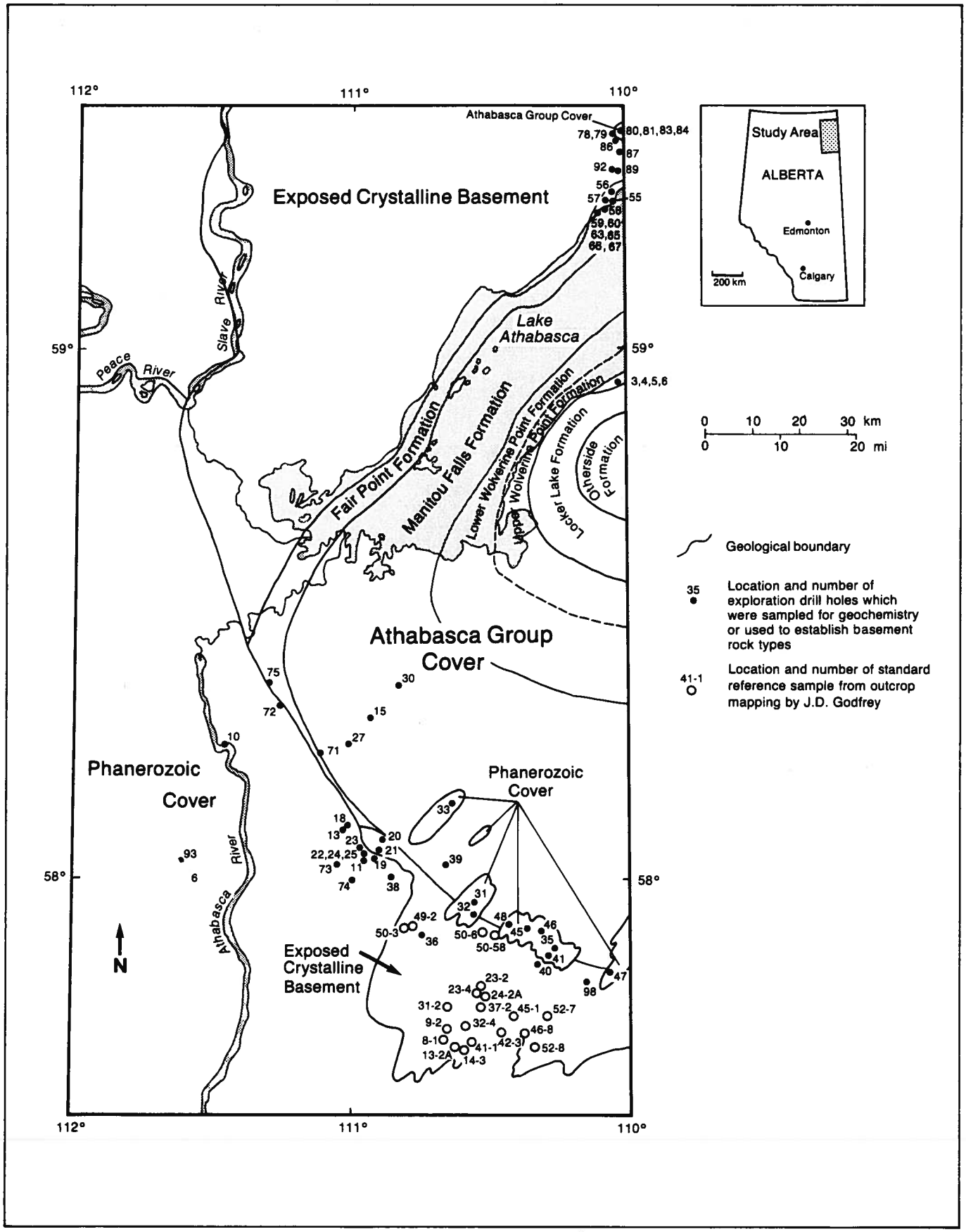

Figure 1. Bedrock geology of the study area, with the location of drill holes that penetrated to basement and standard reference samples in the Marguerite River area (after Wilson, 1985a and mapping by J.D. Godfrey).

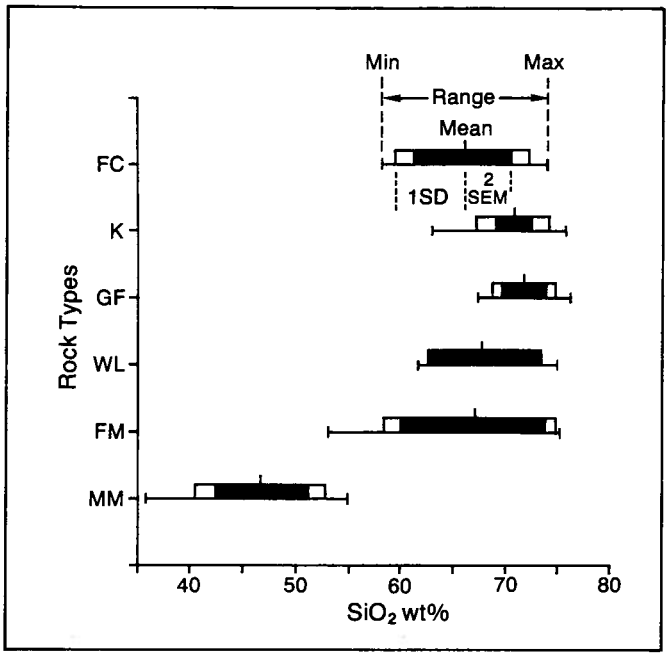

Figure 2. Example of Dice diagram presentation of data. SEM - standard error of the mean. SD - standard deviation. Legend for rock types is on figure 23. (Modified after Jones, 1974 and Sokal, 1965).

n is greater than 30, twice the standard error of the mean represents the 95 percent confidence limit for placement of the mean. Thus, as a guide, if the black bars overlap, the populations can be considered the same, but if they do not, they represent separate populations. This guide is less certain if n is less than 30.

Published Geological Survey of Canada regional aeromagnetic surveys (GSC, 1964a, 1964b; 1983) form the basis for part of the interpretation. The maps are based on total field survey data, and hence the interpretations are qualitative. The basic mapping was done at a 1:250 000 scale and is available as an Alberta Research Council open file map (Wilson, 1985b).

Previous work

Early reconnaissance work on the exposed Precambrian Shield of northeastern Alberta (also referred to as the Alberta Shield) was carried out in the early 1930s (Cameron, 1930; Cameron and Hicks, 1931; Hicks, 1930, 1932) and later by Riley (1960). Mineral prospects on the Alberta Shield were examined by Collins and Swan (1954), and mineral showings in the Andrew, Waugh and Johnson Lakes areas were reported by Godfrey (1958a).

Since the Alberta Research Council commenced detailed work in northeastern Alberta in 1957, numerous district maps and reports have been published (Godfrey, 1961, 1963, 1966, 1970, 1980a, 1980b, 1984, in press; Godfrey and Langenberg, 1986, in press; Godfrey and Peikert, 1963, 1964). The geophysical and geochemical expression of the exposed Precambrian Shield were dealt with by Sprenke et al. (1986) and Goff et al. (1986), respectively. The geochronology was published in Baadsgaard and Godfrey (1967, 1972), Kuo (1972) and Day (1975). Detailed local studies of petrogenesis, metasediments and cataclastics can be found in Peikert (1961, 1963), Watanabe (1961, 1965) and Klewchuck (1972). Metamorphism was dealt with by Godfrey and Langenberg (1978) and Langenberg and Nielsen (1982), and structure by Godfrey (1958b), Langenberg and Ramsden (1980) and Langenberg (1983). The Athabasca Group in Alberta was studied by Wilson (1985a).

General geology

Fresh basement

The basement in the study area is part of the Churchill Structural Province of the Canadian Shield and lies within the Athabasca Mobile Belt (Burwash and Culbert, 1976). The main area of basement outcrop is to the north of Lake Athabasca and comprises a curving, linear body of granite gneisses and associated high-grade metasediments flanked by several distinct grantoid bodies containing areas of metasediments (figure 3).

The Granite Gneiss belt comprises the granite gneisses, high-grade metasediments, minor amphibolite, and small plutons (Godfrey, 1980a, 1980b; 1984). Rb-Sr whole rock isochrons on pegmatites that cut granitoids, gneisses and metasediments in the Charles Lake area show ages of about 2500 Ma (Baadsgaard and Godfrey, 1967; 1972). This indicates an Archean age for the Granite Gneiss belt. The granitoid rocks on either side of this terrain have been subdivided into several distinct plutons (Godfrey 1980a, 1980b; 1984). The major granitoid plutons are the Wylie Lake and Colin Lake plutons to the east of the granite gneisses, the Slave, Arch Lake, La Butte, Francis and Fort Chipewyan Red Granite plutons to the west, and the Thesis Lake and Charles Lake plutons, which occur within the Granite Gneiss belt. Rb-Sr determinations on the granitoids give Aphebian ages: 1893 ± 6 Ma for the Colin Lake Granitoids to the north of the study area (Baadsgaard and Godfrey, 1972), and 1938 ± 29 Ma for the Slave Granitoids (Nielsen et al., 1981). Similar ages are postulated for the other granitoid bodies (Langenberg, 1983).

The metamorphic history of the crystalline basement is examined in Langenberg and Nielsen (1982) and consists of two distinct cycles (figure 4). The first is Archean in age, reached high-pressure granulite facies and affected the high-grade metasediments and granite gneisses. The second cycle of metamorphism is Aphebian in age and shows a three-stage cooling process. The three stages are from moderate pressure granulite facies through low-pressure amphibolite facies to greenschist facies conditions. The second cycle is mainly recorded in the metasedimentary rocks, but can also be recognized in the granitoid rocks.

The low-grade metasediments show evidence of only greenschist facies metamorphism, indicating that they may have been deposited late in the metamorphic history. Since greenschist facies metamorphism is too low for partial melting to occur (Koster and Baadsgaard, 1970) it is unlikely that these low-grade

metasediments are the parent material for the Colin Lake Granitoids as was suggested by Peikert (1961, 1963). It is much more likely that the granitoids are derived by partial melting of the granite gneisses and high-grade metasediments during ultrametamorphism at the height of the second metamorphic cycle (Langenberg and Nielsen, 1982).

The cyclic nature of the geologic history is also indicated by the polyphase deformation as described by Langenberg (1983) (see also figure 4). In the Archean, during the Kenoran orogeny, tight to isoclinal folding affected the gneisses. This phase of deformation may be correlated with the first cycle of metamorphism. At the height of the second metamorphic cycle, diapiric doming of the granitoids produced domes and basins. Domal structures are also present in the Archean Granite Gneiss Complex and have been correlated with the granitoid domes. Thus, the granitoid domes are immature diapirs formed during anatexis of the granite gneisses in the Aphebian around 1900 Ma (Langenberg, 1983).

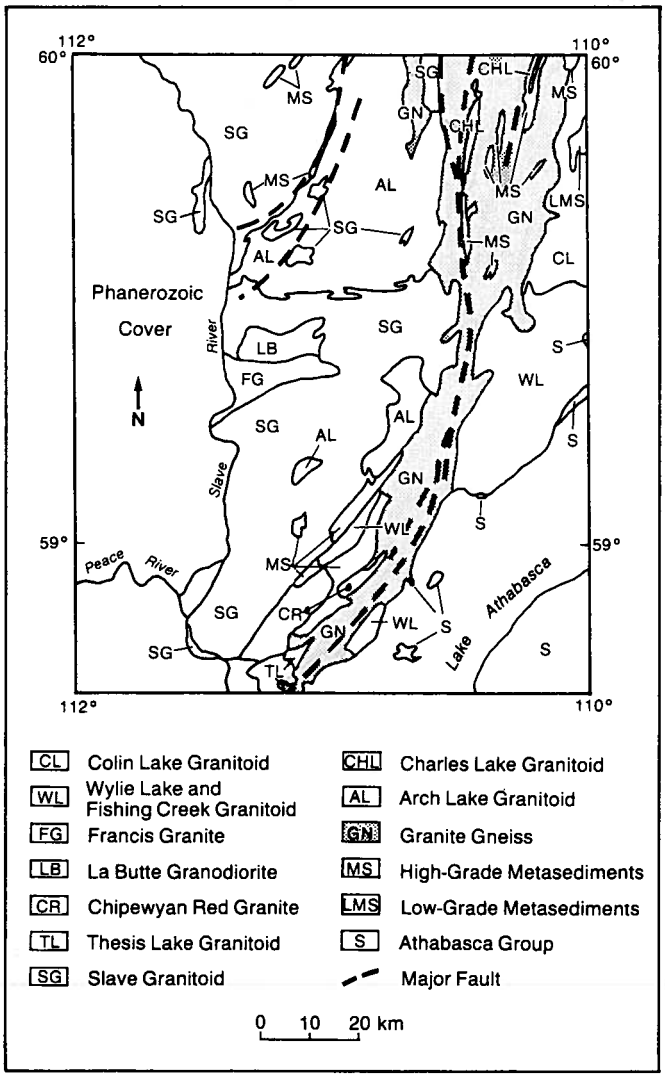

Figure 3. Simplified geological map of the exposed Precambrian Shield north of Lake Athabasca, Alberta (after Godfrey, 1980a, 1980b and 1984, and Langenberg and Nielsen, 1982).

Major faults in the area are expressed as shear zones characterized by mylonites (Watanabe, 1965) and affect most rock units. Greenschist facies minerals within the fault zones indicate a late Aphebian age for the faulting (Langenberg, 1983).

A younger phase of brittle deformation is also present. This late faulting, as well as reactivation of Aphebian fault zones, may have occurred after the deposition of the Athabasca Group.

Altered basement

A saprolite[1] is preserved on the basement rocks beneath the Athabasca Group. This Helikian surface weathering zone may have formed on a more extensive paleoplain (Ambrose, 1964), which is preserved beneath the Athabasca Group (MacDonald, 1980), the Thelon Group (LeCheminant et al., 1983) and the Coppermine Homocline (Kerans et al., 1981). These basins may once have been continuous (Fraser et al., 1970) and the paleoplain may conform to the present exhumed shield surface (Ambrose, 1964). Fairbridge and Finkl (1980) suggest that the paleoplain represents a worldwide chain of events involving prolonged periods of deep chemical weathering, interspersed with briefer periods of instability when the weathered zone was stripped off. If this is the case, then the sub-Athabasca Group saprolite represents the preservation of part of the chemical weathering profile in low-lying areas of the cratonic surface during one of the cratonic instability periods.

The age of the saprolite lies between the age of greenschist metamorphism of the Shield (1790 ± 40 Ma, Baadsgaard and Godfrey, 1972) (figure 5) and deposition of the Athabasca Group. The saprolite is not present beneath the Martin Group in the Beaverlodge area of Saskatchewan. If the weathering

[1]The term saprolite is preferred to the term regolith in this publication. Regolith is a general term for an unconsolidated mantle of rock debris, which may be residual or transported. The term saprolite describes a weathered zone formed in situ and retaining remnant textures from the fresh parent rock. Thus, saprolite is a more accurate description of the paleoweathered zone beneath the Athabasca Group.

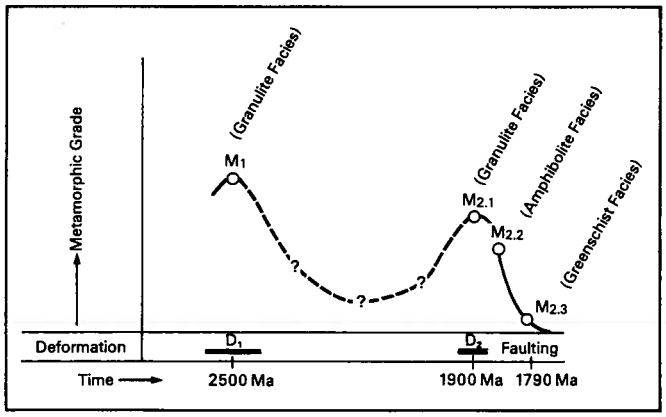

Figure 4. Time scale for the major metamorphic and deformational events affecting the Precambrian Shield of northeastern Alberta (after Langenberg, 1983).

Figure 5. Stratigraphic column with radiometric ages for the Athabasca Basin in Alberta (Athabasca Group stratigraphy from Wilson, 1985a).

Devonian	
Undivided Middle Devonian	
Helikian	
Diabase Dikes (Saskatchewan)	1310 ± 70 Ma (Armstrong and Ramaekers, 1985)
Athabasca Group	
Locker Lake Formation	
Wolverine Point Formation - Upper - Lower	1430 ± 30 Ma (Armstrong and Ramaekers, 1985)
Manitou Falls Formation	
Fair Point	
Saprolite	1632 ± 32 Ma (Fahrig and Loveridge, 1981) 1541 ± 40 Ma 1411 ± 36 Ma (Stevens et al., 1982)
Martin Group (Saskatchewan)	1635 ± 180 Ma (Fraser et al., 1970)
Aphebian	
Granitoids (greenschist facies metamorphism)	1790 ± 40 Ma (Baadsgaard and Godfrey, 1972)
Granitoids (granulite facies metamorphism)	1900 Ma (Nielsen et al., 1981)
Archean	
Pegmatites cutting granite gneiss granitoids and high-grade metasediments	2500 Ma (Baadsgaard and Godfrey, 1967, 1972)

is assumed to be regional, then the saprolite formed after deposition of the Martin Group. Basalts within the Martin Group have been dated at 1635 ± 180 Ma (Fraser et al., 1970), but may be considerably older (Hendry, pers. comm., 1986). A Rb-Sr date of 1632 ± 32 Ma (Fahrig and Loveridge, 1981) and K-Ar ages of 1541 ± 40 Ma and 1411 ± 36 Ma (Stevens et al., 1982) have been obtained on weathered basement rocks from Saskatchewan. The K-Ar ages were obtained close to uranium deposits and were probably affected by later alteration association with mineralization; hence, they are minimum ages. Thus, the age of the saprolite cannot be precisely determined, but it probably formed before 1600 Ma.

Hydrothermal alteration of the basement crosscuts both the saprolite and fresh basement. This alteration is white to pale yellowish-green and is commonly related to fracturing. The age of this alteration is unknown, but it postdates the saprolite and probably the deposition of the Athabasca Group. Locally, the saprolite is bleached immediately below the unconformity. This alteration is probably related to fluid flow within the overlying sediments and not to the fracture-related hydrothermal alteration.

Cover rocks

The Athabasca Group in Alberta consists of a thick sequence of predominantly fluvial clastics with minor interbedded pyroclastics (Wilson, 1985a). In Alberta, the group is more than 1255 m thick and is subdivided into four formations on the basis of clast size, clay content, pyroclastic content and sedimentary structures (figure 6). Evidence of tectonic activity since deposition of the Athabasca Group is limited to fracture zones encountered in some drill holes, offsets of the basal unconformity and formational boundaries between drill holes, and the steep dip of the basement/ Athabasca Group unconformity at Fidler Point. However, the greater evidence of tectonism affecting the basin in Saskatchewan (Ramaekers, 1979, 1980), and the proximity to the Alberta border of the extremely disturbed terrain of the Carswell structure, suggests that the basin in Alberta may be cut by considerably more faulting than thought earlier. This tectonic activity may be related to the brittle phase of deformation present in the exposed Shield, or to the forces that formed the Carswell structure, or they may be multiple reactivation of ancient faults and shear zones.

The Athabasca Group was deposited sometime between the formation of the saprolite and the uranium mineralization and emplacement of dikes. As discussed above, the saprolite probably formed between 1790 Ma and 1600 Ma. Ages for early uranium mineralization at the basement/Athabasca Group unconformity range from 1050 Ma to 1320 Ma (Tremblay, 1982). The oldest age obtained on a diabase dike cutting the Athabasca Group is 1310 ± 70 Ma (Armstrong and Ramaekers, 1985). Armstrong and Ramaekers (1985) also obtained a Rb/Sr age of 1430 ± 30 Ma on fine-grained sediments from the tuffaceous Wolverine Point Formation. This age may be the age of deposition of part of the Athabasca Group, or it may indicate the age of devitrification of the tuffs, thus being a minimum age. The saprolite alteration probably occurred shortly before deposition of the basal Athabasca Group. Thus, deposition of the basal Athabasca

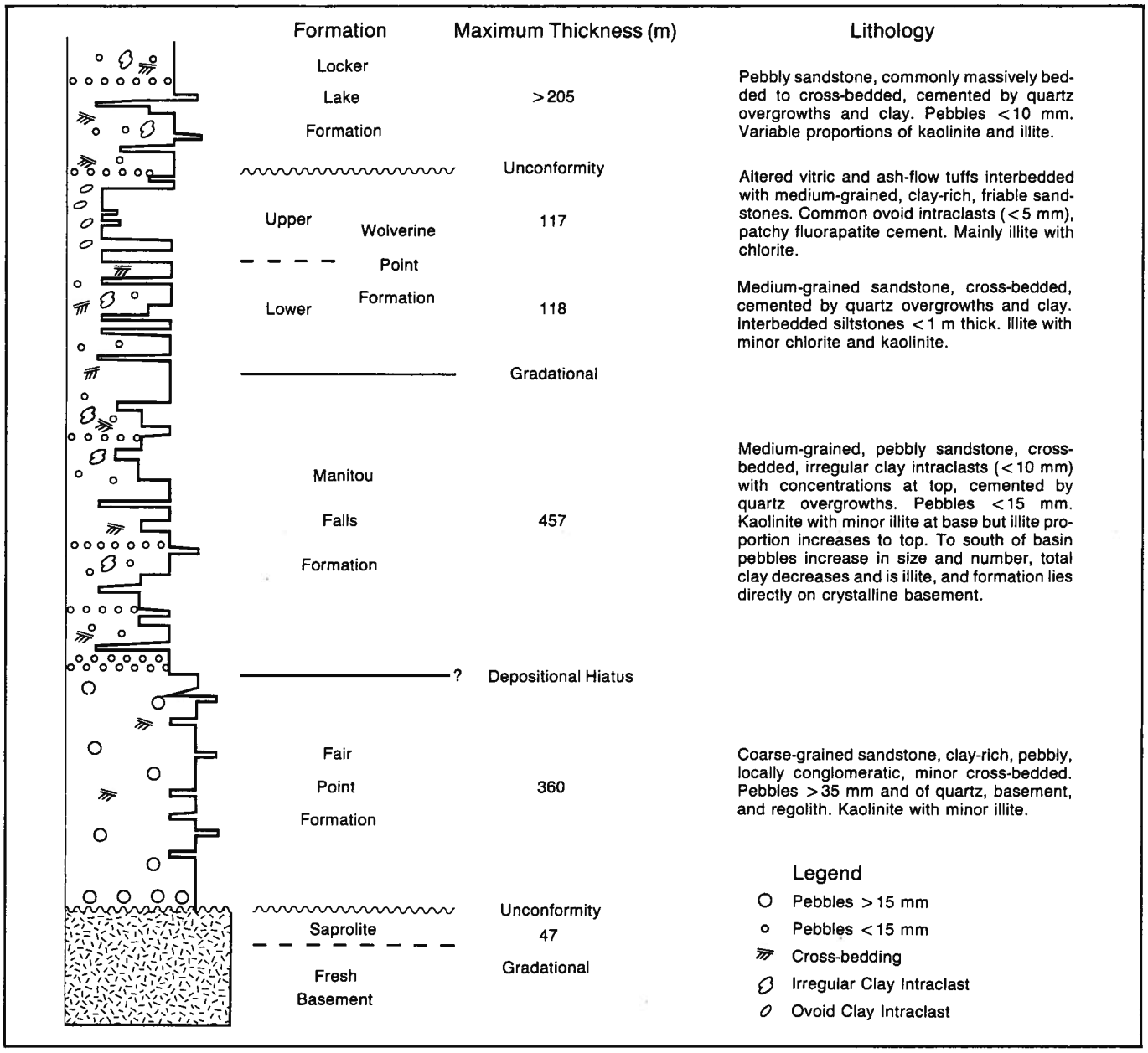

Figure 6. Stratigraphic column for the Athabasca Group in Alberta (after Wilson, 1985a).

Group may have occurred closer to 1600 Ma than the published age suggests.

The Phanerozoic cover consists of Middle to Upper Devonian carbonates and calcareous clastics. In the extreme south and southwest of the area, a thin cover of Cretaceous clastics is present.

Basement topography

Basement topography was a major control on Helikian sedimentation and on the development of the saprolite. In addition, relief on the basement/Athabasca Group unconformity may be an indication of post-Athabasca Group tectonic activity, and this points to prime exploration areas for uranium mineralization (Tremblay, 1982).

Figure 7 is a contour map of the basement surface in the covered portions of the study area. The southern portion of the map has a reasonable distribution of data points and was contoured by computer. However, the contours were extended by hand to the north where there are few data points.

The sparse distribution of data points in some areas of the map makes the definition of detail impossible. However, some features can be noted. Feature (1) is the west-northwest trending fault postulated by Wilson (1985a), and was a major local control on sedimentation. Features (2) and (3) are less pronounced, but may represent fault scarps. Apart from these features, the topography is marked by gentle slopes, indicating no basement offsets.

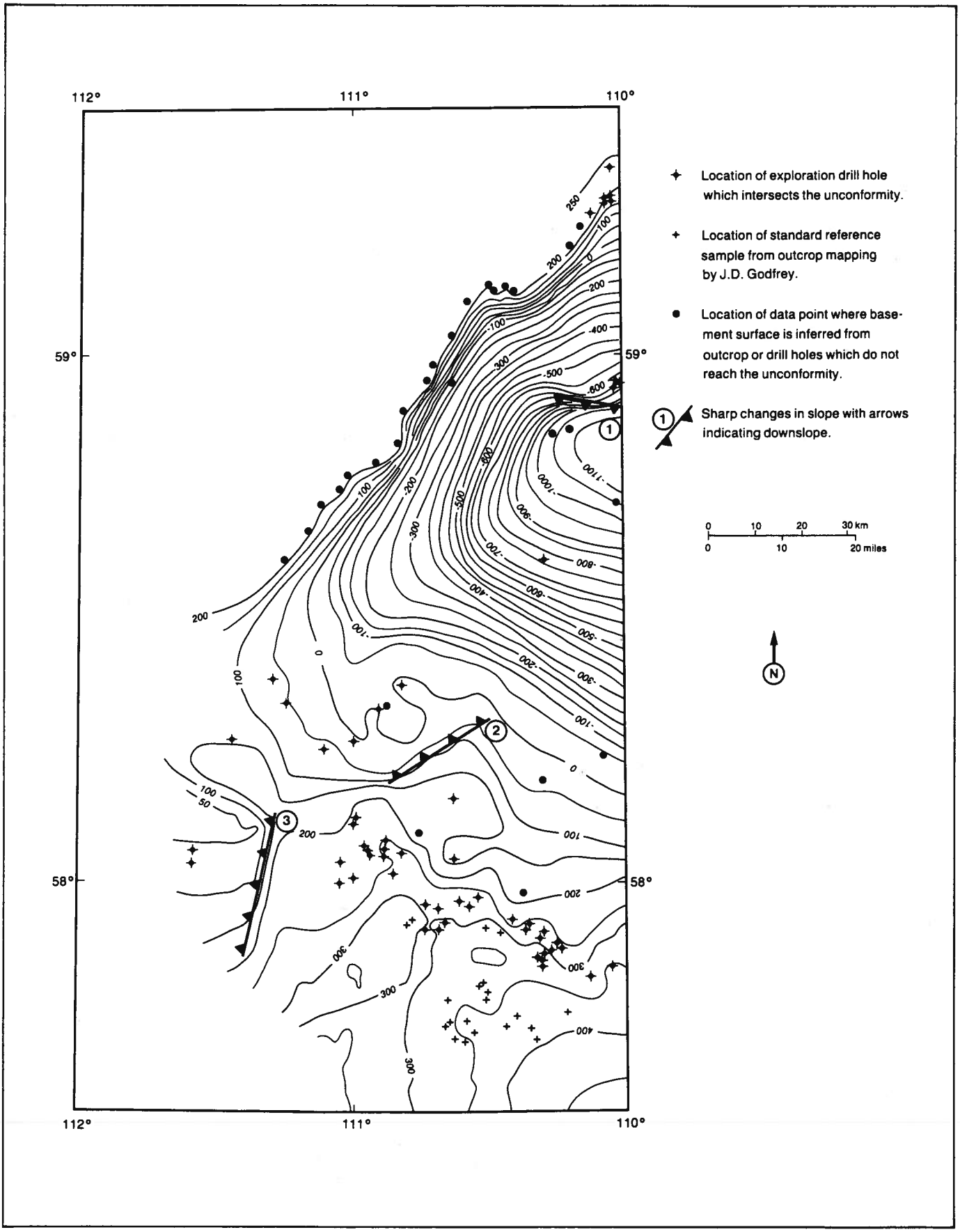

Figure 7. Contour map of the basement surface beneath the Athabasca Group in Alberta. Contour interval is 50 m.

Geology of the fresh basement

Rock descriptions

Forty-four cores that penetrated the fresh basement in the study area were examined. The rock types present in core were visually compared to the outcrop rock types mapped north and south of the Athabasca Basin. In many cases the cores are outside the Athabasca Basin or close to the edge and are easily related to the outcrop rock types. The exceptions are along the southern edge of the basin, where there is only limited basement outcrop data to work with.

The informal nomenclature used here differs from that used by Godfrey (1980a, 1980b, 1984). This is due to the nature of drill core, which does not show field relationships between rock types or even the complete range of one rock type as well as a good outcrop. The granitoid rocks are equivalent to the members of the Wylie Lake pluton. The Wylie Lake Granitoid is probably equivalent to Godfrey's Wylie Lake Granodiorite Phase (Godfrey, 1980a), the Fishing Creek Granitoid is equivalent to the Fishing Creek Quartz Diorite (Godfrey, 1980a) and the Alkali Feldspar-Rich and Grey Foliated Granitoids are probably, at least in part, equivalent to the Leucocratic Granite (Godfrey, 1980a). The mylonitic rocks are broadly equivalent to Godfrey's Granite Gneiss Complex and High-Grade Metasediments (Godfrey, 1980a). The rock types distinguished in core are outlined in table 1 and described below.

Table 1. Major basement rock types present in drill core from northeastern Alberta

Rock type	General characteristics in hand specimen	General characteristics in thin section	Drill holes
Wylie Lake Granitoid	medium-grained equigranular massive to foliated granodiorite to tonalite	plagioclase > > alkali feldspar strained to recrystallized quartz brown biotite clinopyroxene	10, 19, 47, 63, 79, 98
Fishing Creek Granitoid	medium- to coarse-grained equigranular to megacrystic massive variable mafic content granodiorite to tonalite	plagioclase > > alkali feldspar strained quartz brown biotite clinopyroxene myrmekite	20, 57, 59, 71, 72, 73, 74, 75,76, 83
Alkali Feldspar-Rich Granitoid	medium-grained porphyroblastic locally massive to well-foliated granite	alkali feldspar > plagioclase strained to recrystallized quartz brown biotite muscovite clinopyroxene sillimanite epidote orthopyroxene	15, 31, 33, 35, 36, 40, 41, 45, 55, 60, 74, 79, 86, 87, 93
Grey Foliated Granitoid	medium-grained equigranular foliated granite	alkali feldspar = plagioclase strained quartz brown biotite clinopyroxene muscovite	5, 11, 13, 18, 20, 56, 66, 67, 89, 92
Mafic Mylonite	fine-grained protomylonitic to mylonitic textures foliated variable composition mafic	variable feldspar ratios abundant chlorite and other mafic minerals recrystallized streaky quartz mortar textures common green biotite allanite apatite epidote clinopyroxene graphite locally	3, 4, 6, 21, 22, 23, 25, 38, 47
Felsic Mylonite	fine- to medium-grained protomylonitic to mylonitic textures moderately to strongly foliated minor mafic content variable composition	variable feldspar ratios minor chlorite/epidote recrystallized streaky quartz mortar textures common allanite minor green biotite	4, 5, 19, 21, 24, 25, 38, 47

Wylie Lake Granitoid

This is a variable rock type that is commonly present with other rock types in a single drill hole. In hand specimen it is dark greenish gray to brownish red, commonly with pink to red feldspars set in a darker matrix (figure 8). The texture is commonly equigranular and the rock is massive to foliated. The foliation may be more pronounced close to shear or fracture zones. Both the feldspars and the matrix are medium grained. The matrix consists of feldspar, quartz and biotite. Compositionally, the rock ranges from granodiorite to tonalite (figure 9a).

Petrographically this rock type consists of sericitized plagioclase with minor amounts of alkali feldspar, strained to recrystallized streaky quartz, and brown, partly chloritized biotite. Minor to trace amounts of clinopyroxene (with alteration halos), apatite, muscovite, zircon, opaques and fracture filling carbonate are also present. Foliation is defined by the biotite. Where unstrained, the major minerals tend to be equigranular. However, close to fracture zones or faults mortar textures may be approached.

A leucocratic variation of the Wylie Lake Granitoid is present locally. However, since field associations cannot be observed on outcrop, it is not possible to define its relationship to the Wylie Lake Granitoid.

Fishing Creek Granitoid

This rock type is part of the Wylie Lake pluton (Godfrey, 1980a), but is easily recognized in core and hence is considered separately. It occurs as irregular bodies surrounded by other members of the Wylie Lake pluton. In hand specimen, the Fishing Creek Granitoid is medium- to light-gray, with grains of quartz and plagioclase outlined by biotite (figure 10). The mafic content can vary markedly, even in hand specimen. Texturally, the rock is commonly medium-to coarse-grained, although locally fine-grained variations and megacrystic textures are present. Foliation is poor except locally near shear zones where the rock may be gneissic. Compositionally, the rock ranges from tonalite to granodiorite (figure 9b).

In thin section, the Fishing Creek Granitoid is commonly composed of equigranular plagioclase and strained quartz grains with some alkali feldspars in a matrix of brown biotite. Trace amounts of zircon, garnet, apatite, clinopyroxene and opaques are present. Locally, the quartz may be recrystallized to a fine groundmass and the alkali feldspars may form porphyroblasts. The alkali-feldspar grains are commonly surrounded by myrmekitic textures that have corroded the edges of the grain. Myrmekitic textures are not commonly present away from the edges of the alkali feldspar grains.

Alkali Feldspar-Rich Granitoid

The Alkali Feldspar-Rich Granitoid is present throughout the study area in both small and large bodies. They vary considerably in appearance, but generally are light gray to pink, or mottled pink and gray (figure 11). Most commonly they are massive, although well-foliated varieties are present locally. Grain size is medium or rarely fine with no evidence of porphyroblast development. Alkali feldspar generally predominates over plagioclase, and there are minor amounts of biotite, quartz (which may be blue) and garnets. Com-

Figure 8. Typical foliated Wylie Lake Granitoid. Drill hole 47. Top of the core is to the right. Scale is in cm.

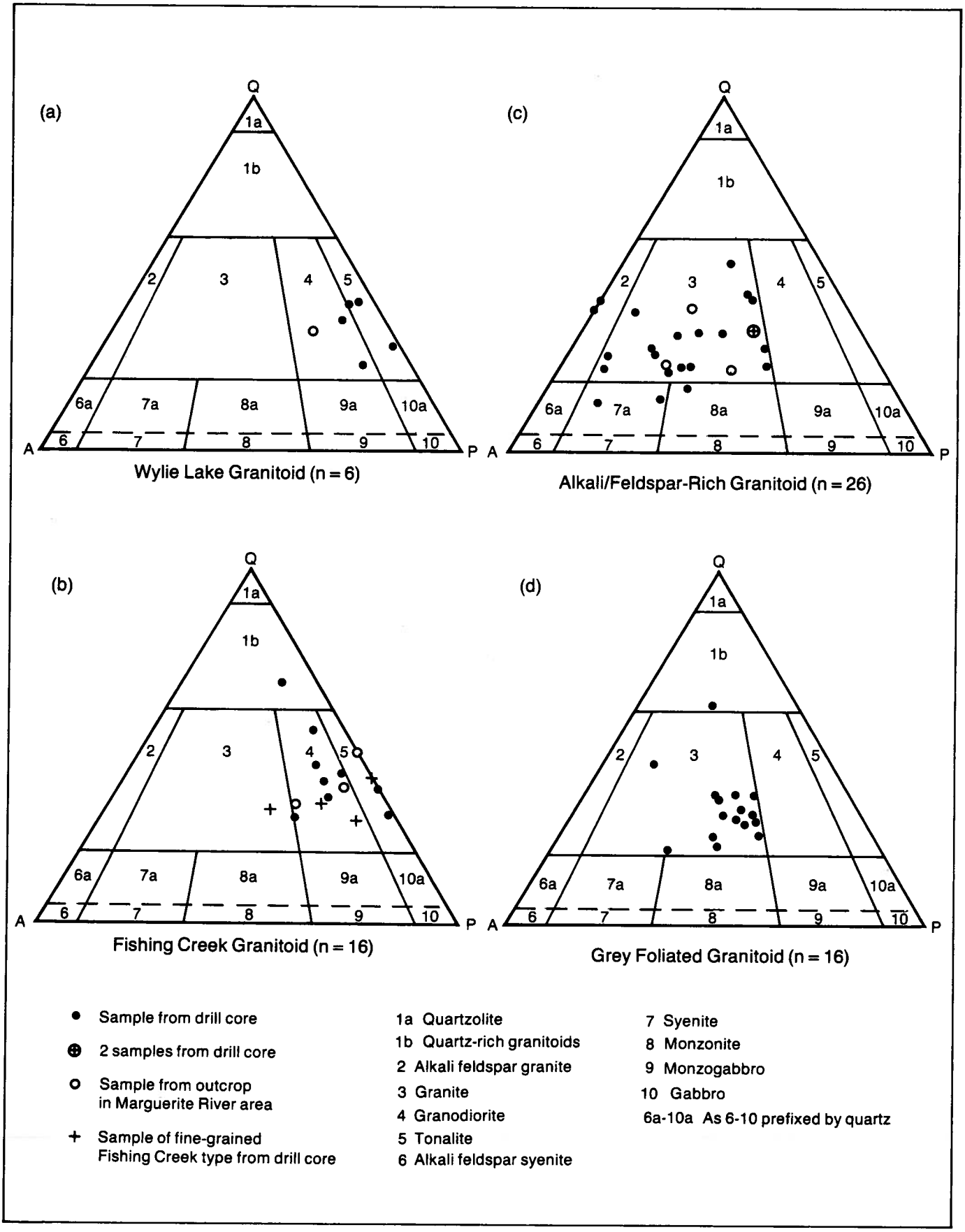

Figure 9. Ternary Quartz (Q) - Alkali Feldspar (A) -Plagioclase (P) plots for the granitoid rocks in the study area. (Field boundaries from Streckeisen, 1976).

Figure 10. Typical Fishing Creek Granitoid. Drill hole 75. Top of the core is to the right. Scale is in cm.

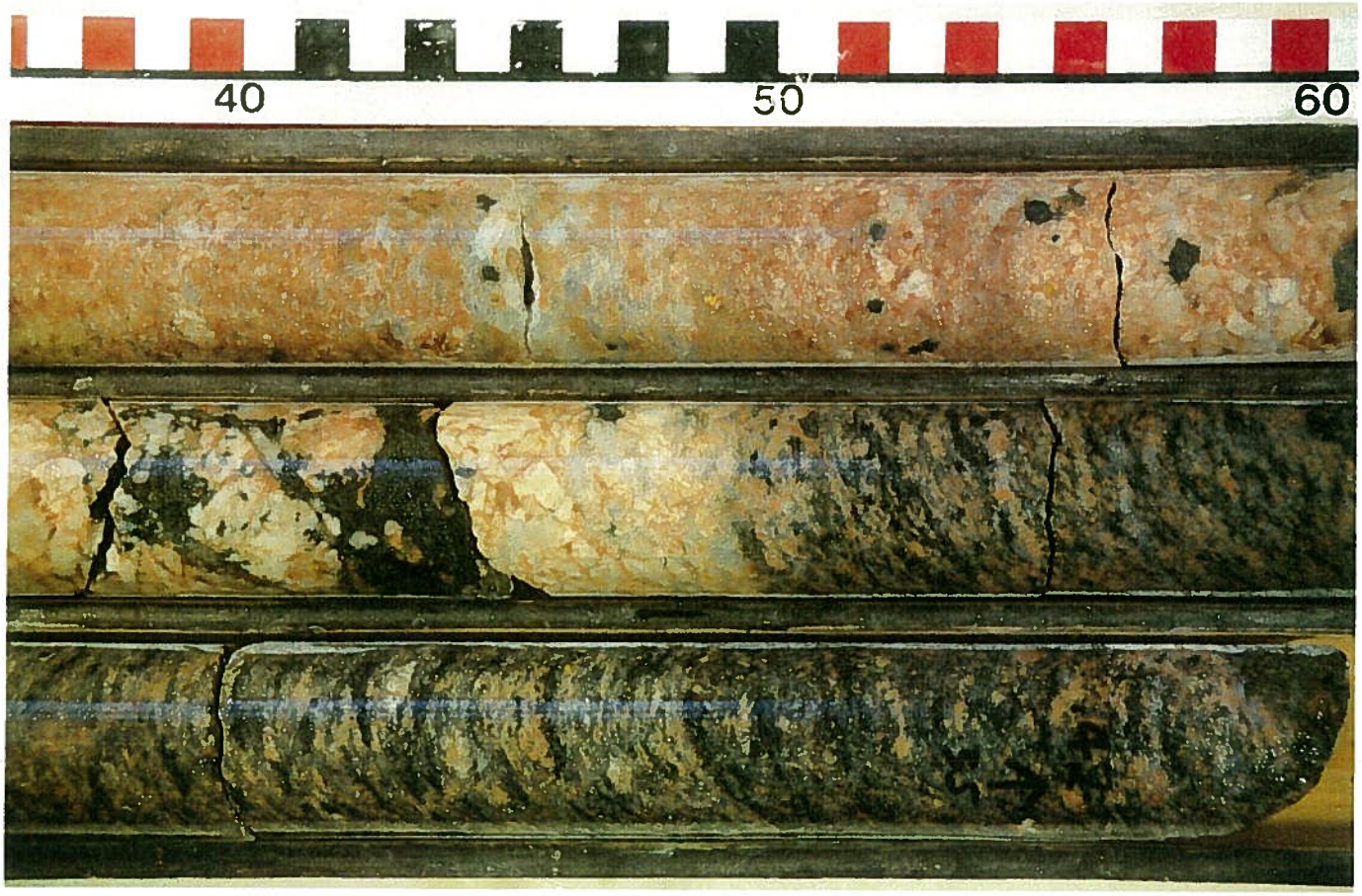

Figure 11. Typical Alkali Feldspar-Rich granitoid. Drill hole 35. Top of the core is to the right. Scale is in cm.

positionally, the rocks fall within the granite field (figure 9c). Some specimens resemble the Wylie Lake Granitoid except for the high alkali feldspar content, suggesting that this rock unit may be an alkali feldspar-enriched equivalent of the Wylie Lake Granitoid.

Petrographically, the rock is composed of equigranular alkali feldspar that may be perthitic and contains inclusions of quartz, plagioclase and myrmekite, and quartz that is commonly strained but is recrystallized close to shear zones. Plagioclase is more or less sericitized, has a smaller grain size than the quartz or alkali-feldspar and may have unsericitized overgrowths (figure 12). Biotite is the predominant mafic mineral and is commonly altered to chlorite. Muscovite is a more prevalent accessory mineral than in the other rock types, and clinopyroxene is present in trace amounts as remnant grains surrounded by alteration halos. Trace amounts of sillimanite (figure 13), garnet, epidote, orthopyroxene, apatite, zircon, monazite and opaques are present. The foliation present in some specimens appears to be due to proximity to fault or shear zones. Carbonate fills late fractures.

The presence of hypersthene in this rock type would classify it as a charnokite (Streckeisen, 1976). However, hypersthene is only rarely present, never reaches five percent of the rock by volume and cannot be recognized in hand specimens. Thus, while charnokite (senso stricto) may be present locally, it is a minor variation of the Alkali Feldspar-Rich Granitoid and cannot be identified without thin section examination.

Grey Foliated Granitoid

Like the Alkali Feldspar-Rich Granitoid, this rock type occurs throughout the study area. The Grey Foliated Granitoid is light to medium gray, commonly well foliated and generally has a low mafic content (figure 14). Medium-grained quartz, alkali feldspar and plagioclase are set in a matrix of biotite with scattered garnets. On a Q-A-P plot, the rock samples plot in a tight group to the right of the granite field (figure 9d). Possibly this rock type represents an alkali feldspar-rich foliated variety of the Fishing Creek Granitoid.

Thin sections of this rock type show large grains of alkali feldspar and strained quartz. Plagioclase grains are generally the same size or smaller than alkali feldspars and quartz grains. Variable amounts of brown biotite, in part altered to chlorite, form the mafic constituent of the rock. Accessory minerals include clinopyroxene, zircon, garnet, muscovite and apatite.

Mylonitic rocks

This rock type is defined on the basis of texture. The mylonitic texture masks other features of the rock, and hence several rock types may be present under this heading. Mylonitic rocks are present in core from drill holes 3, 4, 5, 6, 19, 21, 22, 23, 24, 25, 38, and 47 (figure 1). In general the level of mylonitization does not appear to be as high as it is in outcrop at Marguerite River (Godfrey, 1970).

The mylonitic rocks can be broadly subdivided into a mafic and a felsic type. The Mafic Mylonites predominate and may be derived from a granite gneiss or high-grade metasedimentary parent. The Felsic Mylonites are probably derived from granitoid rocks.

In hand specimen the Mafic Mylonites are dark gray to greenish gray. Commonly, feldspar and quartz are present as pale streaks in a fine-grained matrix containing chlorite and epidote (figure 15). The Felsic Mylonites are gray to pink, and contain porphyroblasts of feldspar in a matrix of crushed feldspar, quartz and chlorite.

In thin section, these rocks have mylonitic textures (figure 16). Streaks of recrystallized quartz, fractured porphyroblasts of alkali feldspar, and partly sericitized grains of plagioclase are common in a fine groundmass of chlorite, biotite, epidote and clay. Locally, within the groundmass grains of pyrite, clinopyroxene, apatite, zircon, hematite and allanite are present. Graphite occurs locally in the chlorite-rich Mafic Mylonite as distorted, whispy streaks commonly associated with late-stage carbonate replacement and fracture fill. In the Felsic Mylonites the groundmass consists of finely broken up feldspar and recrystallized quartz. In one case the mylonite is garnet-rich. Several

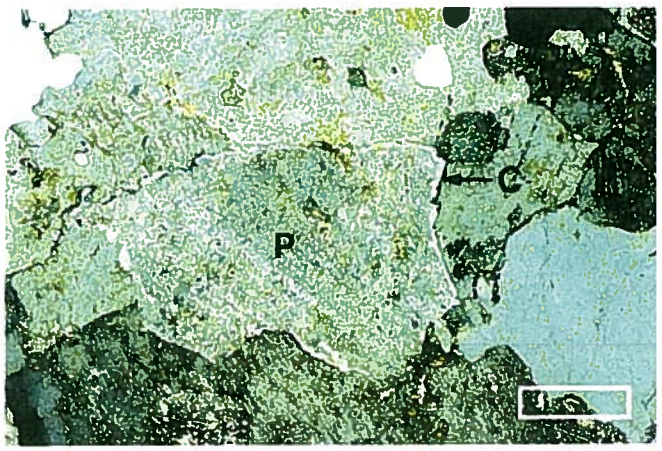

Figure 12. Sericitized plagioclase grain (P) with rim of fresh overgrowth (O). Crossed nicols. JAW84-060-37.6. Scale bar is 0.5 mm long.

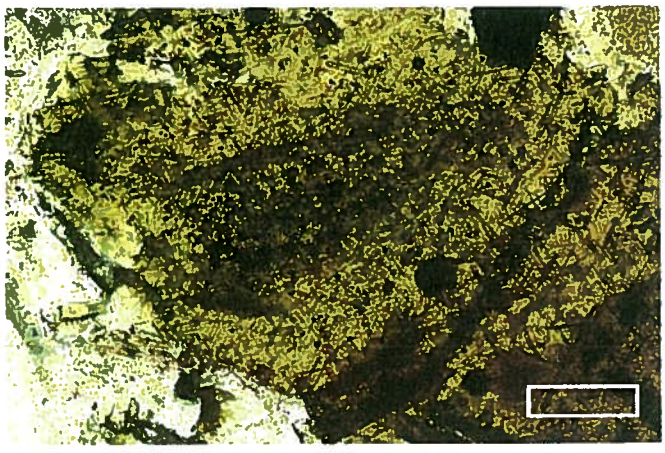

Figure 13. Sillimanite needles in biotite grain. Plane polarized light. JAW84-074-65. Scale bar is 50 μm long.

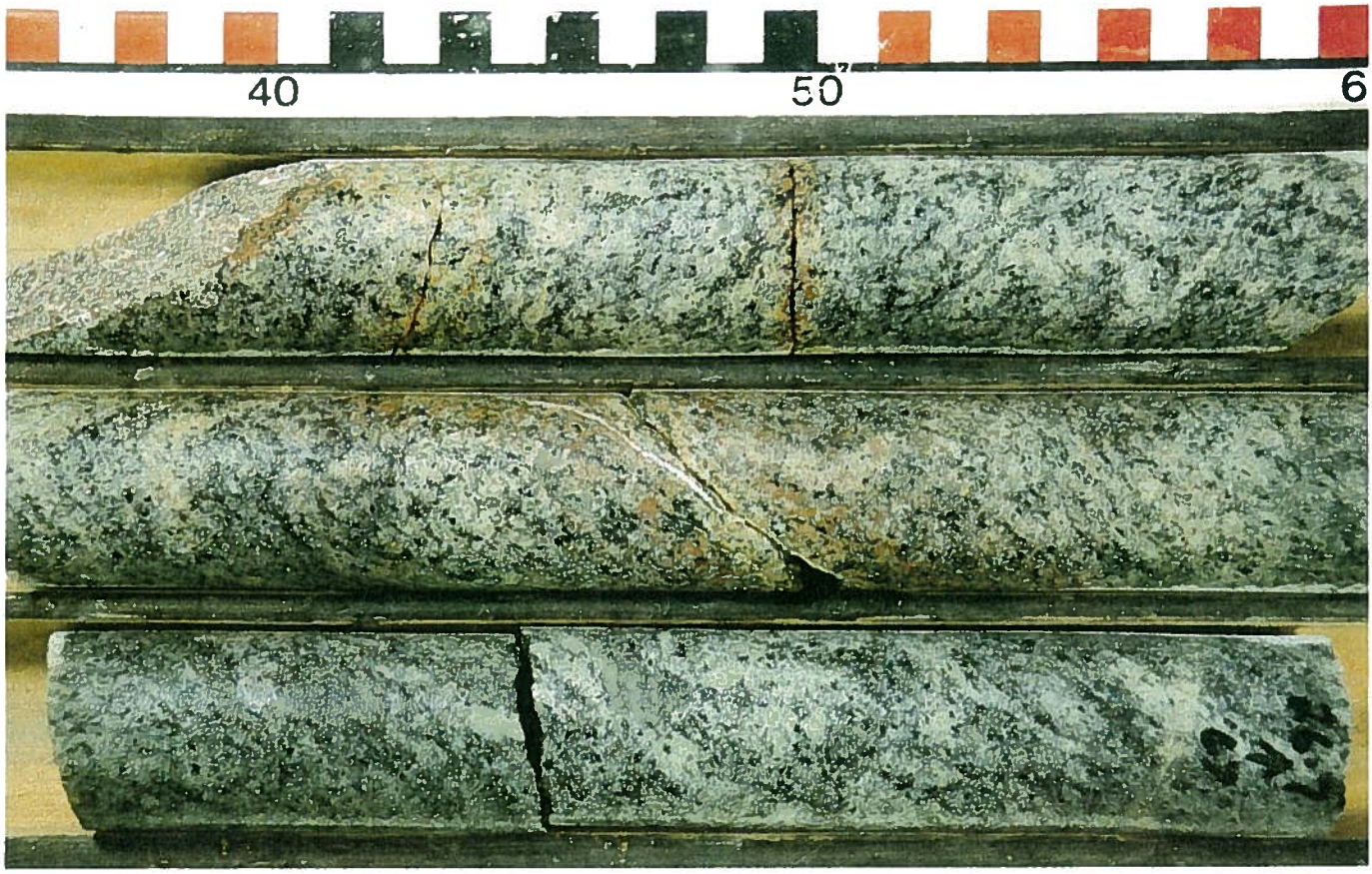

Figure 14. Typical Grey Foliated Granitoid. Drill hole 67. Top of the core is to the right. Scale is in cm.

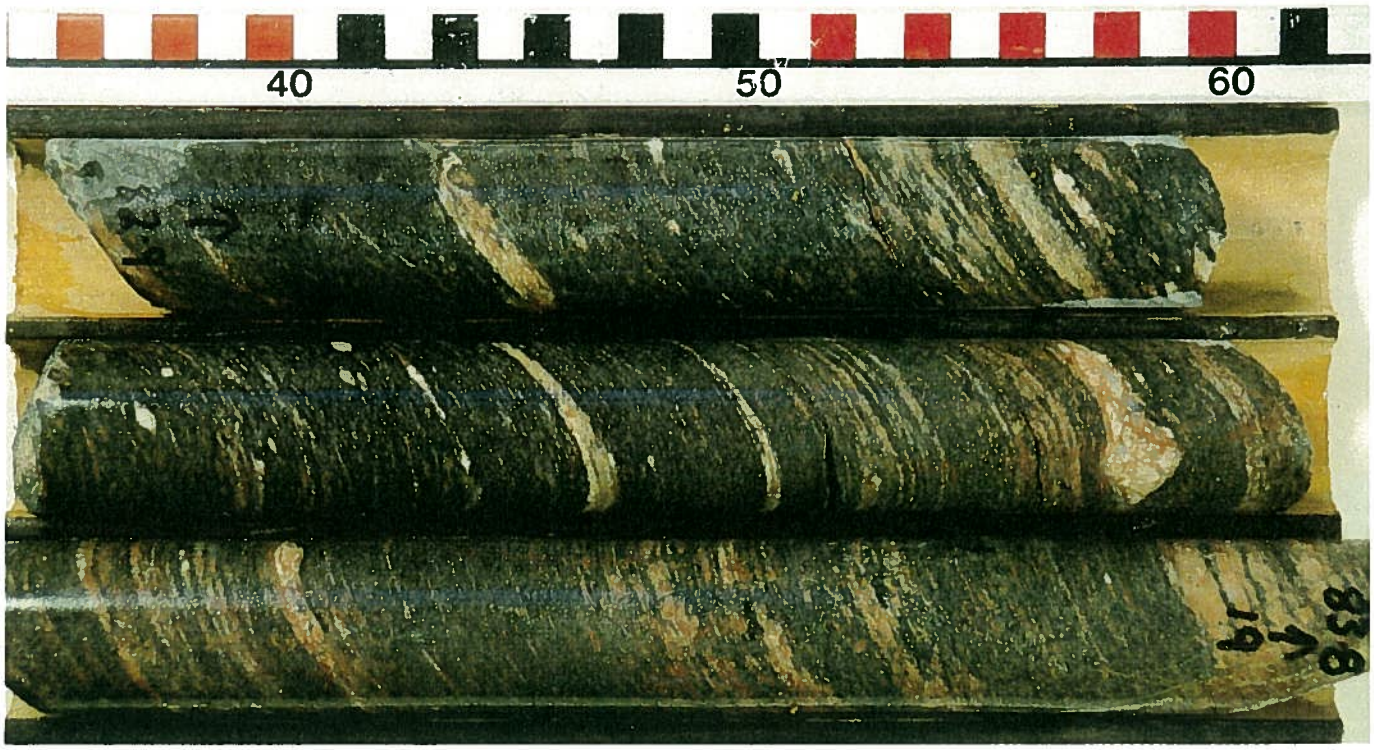

Figure 15. Well-developed Mafic Mylonite. Drill hole 19. Top of the core is to the right. Scale is in cm.

original rock types are represented by the mylonitic rocks although most commonly they appear to be derived from a mafic parent.

Minor rock types

Several minor rock types are present in the drill core examined. These do not comprise an entire core but only short sections of single cores.

Locally, within the predominantly mylonitic rocks of drill holes 19, 22 and 24, and in 30, there are rock types whose textures suggest that they are metasediments. These include quartzites that, in thin section, exhibit a granular texture, and fine-grained, banded rocks whose uniform grain size in thin section suggests a well-sorted arenaceous parent (figure 17). The association of these metasediments with the mylonitic rocks suggests that perhaps some of the mylonitic rocks had a sedimentary parent. In addition, the fine-grained, biotite-rich end member of the Fishing Creek Granitoid in drill hole 75 is similar to metasedimentary rocks farther east in the basin.

Chlorite and epidote are common in the mylonitic rock. Rarely, these rocks can be described as chlorite epidote schists that may contain considerable amounts of apatite. Chlorite and epidote are common in the granite gneiss from outcrop (Godfrey, 1980a) indicating that granite gneiss is present within the zones of mylonitic rocks. Drill core 10 contains gneissic rocks rich in hornblende and biotite. These are probably Godfrey's (1980a) Hornblende Granite Gneiss.

Locally, rocks rich in garnet, sillimanite and cordierite are present. These rocks are present in drill cores 3, 4, 5, and 15 and are similar to both the Peter River Gneisses of Pagel and Svab (1985) and some of the high-grade metasediments of Langenberg and Nielsen (1982). High concentrations of garnets are also locally present (drill core 3) and are similar to the garnetites within the Peter River Gneisses (Pagel and Svab, 1985).

Locally, within several drill cores amphibolites and pyroxenites are present. These are fine-grained, dark gray to black rocks composed predominantly of either amphibole or clino- and orthopyroxene, commonly having intrusive contacts. Nowhere are these rocks present in sequences thick enough to suggest an altered volcanic pile. Probably they represent minor dikes or sills, or thin volcanics intercalated with the metasedimentary rocks. The pyroxene-rich rocks appear to be similar to the two-pyroxene granulite which is present in the Earl River Complex of Pagel and Svab (1985). Pegmatoid intrusions are also present in many drill holes, but are rarely more than 1 m thick.

Present in two cores and in outcrop at Marguerite River is a rock type that, in hand specimen, is pink and consists of coarse to porphyroblastic alkali feldspar crystals up to 2.5 cm across in a matrix of medium-grained plagioclase and fine quartz and mafics. It is not well foliated and approaches a protomylonite in texture. In thin section, the alkali feldspars contain inclusions of all other minerals and are predominantly rectangular. The plagioclase grains are irregular and set in a matrix of recrystallized quartz, green biotite that is more or less altered to chlorite, and epidote with traces of clinopyroxene and zircon. The epidote may locally comprise the most common mineral other than the feldspars. This minor rock type superficially closely resembles the Arch Lake Granitoids of Godfrey (1984). However, its local development and the great distance from the recognized outcrop suggest that it is not part of the main Arch Lake Granitoid body.

Locally, evidence of strain is present in the rocks. Quartz may be highly strained and recrystallized (figure 18), plagioclase may be fractured or show bent twin lamellae, garnet may retain strain shadows even after considerable alteration to chlorite (figure 19) and quartz may show strain patterns and pressure solution at points of grain contact (figure 20).

Geophysical data

This portion of the study presents a qualitative comparison of variations in magnetic field intensity over exposed regions of the Shield in the study area with those over covered areas. Magnetic data were chosen because good regional data exist (Geological Survey

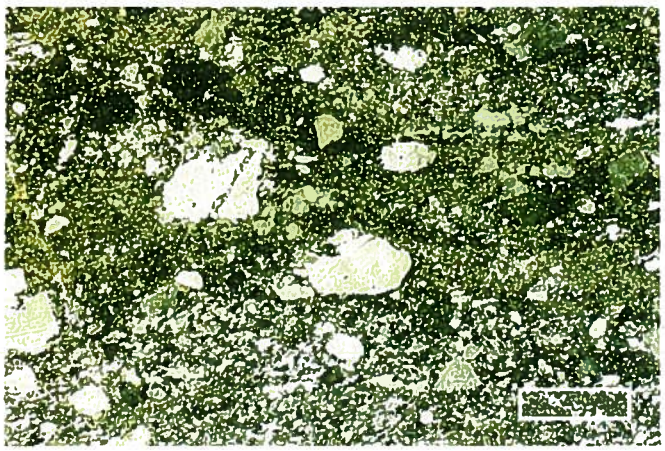

Figure 16. Mylonite. Crossed nicols. JAW84-023-85. Scale bar is 0.5 mm long.

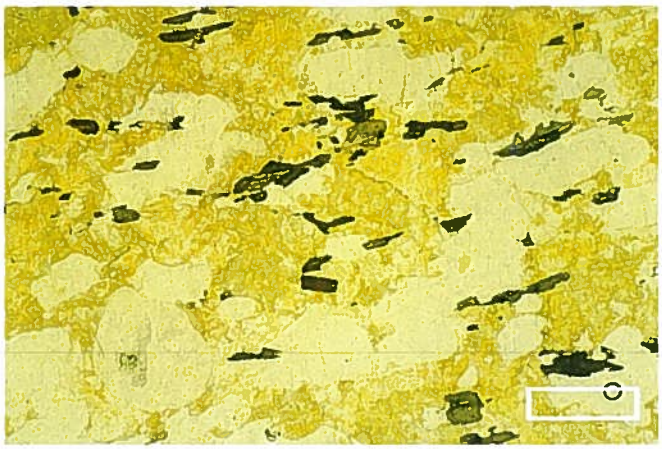

Figure 17. Possible metasedimentary rock. Crossed nicols. JAW84-030-279.3. Scale bar is 0.5 mm long.

Figure 18. Strained, partially recrystallized quartz. Crossed nicols. JAW84-023-63. Scale bar is 0.5 mm long.

of Canada 1964a, 1964b; 1983), and because the magnetic field can be detected beneath considerable thicknesses of cover rocks.

Figure 21 shows the simplified magnetic character for the study area. Areas of high and low magnetic value are outlined, and linear highs and lows marked. The figure takes no account of the possible masking effects of the cover rocks. However, the cover rocks appear to have only minimal effect on the magnetic signature, probably only being noticeable as a damping of the signal where the Athabasca Group is thickest.

The magnetic pattern is dominated by a broad linear high running from northeast to southwest across the area. The high has sharp edges and contains areas of low magnetic signature. Long, pronounced magnetic lows are present within, and strongly aligned with, the high. Linear highs are also present within the feature but tend to be short features. To the southwest, the linear high widens and its orientation swings around to north/south. It is flanked by two distinct high areas, which are characterized by short highs and lows that are less strongly aligned. These highs are separated from the main linear high by sinuous linear lows.

To the northwest of the linear belt, the magnetic signature is low, except for rare, short, linear highs and, in the extreme west and north, areas of high magnetic signature. These high areas are characterized by short linear highs and lows with no strong overall alignment.

To the southeast of the linear high, the area can be subdivided on the basis of the magnetic signature. The northern half of this area has a very flat, low magnetic signature with only rare, short linear lows and isolated high areas. The southern half is characterized by numerous irregular to linear magnetic highs and linear lows. The linear elements of this southern area are aligned northwest to southeast at approximately right angles to the main linear high bisecting the area.

Interpretation

An interpretation of the magnetic patterns over the exposed shield of northeastern Alberta is presented in Sprenke et al. (1986). They found that there were two types of magnetic anomalies present: 1) linear, aligned anomalies due to local shear and regional metamorphism, and 2) circular anomalies due to original magmatic conditions. In general, most granitoids produce magnetic lows, and granite gneiss produces magnetic highs. It was found that an increase in the mafic content of the granitoids does not substantially increase its magnetic signature. Mylonite zones are related to deep-seated regional shearing and, consequently, commonly lie close to linear magnetic anomalies. Fault traces commonly show low linear magnetic values. Since metasedimentary rocks have magnetic values that are average for the shield, they appear as relative lows when they occur within areas of granite gneiss having high magnetic signatures.

Figure 22 shows the mapped shield geology (Godfrey, 1970; 1980a, 1980b; 1984; in press) and an interpretation beneath the cover based on drill hole data and magnetic pattern (Wilson, 1985b). North of Lake Athabasca the linear magnetic high bisecting the area coincides with the Granite Gneiss belt, and the linear lows within it to major fault zones. Thus, the Granite Gneiss belt and the associated faults can be traced to

Figure 19. Altered garnet (G) with a pressure shadow of chlorite (C). Plane polarized light JAW84-005-830. Scale bar is 0.5 mm long.

Figure 20. Stress patterns in two quartz grains. Note formation of solution features where grains are in contact. Crossed nicols. JAW84-015-222. Scale bar is 0.5 mm long.

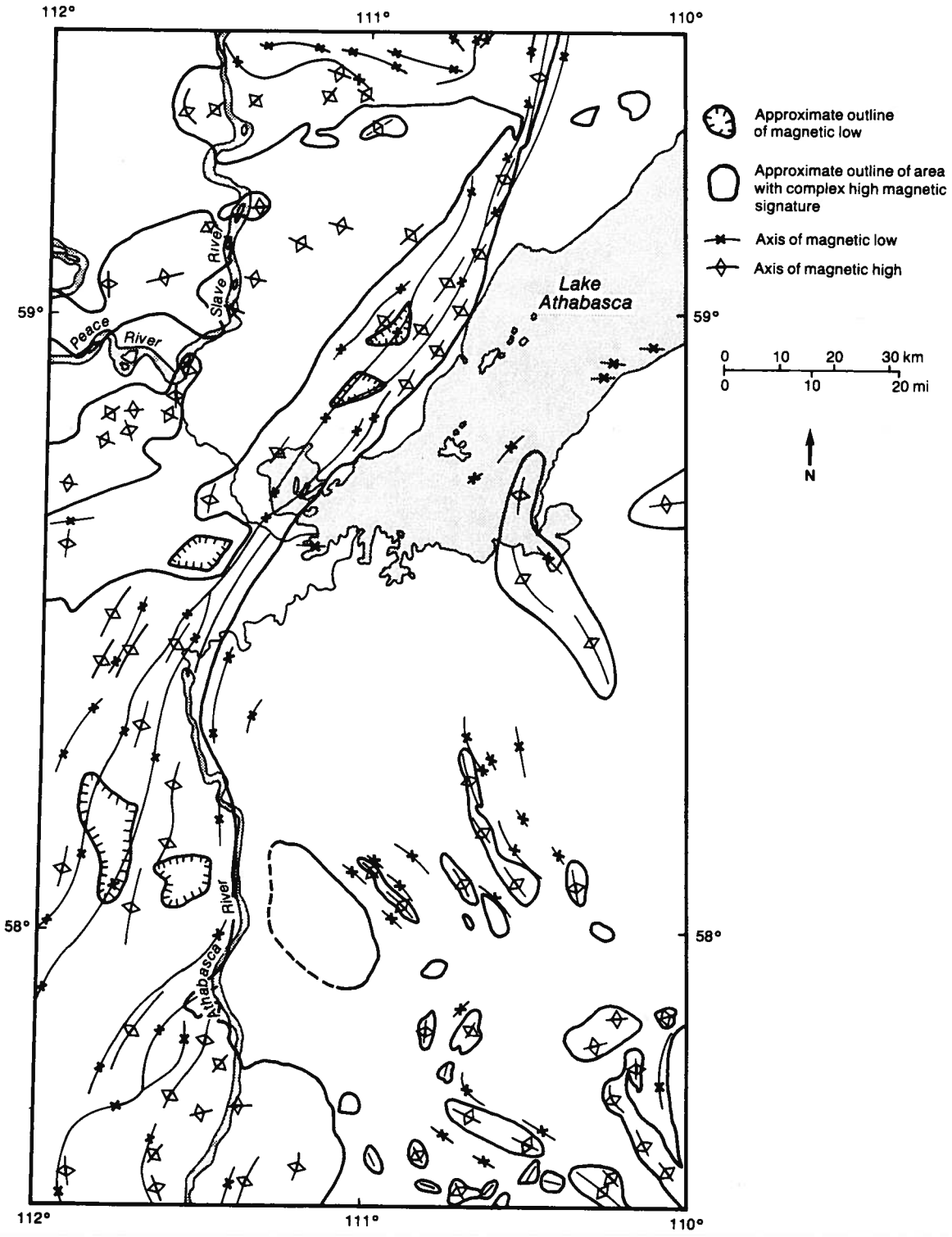

Figure 21. Major magnetic features in the study area.

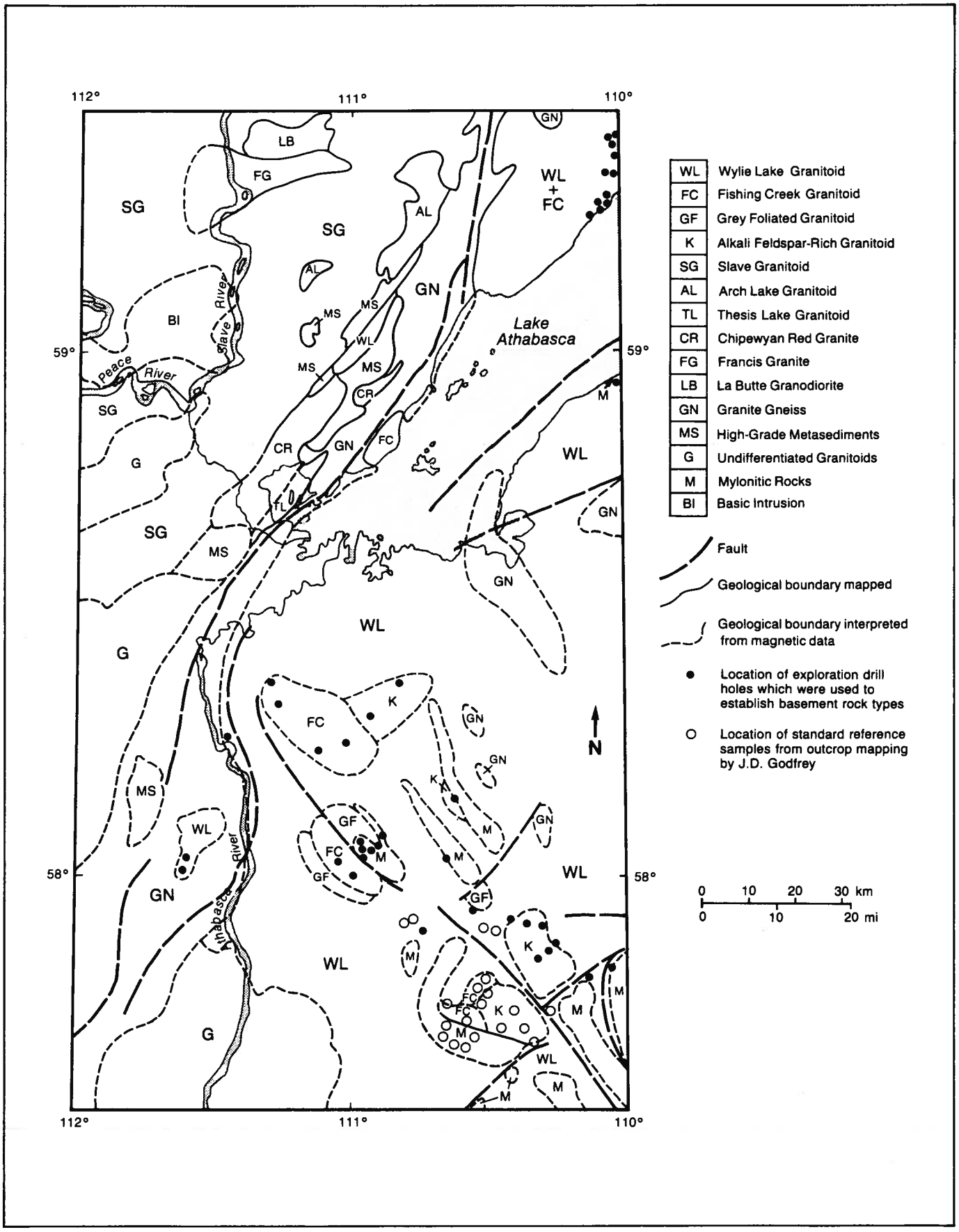

Figure 22. Basement geology in the study area (simplified from Godfrey, 1970, 1980a, 1980b and 1984, and Wilson, 1985b).

the southwest beneath the cover. Areas of low magnetic signature within the Granite Gneiss belt are interpreted as areas of metasediments or granitoids. Major faults flank the granite gneisses in the southwest and separate them from the two other magnetic highs. The high to the north of the Granite Gneiss belt is interpreted as a granitoid body, possibly a continuation of the Chipewyan Red Granite pluton (Sprenke et al., 1986). The area to the south of the granite gneisses may represent another distinct granitoid body, although it continues for some distance south of the study area and an increase in the number of strongly linear features suggests an increase in the granite gneiss component.

Northwest of the Granite Gneiss belt, the area of low magnetic signature is interpreted as a continuation of the exposed Slave Granitoids. In the extreme north, the magnetic high running east to west can partly be accounted for by the presence of the La Butte Granodiorite and the Francis Granite; however, a large part of it is lithologically indistinguishable from the bulk of the Slave Granitoids. The Francis Granite does not extend far beneath the Phanerozoic cover (Sprenke et al., 1986). The magnetic high north of the Peace River is interpreted by Sprenke et al. (1986) to be a "relatively homogenous basic intrusion." The high area to the south of the Peace River is probably a distinct granitoid body.

The area to the southeast of the Granite Gneiss belt is largely covered by the Athabasca Group. The uniformity of the background magnetic signature and its similarity to the area north of Lake Athabasca suggest that the bulk of this area is underlain by rocks of the Wylie Lake pluton. This is a complex pluton consisting of several distinct granitoid rock types. The pluton extension south is confirmed by the presence throughout of core from the distinctive Fishing Creek Granitoid. The distribution in drill core of both the Grey Foliated Granitoid and the Alkali Feldspar-Rich Granitoid indicate that they are variations of the Fishing Creek and Wylie Lake Granitoids.

This large area of Wylie Lake pluton rocks can be broadly subdivided into a northern and a southern half. The northern half contains only two distinct magnetic highs, a sinuous one at Old Fort Bay and one to the east that straddles the Saskatchewan border. If these features represent basement variation, they are probably bodies of granite gneiss.

The southern half of the Wylie Lake pluton is marked by numerous linear and non-linear magnetic highs. This area corresponds to domain E of Wallis (1970) and the Firebag domain of Lewry et al. (1978). One of these linears is present in outcrop in the Marguerite River Area (Godfrey, 1970) and is composed of mylonite. Thus, many of these linear highs probably represent deep-seated shear zones within the Wylie Lake pluton. The magnetic highs in this area that are not linear may represent areas of granite gneiss.

If some of the magnetic highs in the southeast area do represent remnants of granite gneiss, this part of the Wylie Lake pluton may represent a higher level in the pluton, with roof pendants of surviving Archean gneisses. The presence of metasedimentary rocks in some cores supports the idea of remnants of pre-granitoid formation rocks.

The northwest orientation of the shear zones is parallel to magnetic trends present south of the study area (Geological Survey of Canada, 1983). This northwest trend occurs on the axis of what appears to be a major flexure in the Granite Gneiss belt (Geological Survey of Canada 1983, figures 21 and 22), and this may account for the structural complexity in the area.

The enrichment in alkali feldspar observed in two of the granitoid rock types may be due to magmatic segregation during the ultrametamorphism that produced the granitoids, or it could be the result of potassium metasomatism (Burwash and Culbert, 1976). The latter is suggested by the presence of the enriched rocks in an area where faulting and shear zones are common.

Strongly linear magnetic lows, representing fault traces, commonly cannot be distinguished against the low magnetic character of the granitoid rocks. In the southeast of the study area, two major faults are postulated on the basis of magnetic lows, offsets of magnetic highs and drill hole data. The southwest-trending fault in the southeast of the area is an extension of a major linear feature present in the aeromagnetic maps of Saskatchewan (Geological Survey of Canada 1964c, 1966). It is responsible for a large offset of the mylonite zone that crosses the Marguerite River outcrop area. This fault is apparently offset by the southeast-trending fault running along Richardson River. This fault, or splays from it, are responsible for the mylonitic rocks present in drill holes 19, 21, 22, 23, 24, 25, and 38, and was first noted by Eldorado Nuclear Limited geologists during their exploration for uranium in the mid 1970s (Laanela, 1977; Fortuna, 1979).

The fault on figure 22 paralleling the south shore of Lake Athabasca is the postulated extension of the Black Bay Fault (Macdonald and Broughton, 1980). The major fault to the south of Lake Athabasca is a probable extension of the Grease River Shear Zone (Macdonald and Broughton, 1980). Neither of these faults can be traced completely across the Wylie Lake pluton, but they may connect with the major faults which apparently separate the Granite Gneiss belt from the granitoid body in the southwest corner of the study area.

Tona et al. (1985), in their discussion of the geology of the Carswell Structure, show the Deranger Creek Fault extending into Alberta to the south of the extension of the Grease River Shear Zone. This fault is not seen as a separate feature in Alberta (Geological Survey of Canada 1964b).

Geochemical data

Tables 2 and 3 present the major and trace element analyses for 58 samples of fresh basement core. The data for the major rock types are presented as Dice diagrams (see methods section for explanation of diagrams) in figures 23 and 24.

Table 2. Major element analyses for fresh basement rock types

Analysis Number	Hole Number	Depth (m)	Rock Type	Major Elements (weight percent oxide) SiO_2	P_2O_5	CaO	MgO	Na_2O	K_2O	Al_2O_3	$Fe_2O_{3(T)}$*	TiO_2	LOI	Total Percent
101	47	99.2	WL	66.34	0.23	2.42	2.24	3.65	3.60	16.54	4.36	0.69	1.5	101.57
125	63	26.2	WL	68.05	0.07	0.97	2.97	2.77	2.70	14.74	5.36	0.62	3.4	101.65
12	10	88.4	WL	61.74	0.19	4.13	1.51	5.27	2.94	17.77	4.93	0.42	0.8	99.70
29	19	48.5	WL	74.90	0.06	1.12	0.29	6.82	1.64	15.03	0.56	0.05	0.7	101.17
153	74	97.5	FC	73.72	0.03	1.57	1.11	2.46	2.11	10.21	2.86	0.54	0.4	95.01
37	20	62.5	FC	61.20	0.07	3.15	2.51	3.24	2.76	17.10	5.08	0.73	0.9	96.74
121	59	34.6	FC	74.15	0.07	1.36	1.26	2.90	3.42	14.84	3.00	0.35	1.3	102.65
115	57	27.9	FC	66.98	0.32	3.29	2.42	3.17	2.88	15.88	5.08	0.62	1.2	101.84
159	75	170.1	FC	66.02	0.25	2.39	1.58	2.54	4.68	15.21	3.43	0.34	0.6	97.04
160	75	180.8	FC	58.10	0.18	3.50	3.27	2.84	3.12	16.82	7.36	0.78	0.6	96.57
163	76	216.0	FC	61.31	0.20	3.64	2.86	3.51	2.15	15.40	5.72	0.76	0.5	96.05
15	13	102.7	GF	73.83	0.05	0.77	0.50	2.47	7.02	14.18	0.89	0.13	0.6	100.44
129	66	27.9	GF	76.18	0.07	0.68	1.00	1.81	4.80	14.46	1.46	0.15	1.7	102.31
20	18	79.1	GF	72.97	0.05	1.61	0.77	3.04	4.98	14.74	1.66	0.23	0.7	100.75
140	67	29.4	GF	68.27	0.07	1.01	1.03	2.15	5.64	14.08	2.23	0.26	1.1	95.84
141	67	26.9	GF	67.41	0.06	1.40	0.93	2.59	4.56	14.08	2.46	0.26	0.9	94.65
139	67	25.5	GF	68.48	0.06	1.29	1.08	2.34	4.98	14.27	2.45	0.30	1.1	96.35
11	5	845.0	GF	73.08	0.10	0.80	0.66	2.56	5.70	14.46	2.32	0.22	0.7	100.71
35	20	31.6	GF	74.69	0.07	0.87	0.40	2.03	6.36	13.51	1.17	0.03	0.7	99.83
112	56	42.4	GF	71.80	0.05	0.97	1.56	2.28	5.58	14.74	3.43	0.36	1.7	102.47
70	35	143.8	K	63.02	0.07	0.33	0.41	2.19	8.34	14.55	0.55	0.08	0.7	90.24
89	41	107.6	K	73.08	0.14	1.30	0.98	2.77	6.36	14.46	2.49	0.46	0.5	102.54
178	86	9.3	K	64.63	0.05	0.24	1.54	1.32	4.74	14.18	2.60	0.27	1.9	91.47
152	74	92.0	K	69.87	0.06	1.71	1.03	3.92	3.72	14.18	2.07	0.31	1.0	97.87
72	36	57.2	K	69.23	0.10	2.31	1.38	2.90	3.12	14.65	2.65	0.30	1.2	97.84
95	45	124.0	K	75.86	0.09	0.60	0.91	2.43	7.26	14.84	1.36	0.30	0.7	104.35
180	87	24.5	K	70.83	0.15	0.25	1.21	0.05	5.64	14.27	1.84	0.18	2.4	96.82
182	87	22.5	K	73.51	0.10	0.38	0.53	0.32	9.60	14.55	0.34	0.02	1.3	100.65
19	15	231.6	K	73.51	0.08	0.70	0.29	3.11	5.46	15.12	0.94	0.05	0.6	99.86
147	74	72.9	K	67.62	0.07	0.60	1.15	1.39	7.14	13.42	2.09	0.39	1.6	95.47
57	31	108.3	K	71.58	0.11	0.27	1.21	1.28	6.48	12.29	1.20	0.55	1.0	95.97
187	93	239.3	K	73.08	0.04	0.38	0.24	2.12	8.10	14.65	0.39	0.02	0.8	99.82
149	74	81.2	K	69.02	0.10	2.17	0.77	3.24	3.72	14.08	2.73	0.41	0.7	96.94
109	55	62.3	K	70.62	0.09	1.39	1.61	1.82	5.22	15.12	3.22	0.36	2.1	101.55
69	35	143.0	K	75.44	0.04	0.14	0.56	0.55	6.12	10.96	0.55	0.03	0.6	94.99
167	79	18.7	K	71.69	0.07	0.58	0.67	3.24	5.04	15.50	0.96	0.09	1.5	99.34
150	74	82.0	K	68.27	0.11	1.08	1.29	2.25	5.88	12.85	3.65	0.46	0.6	96.44
64	33	181.8	K	75.44	0.04	0.14	0.56	0.55	6.12	10.96	0.55	0.03	1.3	95.69
76	38	99.4	MM	54.89	0.26	2.76	8.13	2.52	1.62	15.40	8.87	0.81	4.4	99.66
42	23	56.3	MM	44.73	1.14	3.36	5.56	1.32	3.72	14.55	15.94	2.94	4.0	97.26
43	25	99.0	MM	41.62	0.28	0.13	6.39	0.09	1.25	18.43	21.09	1.85	7.1	98.23
31	19	51.0	MM	35.74	0.08	0.16	9.46	0.01	1.87	18.24	24.52	2.84	7.0	99.92
30	19	50.5	MM	46.97	0.08	0.77	7.14	4.52	2.88	18.24	13.23	1.69	3.0	98.52
28	19	48.0	MM	48.58	0.21	9.31	9.21	1.22	1.82	15.69	13.08	0.99	2.2	102.31
26	19	36.6	MM	48.26	0.93	6.30	11.29	0.07	2.21	14.27	9.51	1.32	7.0	101.16
5	4	919.5	MM	53.50	0.07	0.08	5.64	0.06	3.54	20.98	8.22	0.87	6.3	99.26
27	19	40.4	FM	72.76	0.07	0.85	0.81	3.58	6.18	15.88	1.16	0.14	0.7	102.13
38	21	28.8	FM	61.53	0.08	3.64	0.72	6.48	2.82	18.71	3.15	0.37	1.0	98.50
33	19	61.8	FM	66.66	0.44	2.73	1.23	5.81	2.03	17.39	3.79	0.43	0.8	101.31
10	5	836.8	FM	73.51	0.11	0.23	1.13	2.07	5.94	13.89	1.49	0.21	1.4	99.98
78	38	99.6	FM	75.01	0.06	0.84	0.34	3.11	6.78	13.70	0.84	0.12	0.7	101.50
44	25	102.4	FM	53.18	0.76	3.29	4.48	0.00	0.92	11.53	16.09	0.47	5.7	96.42
161	75	186.8	INT	66.45	0.12	1.26	0.56	3.04	7.02	16.35	0.90	0.20	0.6	96.50
162	76	206.3	INT	74.26	0.03	1.43	0.36	2.70	3.84	12.00	0.29	0.03	0.8	95.74
151	74	91.8	INT	44.94	0.18	5.39	7.14	0.63	5.40	14.27	12.73	1.50	4.6	96.78
39	22	90.0	MS	52.86	0.07	0.24	1.89	0.13	6.12	20.79	4.72	0.94	6.3	94.06
50	30	279.3	MS	71.26	0.03	0.06	1.71	0.48	7.50	13.14	0.89	0.15	1.9	97.12
51	30	286.3	PX	72.87	0.09	0.31	0.28	2.38	7.44	13.70	0.47	0.03	0.4	97.97

*Iron is total iron calculated as Fe_2O_3, WL - Wylie Lake Granitoid, FC - Fishing Creek Granitoid, GF - Grey Foliated Granitoid, K - Alkali Feldspar-Rich Granitoid, MM - Mafic Mylonite, FM - Felsic Mylonite, INT - Minor Intrusives, MS - High-Grade Metasediments, PX - Pyroxenite

Table 3. Trace element analyses for fresh basement rock types

Analysis Number	Hole Number	Depth (m)	Rock Type	Trace Elements (ppm)										
				Mn	Pb	Ba	V	Ni	Co	Sr	Zn	As	C	U
101	47	99.20	WL	300	30	1850	60	30	35	400	70	1	900	1
125	63	26.20	WL	570	20	245	90	25	40	100	70	4	2600	9
12	10	88.40	WL	610	40	1570	50	75	70	490	80	2	800	0
29	19	48.50	WL	63	20	900	20	100	60	150	30	4	900	0
153	74	97.50	FC	140	30	600	60	15	45	190	60	1	200	1
37	20	62.50	FC	235	30	305	80	90	50	190	110	4	100	14
121	59	34.60	FC	210	35	720	40	20	45	140	55	1	600	3
115	57	27.90	FC	500	35	525	80	25	45	275	105	1	1000	5
159	75	170.10	FC	370	50	1650	20	20	60	300	65	2	200	2
160	75	180.80	FC	640	20	555	150	10	50	370	130	1	100	2
163	76	216.00	FC	585	30	195	50	50	45	270	15	1	200	2
15	13	102.70	GF	39	45	1195	20	50	65	150	30	1	300	5
129	66	27.90	GF	91	45	785	20	10	45	130	10	1	200	3
20	18	79.10	GF	118	52	1580	20	50	50	135	35	2	400	3
140	67	29.40	GF	205	65	1100	60	20	55	180	55	1	700	3
141	67	26.90	GF	385	65	1090	60	20	55	185	60	1	900	3
139	67	25.50	GF	185	65	910	80	20	100	185	65	1	1100	2
11	5	845.00	GF	295	54	465	20	80	50	100	40	2	300	4
35	20	31.60	GF	380	60	825	20	35	60	175	10	1	600	14
112	56	42.40	GF	255	60	2210	40	40	45	275	60	1	1100	1
70	35	143.80	K	38	55	845	20	45	50	125	20	3	200	0
89	41	107.60	K	315	35	1840	20	45	35	185	70	4	300	1
178	86	9.30	K	104	35	810	20	20	50	25	25	2	600	7
152	74	92.00	K	230	15	1550	30	15	100	250	25	1	1400	1
72	36	57.20	K	310	35	1260	30	35	50	290	50	2	200	2
95	45	124.00	K	53	50	920	20	15	50	150	50	1	200	5
180	87	24.50	K	114	40	535	20	10	50	25	15	1	600	42
182	87	22.50	K	39	90	2575	20	20	75	175	10	2	1300	2
19	15	231.60	K	205	59	195	20	70	50	75	15	1	200	9
147	74	72.90	K	75	45	1675	25	25	55	200	30	1	1000	2
57	31	108.30	K	31	75	1230	20	30	65	170	20	2	100	5
187	93	239.30	K	29	65	1255	20	35	65	150	10	1	900	4
149	74	81.20	K	168	40	1565	20	15	55	250	35	1	600	2
109	55	62.30	K	197	50	1660	20	20	50	250	25	3	1500	7
69	35	143.00	K	96	40	1100	20	25	75	375	65	1	400	2
167	79	18.70	K	71	55	1290	20	20	40	225	20	1	1100	4
150	74	82.00	K	205	30	2640	40	15	85	250	35	2	800	2
64	33	181.80	K	96	45	200	20	20	60	50	25	2	200	2
76	38	99.40	MM	735	15	580	125	40	50	200	110	3	1600	3
42	23	56.30	MM	805	30	1760	120	35	60	340	150	1	300	0
43	25	99.00	MM	610	30	100	60	700	45	350	105	3	600	8
31	19	51.00	MM	2300	5	220	200	255	70	10	245	1	300	4
30	19	50.50	MM	1260	35	915	150	245	70	100	190	2	300	4
28	19	48.00	MM	2320	30	1085	275	170	60	245	165	1	500	0
26	19	36.60	MM	1060	45	2265	210	190	70	555	125	2	4700	5
5	4	919.50	MM	255	8	390	165	215	50	25	25	8	4000	4
27	19	40.40	FM	128	35	2720	20	35	50	190	20	1	100	1
38	21	28.80	FM	380	50	480	50	100	50	380	70	1	500	10
33	19	61.80	FM	280	15	1425	50	85	60	370	50	4	100	1
10	5	836.80	FM	69	51	490	20	130	125	80	15	2	200	5
78	38	99.60	FM	68	70	1045	20	50	100	180	20	1	1300	3
44	25	102.40	FM	6600	65	100	200	180	60	50	75	3	6100	5
161	75	186.80	INT	90	70	1715	20	10	60	380	20	1	300	1
162	76	206.30	INT	72	30	910	20	20	80	270	10	3	700	2
151	74	91.80	INT	1300	100	780	260	100	70	125	165	1	8200	1
39	22	90.00	MS	320	10	1010	320	45	35	50	35	3	4300	1
50	30	279.30	MS	17	30	670	20	65	35	60	35	5	100	5
51	30	286.30	PX	58	80	710	20	90	80	75	15	2	400	4

WL - Wylie Lake Granitoid, FC - Fishing Creek Granitoid, GF - Grey Foliated Granitoid, K - Alkali Feldspar-Rich Granitoid, MM - Mafic Mylonite, FM -Felsic Mylonite, INT - Minor Intrusives, MS - High-Grade Metasediments, PX - Pyroxenite

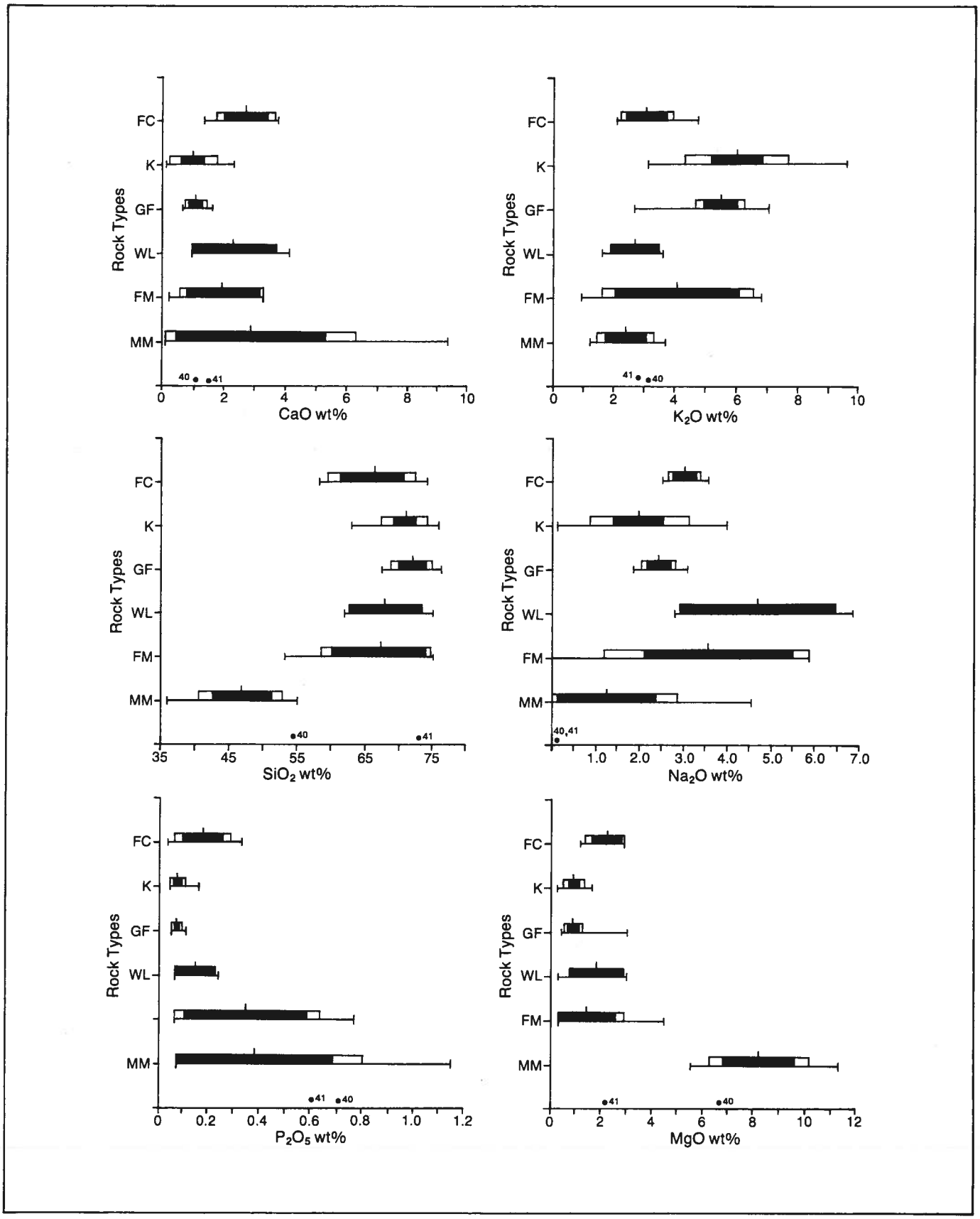

Figure 23. Dice diagrams of major element data for major rock types (continued over page).

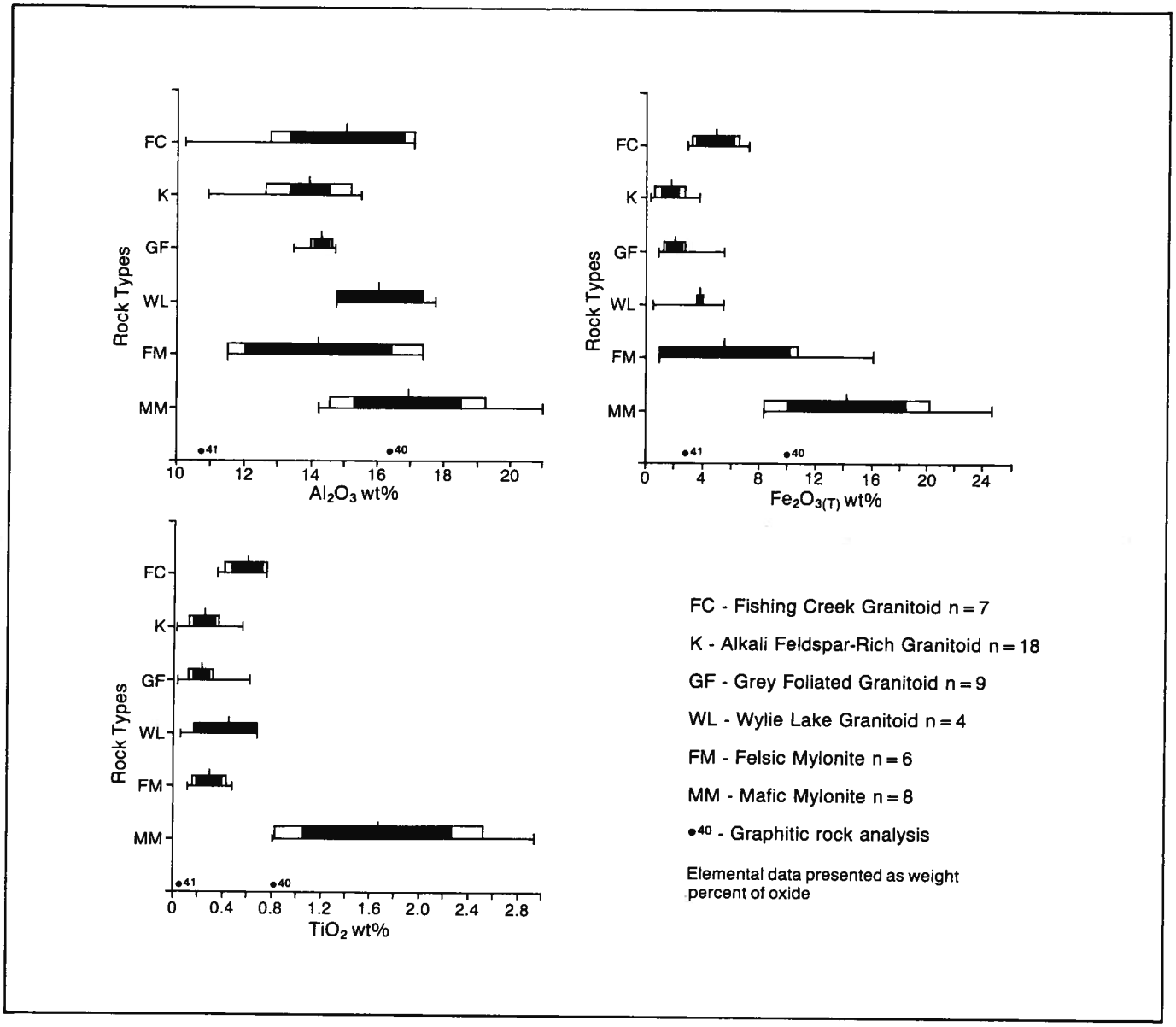

Figure 23. (continued)

The Dice diagrams qualitatively indicate some relationships between the rock types. If the black portions of the bars overlap, this is taken to indicate a close relationship between the rock types; if they are distinct, it indicates a lack of relationship between the rock types. The already perceived close relationship between the Fishing Creek and Wylie Lake Granitoids and the Grey Foliated and Alkali Feldspar-Rich Granitoids is supported by the common overlap of all four bars. However, the rock types plot as pairs with the Grey Foliated and Alkali Feldspar-Rich Granitoids plotting slightly higher than the other two for Si and Co, slightly lower for P, Ca, Mg, Al, Ti, Mn and Sr, and with no obvious paired relationship for Ba, V, Ni, Zn, As, C and U. The bars do not overlap between the pairs for Na, Fe, K and Pb. The low Na and high K for the Grey Foliated and Alkali Feldspar-Rich Granitoids can be explained by the obvious difference in feldspar content.

The Mafic Mylonites show no overlap with the granitoid rocks in the cases of Si, Mg, Fe, Ti, Mn and V, and are offset from the general granitoid trend for P, Ni and Zn. This is a consequence of the probable different origin for the bulk of the Mafic Mylonite rocks. The Felsic Mylonites commonly have a wide range, which overlaps all other rock types, indicating that they are derived from the parent rocks for both the granitoids and Mafic Mylonites.

Figure 25 shows data for the rock types plotted on a commonly used ternary diagram. The data for the granitoid rocks and Felsic Mylonites plot largely in the granite field with minor overlap into the adamellite field. The Mafic Mylonites plot over a much wider range, lying in the tonalite, granodiorite, trondhjemite and the unnamed field, as well as the granite and adamellite fields.

Figure 26 presents three different plots of the geochemical data. In all cases, the granitoids and

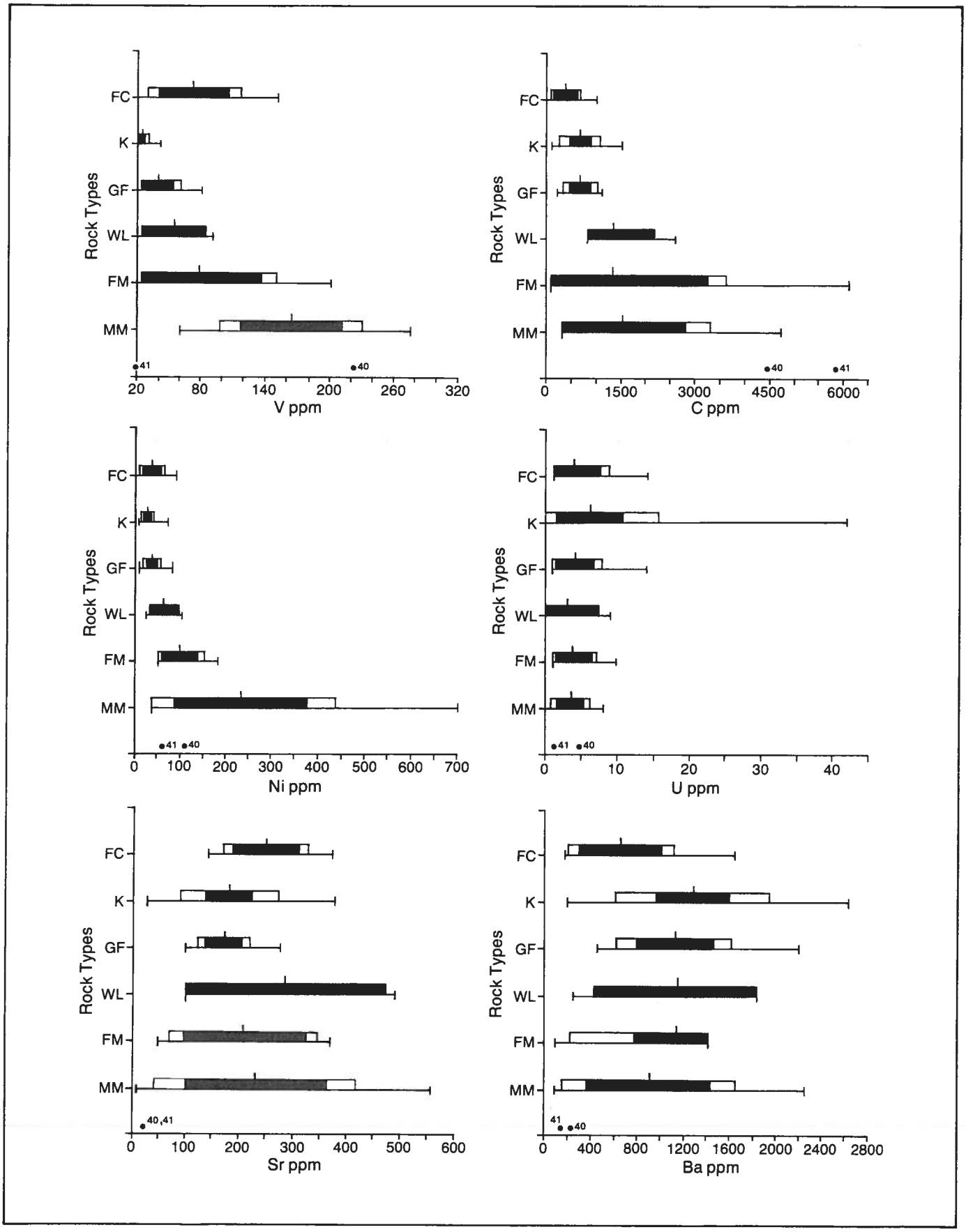

Figure 24. Dice diagrams of trace element data for major rock types (continued over page).

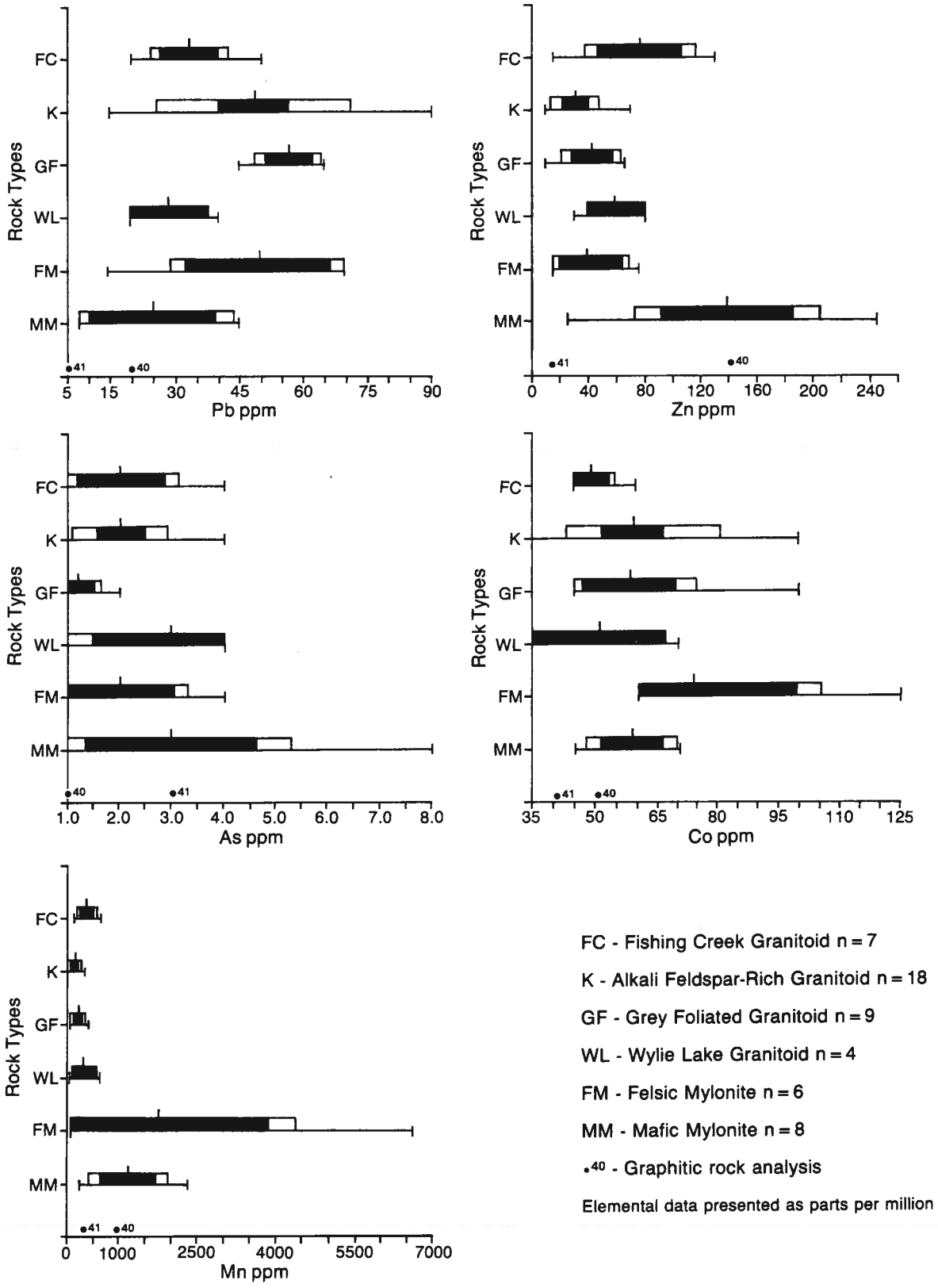

Figure 24. (continued)

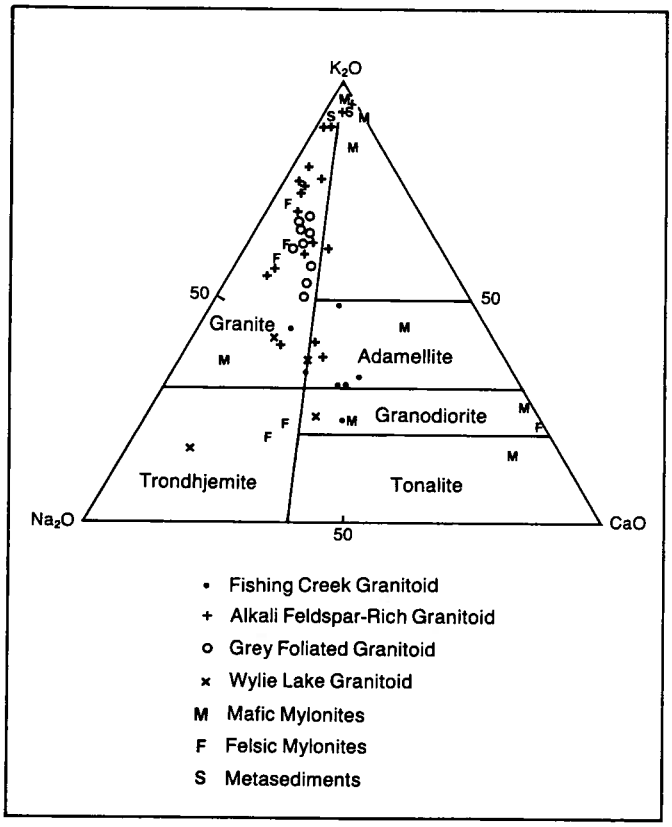

Figure 25. K_2O, Na_2O, CaO ternary plot of major rock type data.

most of the Felsic Mylonites plot as a distinct group or trend, with the Mafic Mylonites plotting separately. The Mafic Mylonites and the Felsic Mylonite that plots with them in figure 15b and c may have a common origin.

Two analyses of metasedimentary rocks are plotted on figures 23-25. In figure 25, both plot with a cluster of three Mafic Mylonite and four granitoid samples. The three graphs in figure 26 show the metasediments plotting with the loose granitoid clusters, except for one sample in 26c, which appears to plot with the Mafic Mylonites.

Appendix A presents the geochemical results from each major element plotted against a modification of the Larsen Index (MLI) [$(SiO_2 + K_2O - CaO - MgO)/3$ after Goff et al., 1986]. The four granitoid rock types plot as a distinct group, commonly with an obvious trend. There is a lot of mixing of the granitoid rock types, but in many cases the alkali feldspar enriched granitoids and the others plot at opposite ends of the trend. The Mafic Mylonites plot as a separate group in every case. In cases where trends are obvious in the granitoids and the Mafic Mylonites, they are commonly different (CaO, MgO, K_2O, Al_2O_3, $Fe_2O_3(T)$).

Of the six samples of Felsic Mylonite plotted, one plots with the Mafic Mylonites and the others plot with the granitoid clusters. This may be a reflection of origin. Similarly, with the plots of two samples that exhibit metasedimentary textures, there is a tendency for one of them to plot with the Mafic Mylonites, or at least off the granitoid trend, and the other with the granitoids.

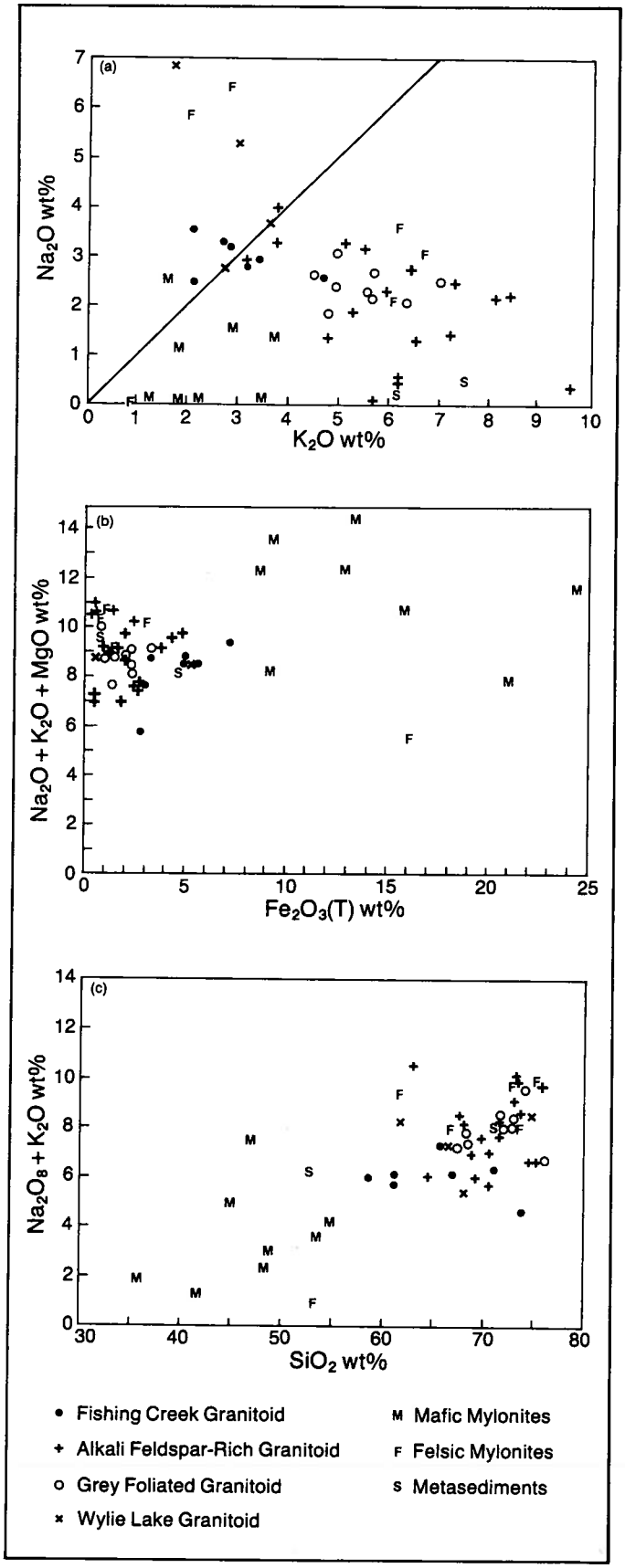

Figure 26. Plots of (a) Na_2O vs. K_2O, (b) $Na_2O + K_2O + MgO$ vs. $Fe_2O_3(T)$ and (c) $Na_2O + K_2O$ vs. SiO_2 for major rock type data.

Some oxides such as P_2O_5 do not plot on a well-defined trend, and there is some overlap between the granitoids and Mafic Mylonites. This may reflect the presence of minerals not related to the genesis of the rock. In the case of P_2O_5, authigenic crandallite group minerals may be present within the basement (Wilson, 1985c).

Tables 4 and 5 present the geochemical analyses for the twenty standard reference samples obtained by J.D. Godfrey during the course of his mapping of the Marguerite River area of basement outcrop (Godfrey, 1970). The location of these samples is given in figure 1 and in Wilson (1985b).

Appendix B shows the plots of the analyses for the major elements from the Marguerite River outcrop samples plotted against a modification of the Larsen Index. Care should be taken in directly comparing these results with Appendix A, since these are ob-

Table 4. Major element analyses for standard reference samples from the Marguerite River area

Analysis Number	Sample Number	Rock Type	Major Elements (weight percent oxide)												
			SiO_2	TiO_2	Al_2O_3	Fe_2O_3	MgO	CaO	Na_2O	K_2O	MnO	P_2O_5	LOI	H_2O	Total
2	50-3	WL	60.27	1.94	14.74	7.76	1.58	3.50	3.02	4.87	0.07	0.86	1.13	0.19	99.00
5	23-2	FC	71.97	0.35	14.37	2.04	0.46	0.66	2.96	6.84	0.01	0.09	0.47	0.07	100.29
6	23-4	FC	73.44	0.03	14.21	1.02	0.11	0.79	3.29	6.20	0.02	0.09	0.36	0.07	99.63
7	24-2A	FC	69.80	0.40	15.34	2.73	1.09	2.74	3.75	3.16	0.03	0.12	0.87	0.15	100.18
12	32-4	FC	61.27	0.68	20.11	4.11	2.98	5.02	3.38	1.86	0.01	0.21	0.61	0.08	100.42
16	46-8	FC	70.95	0.41	16.63	1.18	0.71	1.93	3.46	4.33	0.03	0.09	0.52	0.06	100.30
1	49-2	GF	73.60	0.10	14.66	1.13	0.36	0.60	4.55	4.45	0.03	0.11	0.48	0.13	100.20
9	37-2	K	73.09	0.14	13.76	1.56	0.56	0.41	3.17	6.22	0.02	0.09	0.83	0.12	99.97
11	45-1	K	75.69	0.05	13.69	0.59	0.13	0.87	3.04	5.65	0.03	0.08	0.35	0.08	100.25
15	42-3	K	73.72	0.03	14.93	0.21	0.07	0.28	5.51	4.58	0.01	0.09	0.28	0.12	99.83
19	52-8	K	73.24	0.12	14.16	1.19	0.24	0.50	2.65	7.05	0.02	0.10	0.28	0.08	99.63
8	31-2	MM	67.06	0.42	15.34	4.33	1.70	2.90	3.53	3.54	0.06	0.14	0.76	0.18	99.96
14	8-1	MM	65.66	0.45	15.73	4.29	1.25	2.54	3.88	4.96	0.03	0.25	0.54	0.14	99.72
18	13-2A	MM	61.44	1.68	18.41	3.46	1.36	3.07	3.12	5.34	0.07	0.70	1.01	0.21	99.86
3	50-6	FM	68.97	0.41	14.44	3.55	1.31	2.49	3.46	4.48	0.07	0.20	0.71	0.14	100.23
4	50-5B	FM	69.87	0.42	14.50	3.47	1.31	1.80	3.36	3.88	0.06	0.16	1.00	0.10	99.93
13	9-2	FM	75.15	0.05	15.65	0.26	0.08	0.88	4.86	5.36	0.03	0.09	0.27	0.18	99.86
17	41-1	FM	69.99	0.31	15.91	1.42	0.54	0.58	3.87	6.62	0.02	0.10	0.62	0.17	100.15
20	14-3	FM	72.20	0.20	14.08	1.82	0.61	1.18	4.11	5.40	0.02	0.06	0.36	0.15	100.19
10	52-7	PX	51.73	0.70	14.51	11.90	8.29	10.21	1.98	0.83	0.25	0.09	0.43	0.07	100.99

WL - Wylie Lake Granitoid, FC - Fishing Creek Granitoid, GF - Grey Foliated Granitoid, K - Alkali Feldspar-Rich Granitoid, MM - Mafic Mylonites, FM - Felsic Mylonite, PX - Pyroxenite

Table 5. Trace element analyses for standard reference samples from the Marguerite River area

Analysis Number	Sample Number	Rock Type	Trace Elements (ppm)						
			Ba	Nb	Zr	Y	Sr	Rb	Zn
2	50-3	WL	2029	50	1190	27	418	193	128
5	23-2	FC	644	18	232	14	134	241	53
6	23-4	FC	550	17	116	31	148	205	5
7	24-2A	FC	640	35	186	7	243	173	93
12	32-4	FC	274	30	195	42	259	147	93
16	46-8	FC	1178	25	290	21	305	162	54
1	49-2	GF	540	35	79	22	135	138	18
9	37-2	K	396	17	181	21	96	261	24
11	45-1	K	644	22	95	14	149	190	4
15	42-3	K	64	18	5	8	23	253	1
19	52-8	K	261	22	83	22	75	262	37
8	31-2	MM	600	32	147	20	325	207	49
14	8-1	MM	2359	24	285	27	636	127	26
18	13-2A	MM	2035	53	1312	29	366	206	180
3	50-6	FM	946	25	169	17	264	230	53
4	50-5B	FM	693	21	196	27	226	247	68
13	9-2	FM	109	25	22	11	48	170	1
17	41-1	FM	972	34	107	14	338	154	34
20	14-3	FM	1697	23	123	15	354	129	6
10	52-7	PX	161	7	38	19	151	36	105

WL - Wylie Lake Granitoid, FC - Fishing Creek Granitoid, GF - Grey Foliated Granitoid, K - Alkali Feldspar-Rich Granitoid, MM - Mafic Mylonite, FM - Felsic Mylonite, PX - Pyroxenite

tained by wet chemical analyses and not atomic absorption spectroscopy. However, the Marguerite River samples show broadly the same trends as do Athabasca Basin samples. The differences are that, with the exception of one sample of P_2O_5 and TiO_2, all the Mafic Mylonites from the outcrop samples plot with the granitoid group. One Fishing Creek Granitoid analysis plots away from the group for CaO and Al_2O_3, and the Wylie Lake Granitoid sample plots away from the granitoid group for P_2O_5 and TiO_2. Fe_2O_3 graphs are on different scales because, for the core samples, they show total iron calculated as Fe_2O_3, while the Marguerite River samples represent strictly Fe_2O_3.

Discussion

The fresh basement rocks present beneath the Athabasca Group in Alberta can be related petrographically, geophysically and geochemically to a variety of rocks present in nearby outcrop. The basement consists of four granitoid rock types and a variety of mafic and felsic rocks that have been more or less mylonitized.

The granitoid rocks consist of two granodioritic to quartz-dioritic rock types (Wylie Lake Granitoid and Fishing Creek Granitoid) and two granitic rock types (Grey Foliated Granitoid and Alkali Feldspar-Rich Granitoid). The Wylie Lake and Fishing Creek Granitoids are directly comparable to rock units mapped by Godfrey (1980a) north of Lake Athabasca. The Grey Foliated and Alkali Feldspar-Rich Granitoids may in part represent the leucocratic granite of Godfrey (1980a). These latter two granitoids are alkali feldspar-enriched variations of the former, either as a result of original differences in the parent rock or later potassium metasomatism. All the granitoids were probably derived from partial melting of the granite gneiss and metasediments (Goff et al., 1986).

The mylonitic rocks represent a number of parent rock types and are broadly divided into Mafic Mylonites and Felsic Mylonites. Geochemical data suggest that many of the Felsic Mylonites were derived from granitoid parent material, whereas the Mafic Mylonites were derived from a geochemically distinct parent. The high mafic content of some of the mylonites and the well-preserved sedimentary textures associated with some mylonitic zones suggest a metavolcanic and a metasedimentary parent, respectively, for much of this material. The mylonites probably represent remnant pendants of granite gneiss, metasediments and metavolcanics surrounded by the granitoid products of ultrametamorphism.

Drill core 10 was drilled on the edge of the Granite Gneiss belt where it curves around to the western end of the Athabasca Basin. The rock here is unmylonitized Hornblende Granite Gneiss.

The garnet-cordierite-sillimanite rocks that are present locally beneath the Athabasca Group are very similar to aluminous metasediments described by Langenberg and Nielsen (1982) from north of Lake Athabasca and to the Peter River Gneiss present at the Carswell structure (Pagel and Svab, 1985). Also present within the granitoids beneath the Athabasca Group are minor pyroxene-rich mafic rocks similar to rocks described by Langenberg and Nielsen (1982) and to parts of the Earl River Complex of the Carswell area (Pagel and Svab, 1985). These metasedimentary rocks are not known to be as common beneath the Athabasca Group as they are north of Lake Athabasca or in the Carswell structure. This may be partly a factor of the lack of data in many parts of the Athabasca Basin. Future exploration work may allow the delineation of more extensive bodies of aluminous and pyroxene metasediments in Alberta.

Geology of the sub-Athabasca Group saprolite

The Proterozoic saprolite present beneath the crystalline basement/Athabasca Group unconformity is closely associated spatially with several important uranium deposits in Saskatchewan (Blaise and Koning, 1985; Wallis, et al., 1983; Ayres, et al., 1983; Hoeve and Sibbald, 1976; Dahlkamp, 1978; and Harper, 1979, 1980). The saprolitic weathering occurred prior to the deposition of the Athabasca Group and prior to the major phase of uranium mineralization. However, recognition of the weathering profiles' petrographic and geochemical character will aid in recognizing anomalous alteration that may be related to economic mineralization.

The formation of chemical weathering zones in contact with the Precambrian atmosphere can be used to indicate the nature of that atmosphere (Gay and Grandstaff, 1980) and the weathering process that occurred (Schau and Henderson, 1983). The prime difficulty encountered is in separating original weathering effects from later diagenetic or hydrothermal effects (Tremblay, 1983) or even from metamorphic effects (Koryakin, 1971). This section presents petrographic descriptions and geochemical analyses of the sub-Athabasca Group saprolite.

Description of the saprolite

The weathering zone beneath the Athabasca Group occurs throughout the entire basin and affects all basement rock types. In Alberta, thicknesses range from 5.5 m to 47 m, with a mean of all cores (where the complete profile is present) of 15 m. The thickness is determined by the rock type (the more schistose the rock type, the thicker the profile) and by the amount of fracturing present, although original conditions such as local topography probably also have an effect. Host rock textures are commonly preserved throughout the paleoweathering profile, hence the use of the term saprolite. The saprolite is well preserved in outcrop at Fidler Point (Wilson, 1985a) where a core-stone of

relatively fresh basement rock is present close to the unconformity (figure 27). The saprolite lacks the silicification observed beneath the Thelon Basin (Ross and Chiarenzelli, 1985).

The saprolite exhibits a marked, laterally correlative color zonation with depth. An upper red hematitic zone is commonly present (figure 28), locally capped by a thin bleached zone (figure 29). At the base of the saprolite is a green chloritic zone (figure 30), and there is a mixed red-green zone between them (figure 31). This zonation bears a striking resemblance to the Hematite, Transitional and Chlorite zones from the Thelon Basin (Chiarenzelli, J.R. pers. comm., 1985) and to the saprolite developed on the meta-semipelite and meta-pelite of Macdonald (1980), although it lacks the prominent white zone of Macdonald's meta-arkose profile. Locally, any one of the zones may be poorly developed or absent, and the sequence may be complicated by the presence of later hydrothermal alteration overprinting the saprolite (figure 32). Mean thicknesses for the different zones are presented in table 6.

Figure 27. Core-stone of fresh basement in the red zone of the saprolite at Fidler Point. Diameter of pencil is approximately 7 mm.

The red zone is composed primarily of three minerals—quartz, kaolinite and hematite—all of which may retain original textures (figure 33). Quartz retains the shape of the original grains, although the grains are commonly fractured and locally are extensively corroded (figure 34); the fractures are filled with clay or healed with chert or quartz overgrowths (figure 35). The surface of the quartz grains are commonly embayed or etched. Kaolinite forms the ground mass of the red zone and may retain the shape of original feldspar grains or may exhibit vermicular textures. Locally, the kaolinite is illitized. The hematite is present as a scattered dust throughout the kaolinite or as "feathery" books that pseudomorph biotite (figure 36). Muscovite is associated with the illite, and there are trace amounts of zircon, apatite and crandallites. The red zone is the best defined zone of the saprolite. Its base is marked by a change from red to green coloration in the core and by the appearance of recognizable biotite or chlorite in thin section.

Figure 28. Red zone of the saprolite. Drill hole 5. Top of the core is to the right. Scale is in cm.

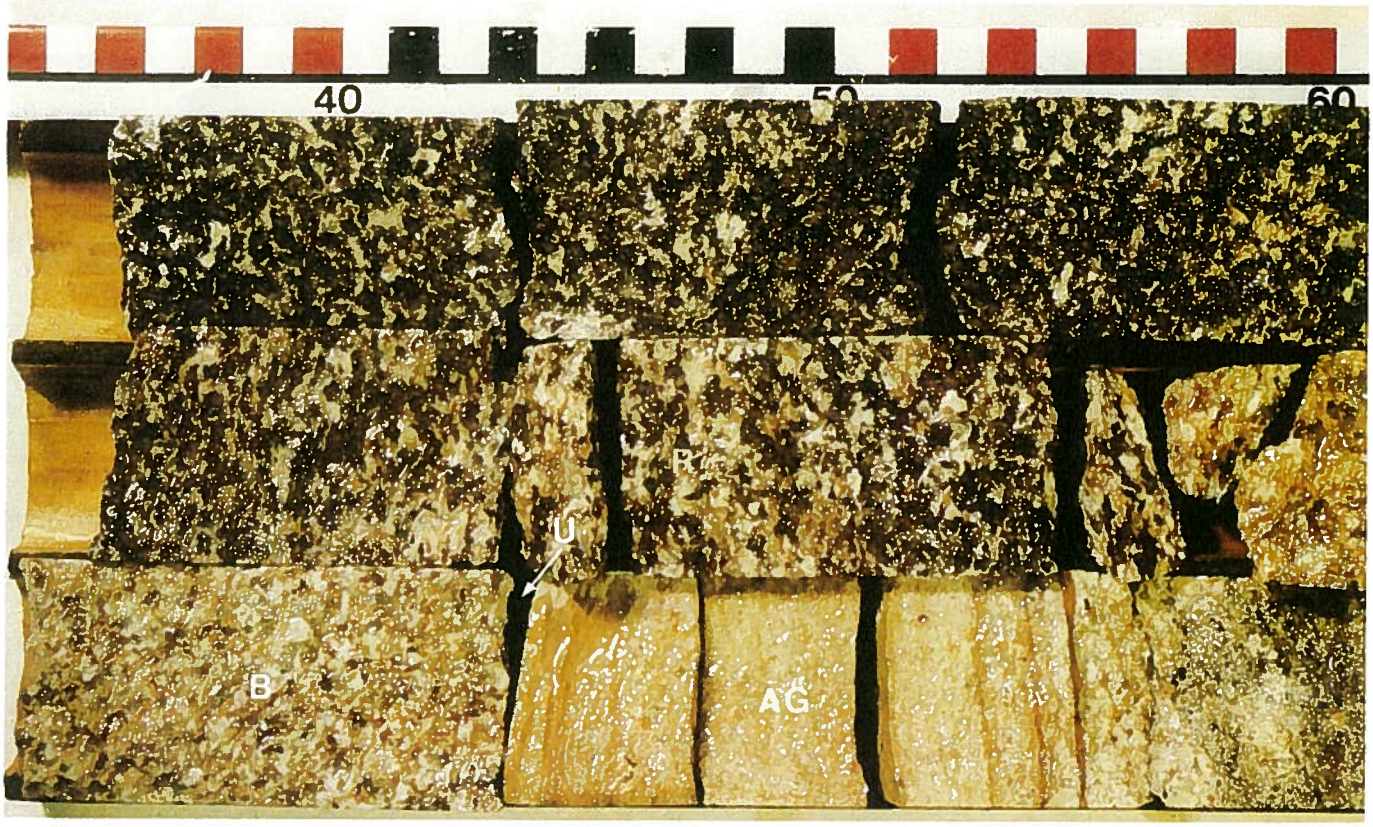

Figure 29. Unconformity (U) between Athabasca Group (AG) sediments and the saprolite. Note the thin bleached zone (B) overprinting the red zone alteration (R). Drill hole 75. Top of the core is to the right. Scale is in cm.

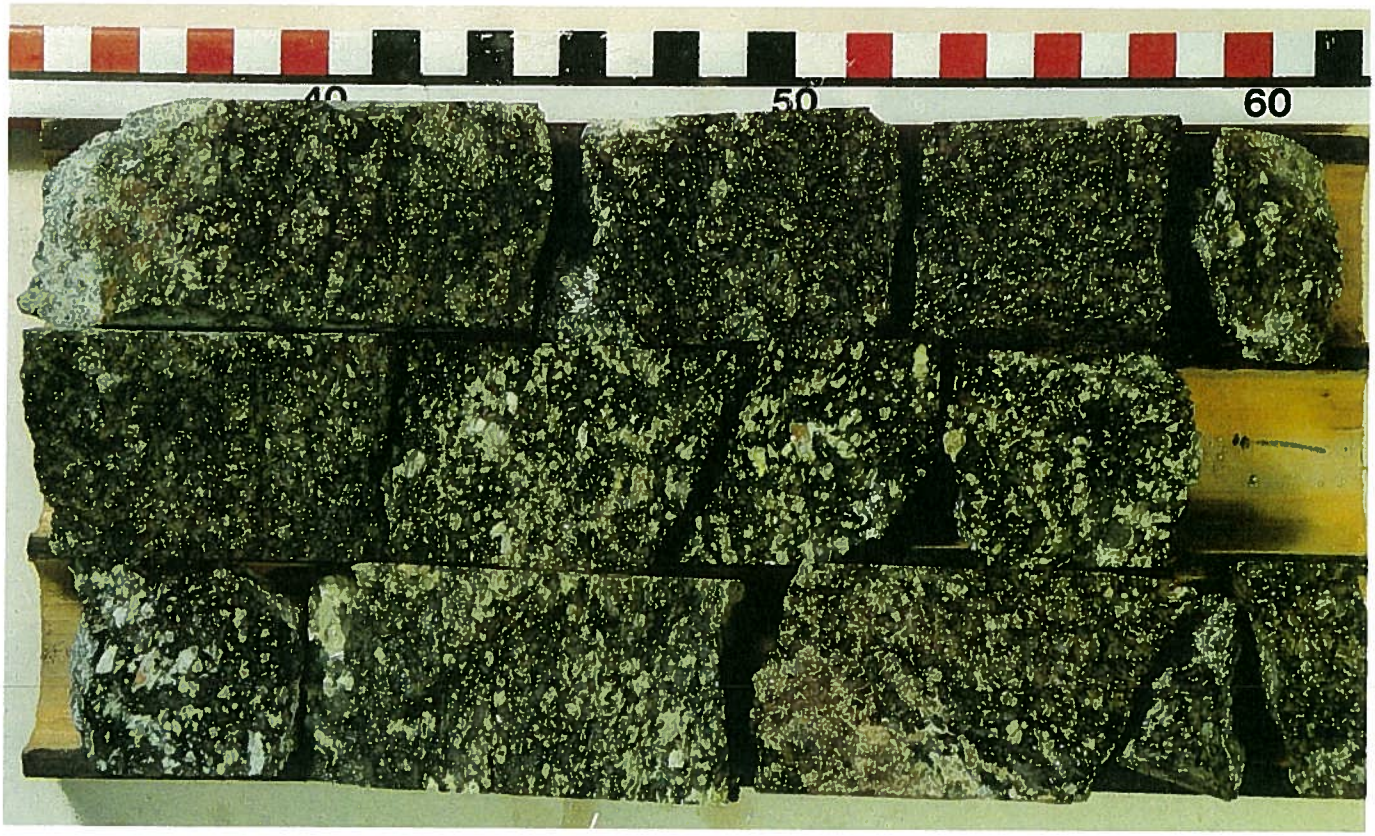

Figure 30. Green zone of the saprolite. Drill hole 75. Top of the core is to the right. Scale is in cm.

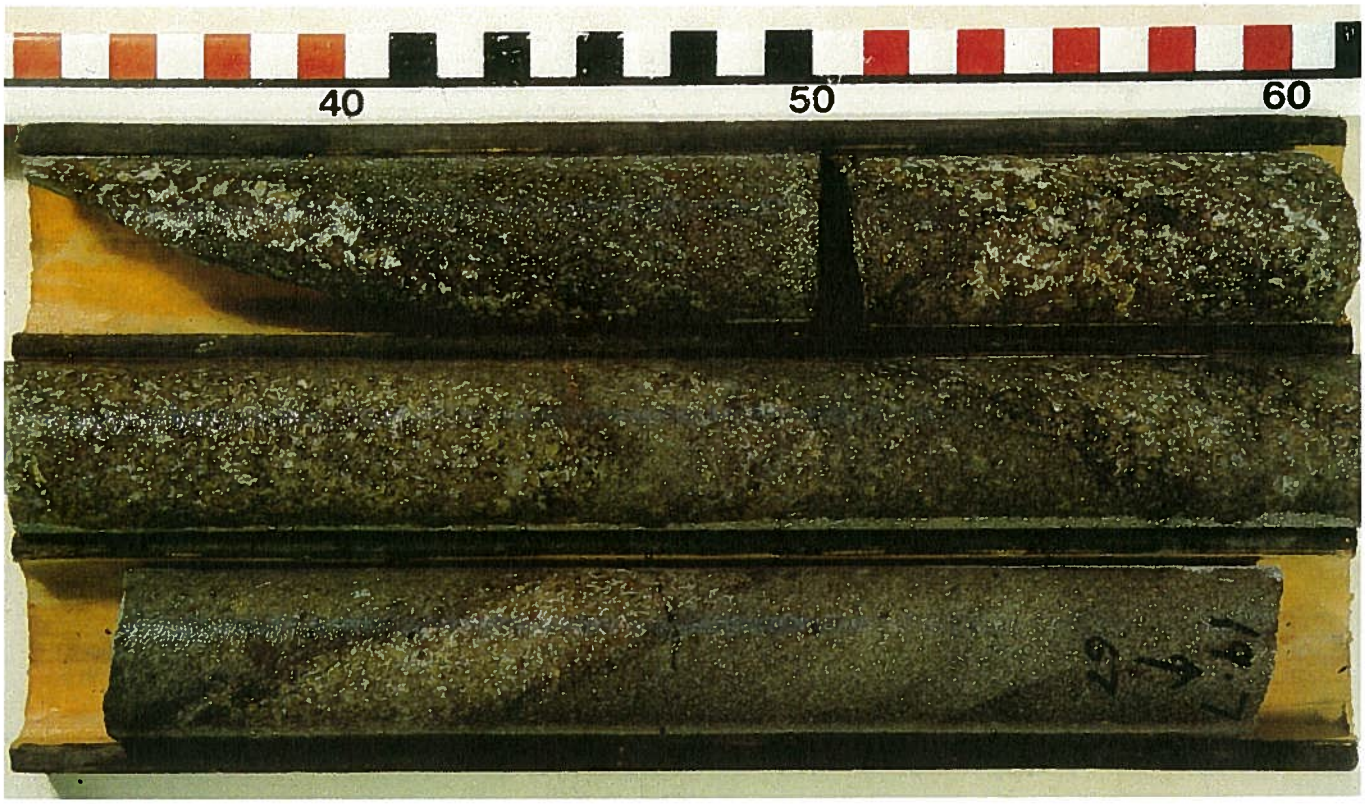

Figure 31. Red/green zone of the saprolite. Drill hole 67. Top of the core is to the right. Scale is in cm.

Figure 32. Hydrothermal alteration around fractures. Hydrothermal alteration (H) crosscuts the red zone of the saprolite. Drill hole 72. Top of the core is to the right. Scale is in cm.

Table 6. Characteristics of the sub-Athabasca Group saprolite

Zone	Range of Thickness (m)	Mean Thickness (m)	Number of cores exhibiting a complete section	Mineralogy	Textures
Bleached	0.1 - 0.9	0.6	15	Major: kaolinite, quartz Minor: illite, muscovite Trace: zircon, hematite, crandallites	As red zone with only ghost pseudomorphs of biotite Illite all replacement of kaolinite
Red	0.2 - 8.9 (26.8)*	4.3 (5.2)†	25 (26)	Major: kaolinite, quartz, hematite Minor: illite, muscovite Trace: zircon, apatite, crandallites	Feathery hematite pseudomorphs of biotite Quartz fractured and etched Illite replacement of kaolinite
Red-Green	0.8 - 20.4	6.5	25	Variable, as red or as green zone	Intermediate between red and green zones
Green	0.4 - 30.4	8.0	17	Major: kaolinite, illite, quartz Minor: biotite Trace: chlorite, feldspar, zircon, crandallites	Biotite fresh with hematite dust lines and traces of chlorite Remnant fresh feldspar Kaolinite and illite are replacements of feldspar

The saprolite is at least partially represented in 40 cores. *The value in parentheses is present where the core is fractured. †Mean in thick, fractured red zone is included.

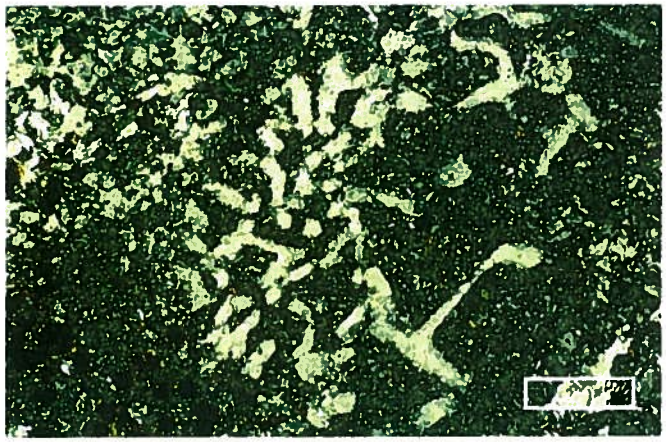

Figure 33. Remnant myrmekitic textures. Red zone of the saprolite. Plane polarized light. JAW84-033-147. Scale bar is 50 μm long.

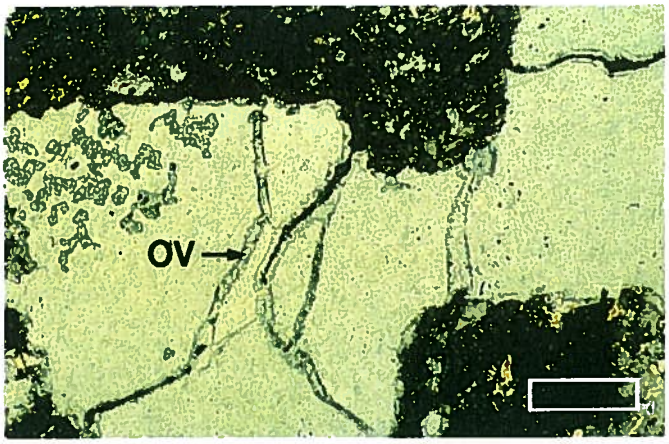

Figure 35. Fractured quartz partly healed by overgrowths (OV). Red zone of the saprolite. Plane polarized light. JAW84-015-220. Scale bar is 200 μm long.

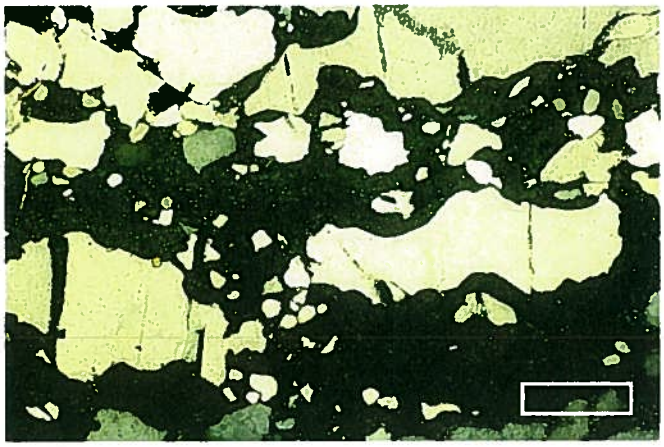

Figure 34. Strongly etched quartz grains. Red zone of the saprolite. Crossed nicols. JAW84-030-259.6. Scale bar is 0.5 mm long.

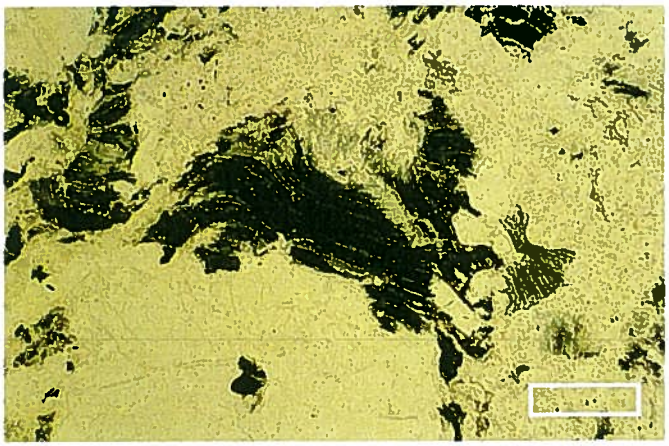

Figure 36. Hematite dust pseudomorphing biotite. Red zone of the saprolite. Plane polarized light. JAW84-058-34.6. Scale bar is 0.5 mm long.

The bleached zone locally overprints the red zone at the unconformity. Texturally, it is identical to the red zone, except that the bulk of the hematite has been removed, leaving only ghosts of the feathery hematite (figure 37).

The red-green zone exhibits characteristics of both the overlying red zone and underlying green zone. In core it is identified by the alternate irregular bands of red and green alteration. In thin section, illite and sericite locally form the matrix, although the illite is still primarily an alteration of kaolinite. Quartz is less fractured than in the red zone, although the edges are still scalloped. Hematite is present in variable amounts, pseudomorphing biotite in the red sections of core, whereas biotite and chlorite predominate in the green sections (figure 38). Quartz lenses occur locally within the chloritized biotite. Trace amounts of zircon, apatite, microcrystalline quartz and crandallites are present. Locally, the shape of the original feldspar grains is retained by kaolinite or illite. The base of this zone is gradational, the hematite gradually decreasing as the fresh biotite and chlorite increase.

The green zone is the least altered of the zones. Quartz is less fractured or etched than the red zone. Biotite is commonly fresh with only minor alteration to chlorite. Illite and sericite are more common than in the above zones and commonly pseudomorph feldspar grains that may have a fresh core. Kaolinite also replaces plagioclase feldspar, and alkali feldspars remain fresh (figure 39). Locally, kaolinite is illitized. The base of this zone grades downward into fresh basement. The green zone exhibits greater textural variation than the others because, in this zone, the rock retains more of the fresh rock textures than do the more altered zones.

Geochemistry of the saprolite

Seventy-nine samples of saprolite alteration from 28 drill cores were analyzed for major and trace elements (tables 7 and 8). These data are presented as Dice diagrams in figures 40 and 41. These figures support the idea that the weathering process that produced the saprolite was a leaching process. For most major and trace elements (Si, Mg, Na, K, Fe, Ti, Mn, Pb, Ba, Ni) the range of values is reduced from fresh rock to saprolite. In addition, the mean values decrease upward through the saprolite profile gradually (Mg, K, V, Zn) or sharply (Ca, Na, Mn, Ba). The remainder stay constant, vary randomly or increase slightly through the profile. For most elements, there is an overlap of two standard errors of the mean between adjacent zones, although the red or bleached zones may not overlap the fresh rock.

Reiche (1943) presents problems with this type of data presentation for weathering profiles. Oxides and elements in a weathering profile are either leached or residual, depending on the type of chemical weathering and their solubility. If the raw data are simply plotted against depth, the residual elements will show an apparent gain, and leached elements an apparent loss. This loss or gain is not necessarily related to an absolute gain or loss to the system. In fact, residual elements may show a gain when they have, in fact, been slightly leached.

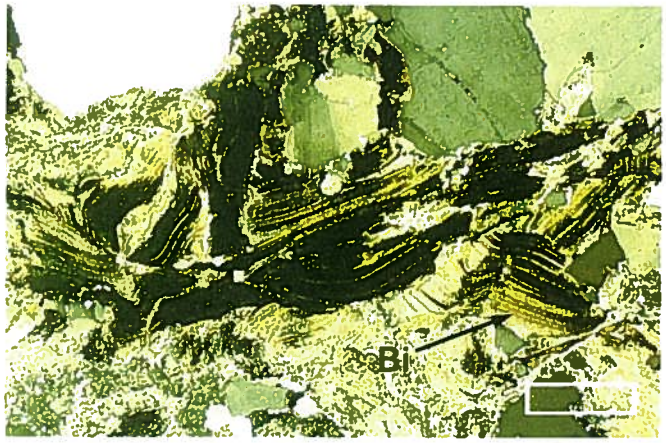

Figure 38. Fresh biotite (Bi) with hematite dust outlining plate separations. Red/green zone of the saprolite. Crossed nicols. JAW84-055-45.5. Scale bar is 0.5 mm long.

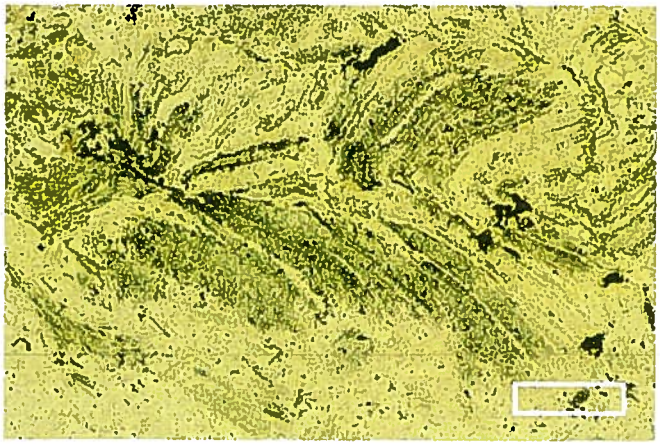

Figure 37. Remnant hematite dust retaining outline of original biotite grain. Bleached zone. Plane polarized light. JAW84-075-154.6. Scale bar is 200 μm long.

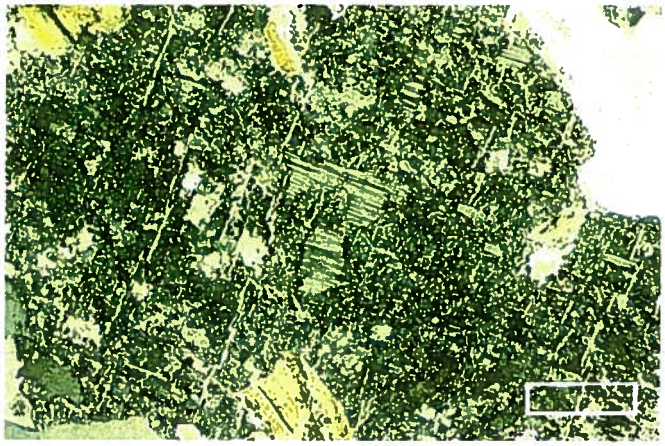

Figure 39. Fresh alkali feldspar inclusion within a plagioclase grain partly altered to kaolinite. Green zone of the saprolite. Crossed nicols. JAW84-067-23.6. Scale bar is 200 μm long.

Table 7. Major element analyses for saprolite alteration (continued over page)

Analysis Number	Hole Number	Depth (m)	Alteration Type	Major elements (weight percent oxide) SiO_2	P_2O_5	CaO	MgO	Na_2O	K_2O	Al_2O_3	$Fe_2O_{3(T)}$*	TiO_2	LOI	Total Percent
1	4	888.6	B	83.46	0.06	0.09	0.34	0.06	2.46	8.51	0.62	0.32	1.7	97.62
45	27	268.0	B	80.79	0.13	0.19	0.33	0.11	2.88	16.54	0.58	0.14	3.8	105.49
118	59	16.4	B	77.68	0.04	0.12	0.26	0.09	1.43	16.73	0.86	0.08	5.1	102.39
60	33	133.4	B	74.58	0.08	0.02	0.06	0.00	0.37	14.08	0.13	0.25	5.1	94.67
113	57	20.9	B	77.79	0.07	0.07	0.13	0.04	0.44	17.67	0.46	0.06	5.9	102.63
154	75	154.6	B	69.76	0.11	0.05	0.19	0.00	0.86	18.81	0.36	0.68	6.4	97.22
53	31	81.0	B	70.73	0.06	0.02	0.06	0.00	0.41	18.33	0.41	0.49	6.7	97.21
96	46	113.3	B	85.28	0.06	0.04	0.11	0.03	0.89	11.34	0.23	0.33	3.5	101.81
116	58	33.8	B	71.37	0.17	0.05	0.32	0.03	1.12	20.32	0.58	0.21	6.6	100.77
142	72	192.8	B	74.79	0.04	0.04	0.07	0.01	0.22	16.07	0.21	0.45	6.0	97.90
4	4	896.8	G	61.42	0.07	0.05	3.49	0.08	5.34	20.70	2.76	0.73	4.4	99.04
138	67	23.6	G	69.02	0.06	0.11	2.11	0.19	4.80	13.99	2.59	0.29	3.1	96.26
80	39	182.4	G	71.37	0.05	0.03	0.10	0.05	0.82	20.98	0.45	0.04	7.1	100.99
48	30	268.9	G	67.73	0.18	0.38	3.09	0.02	4.26	14.74	3.15	0.58	4.4	98.53
82	39	188.7	G	78.65	0.18	0.04	0.35	0.06	1.61	15.31	1.46	0.19	4.4	102.25
88	41	100.0	G	74.69	0.06	0.07	3.57	0.10	2.46	15.12	2.02	0.63	4.2	102.92
144	72	195.2	G	70.73	0.21	0.26	0.60	0.02	1.43	14.93	2.10	0.39	4.9	95.57
145	72	197.4	G	72.12	0.15	0.26	1.21	0.07	3.66	14.08	2.22	0.41	2.7	96.88
8	5	831.0	G	73.51	0.12	0.19	3.22	0.02	2.70	14.84	1.29	0.28	4.2	100.37
157	75	167.5	G	63.56	0.19	0.39	4.81	0.02	3.00	15.21	4.22	0.50	5.1	97.00
9	5	832.4	G	72.97	0.11	0.10	2.21	0.15	6.12	13.99	1.49	0.28	2.6	100.02
120	59	33.9	G	70.19	0.07	0.17	3.30	0.11	3.12	14.55	2.59	0.38	4.2	98.68
91	45	110.7	R	78.22	0.03	0.02	0.03	0.04	0.18	18.14	0.22	0.03	6.3	103.21
65	35	131.9	R	68.48	0.04	0.02	0.13	0.00	0.46	17.29	3.00	0.32	6.4	96.14
122	63	10.1	R	76.61	0.05	0.04	0.31	0.03	2.18	14.93	2.86	0.31	3.8	101.12
126	63	23.8	R	68.27	0.07	0.83	2.71	0.05	3.60	16.35	3.86	0.71	5.0	101.45
16	15	219.8	R	76.18	0.05	0.01	0.14	0.01	1.00	16.07	2.00	0.38	5.1	100.94
131	67	17.6	R	72.12	0.05	0.04	0.21	0.01	0.83	18.33	3.65	0.70	7.5	103.44
47	30	260.0	R	71.05	0.09	0.03	0.08	0.00	0.16	17.39	2.93	0.41	6.3	98.44
46	27	269.4	R	65.16	0.18	0.25	3.74	0.00	3.60	15.59	4.65	0.49	4.0	97.66
130	67	16.7	R	66.88	0.06	0.03	0.33	0.03	1.39	23.34	0.67	0.04	6.0	98.77
6	5	824.0	R	72.55	0.05	0.00	0.19	0.00	1.14	16.25	1.99	0.37	5.3	97.84
177	84	33.2	R	68.80	0.08	0.04	0.33	0.00	2.29	18.52	1.33	0.16	5.3	96.85
143	72	193.5	R	70.41	0.13	0.05	0.07	0.01	0.28	16.44	2.86	0.37	6.1	96.72
104	48	142.7	R	46.01	0.11	0.05	0.08	0.03	0.41	36.57	3.43	0.38	13.0	100.07
59	32	99.0	R	65.06	0.08	0.03	0.09	0.00	0.88	19.56	3.79	0.54	6.7	96.73
106	55	45.2	R	73.40	0.18	0.24	0.58	0.06	1.40	17.77	1.57	0.45	5.7	101.35
90	45	110.5	R	78.00	0.07	0.03	0.10	0.06	0.57	16.82	1.47	0.25	5.7	103.07
61	33	134.0	R	75.22	0.13	0.03	0.06	0.00	0.22	14.65	0.51	0.27	5.4	96.49
119	59	16.6	R	59.39	6.98	10.64	0.13	0.02	0.89	15.21	2.86	0.07	4.7	100.89
132	67	18.0	R	76.18	0.14	0.18	0.40	0.00	0.82	16.54	2.62	0.67	4.3	102.85
2	4	893.0	R	53.82	0.09	0.06	3.74	0.09	5.88	25.52	2.30	0.97	5.7	98.17
170	80	10.0	R	67.20	0.05	0.05	0.41	0.01	2.82	15.78	4.79	0.45	4.0	95.56
98	46	115.4	R	75.86	0.06	0.03	0.16	0.02	1.25	18.14	1.63	0.26	5.6	103.01
171	80	11.7	R	71.05	0.25	0.06	0.24	0.00	1.94	15.97	2.12	0.15	4.5	96.28
155	75	156.4	R	56.82	0.61	0.99	1.58	0.02	2.88	19.47	8.08	0.87	5.6	96.92
175	83	16.3	R	71.90	0.11	0.04	0.14	0.00	0.66	16.54	1.13	0.17	5.7	96.39
99	47	88.0	R	62.38	0.34	0.55	6.56	0.02	1.52	18.81	2.22	1.00	6.7	100.10
54	31	81.4	R	70.41	0.06	0.02	0.05	0.00	0.29	17.29	2.75	0.28	6.3	97.45
85	41	88.3	R	68.16	0.06	0.02	0.11	0.04	0.92	22.11	1.12	0.44	7.3	100.28
114	57	21.4	R	70.94	0.39	0.49	0.26	0.03	0.46	17.86	4.79	0.68	6.2	102.10
97	46	113.4	R	67.52	0.25	0.22	0.29	0.04	0.65	15.50	10.15	0.64	7.6	102.86
172	81	19.7	R	69.66	0.13	0.03	0.29	0.00	2.09	16.44	2.56	0.27	4.7	96.17
176	84	32.6	R	66.77	0.11	0.04	0.20	0.00	1.39	18.99	2.10	0.81	6.2	96.61
117	58	34.8	R	67.84	0.64	0.88	0.32	0.02	0.80	18.71	4.29	0.85	6.2	100.55
86	41	92.4	R	73.08	0.05	0.02	0.06	0.04	0.50	16.35	1.30	0.31	5.7	97.41
103	48	136.6	R	64.52	0.10	0.04	0.05	0.02	0.01	23.53	3.29	0.47	8.6	100.63
56	31	94.5	RG	71.58	0.12	0.21	1.01	0.09	3.18	15.03	2.83	0.30	3.4	97.75
135	67	21.7	RG	75.01	0.04	0.08	2.08	0.02	3.30	15.88	1.36	0.33	3.6	101.70
156	75	161.6	RG	69.98	0.10	0.17	1.00	0.01	4.14	15.12	1.30	0.59	2.8	95.21
134	67	21.0	RG	72.65	0.07	0.09	2.03	0.02	3.54	15.69	3.36	0.37	3.4	101.22
49	30	265.3	RG	68.16	0.17	0.22	0.57	0.00	4.98	18.05	1.53	0.02	3.2	96.90

Table 7. (continued)

Analysis Number	Hole Number	Depth (m)	Alteration Type	Major elements (weight percent oxide) SiO_2	P_2O_5	CaO	MgO	Na_2O	K_2O	Al_2O_3	$Fe_2O_{3(T)}$*	TiO_2	LOI	Total Percent
3	4	894.0	RG	74.47	0.08	0.15	2.69	0.12	2.46	12.19	2.47	0.47	3.4	98.50
133	67	19.7	RG	69.12	0.17	0.25	2.04	0.04	2.76	18.81	2.43	0.78	5.2	101.60
94	45	118.9	RG	78.11	0.06	0.12	2.57	0.04	2.46	13.89	1.74	0.37	3.9	103.26
174	81	27.0	RG	72.65	0.10	0.04	0.41	0.00	3.66	14.93	2.73	0.13	2.6	97.25
137	67	23.1	RG	74.04	0.07	0.17	3.27	0.04	2.46	15.97	1.96	0.35	4.5	102.83
158	75	169.4	RG	60.88	0.21	0.35	5.31	0.01	2.36	15.59	5.79	0.57	5.1	96.17
7	5	830.0	RG	69.98	0.09	0.11	3.57	0.01	2.46	15.50	1.76	0.26	4.4	98.14
105	48	147.2	RG	76.83	0.05	0.04	0.13	0.03	2.06	15.50	3.29	0.23	4.0	102.16
136	67	22.0	RG	67.30	0.25	0.41	1.51	0.04	5.58	20.88	1.54	0.04	3.8	101.35
173	81	20.3	RG	66.66	0.08	0.03	0.30	0.00	2.22	17.20	2.59	0.30	4.9	94.28
87	41	97.7	RG	71.69	0.19	0.12	2.16	0.05	3.72	17.58	3.22	0.55	3.9	103.18
79	39	173.1	RG	60.99	0.03	0.04	0.15	0.09	1.36	27.22	2.67	0.04	8.9	101.49
17	15	222.0	RG	78.86	0.04	0.00	0.07	0.00	0.67	16.16	0.56	0.03	5.3	101.69
110	56	40.4	RG	71.58	0.05	0.10	3.57	0.04	2.28	15.78	5.72	0.07	4.4	103.59
92	45	116.5	RG	75.86	0.09	0.07	1.00	0.06	4.38	16.35	1.66	0.50	2.9	102.87
68	35	139.4	RG	70.94	0.09	0.11	1.46	0.00	1.98	15.50	2.55	0.33	4.7	97.66
107	55	45.5	RG	66.23	0.07	0.04	1.29	0.05	2.06	18.14	7.15	0.85	5.5	101.38

*Iron is total iron calculated as Fe_2O_3, B - Bleached Zone, R - Red Zone, RG - Red-Green Zone, G - Green Zone

The most easily applied technique of overcoming this problem is to portray gains and losses relative to an element that is assumed to be immobile. The element most commonly assumed to be immobile is aluminum, because of its low solubility in surface environments. Figure 42 shows the mean gain and loss of each element for each alteration zone, assuming aluminum constant. Figures 43 to 45 display the same data for three cores representing three of the major rock types present in the study area (Fishing Creek, Alkali Feldspar-Rich and Grey Foliated Granitoids).

The results obtained with aluminum constant may be invalid if the volume of the rock changes during weathering. Since weathering is predominantly a leaching process, a volume reduction through a profile is likely. Volume relationships can be estimated by using the procedure outlined by Gresens (1967). MacDonald (1980) applied both the aluminum constant and the Gresens procedures to sub-Athabasca Group weathered samples from Saskatchewan and found a close agreement between the results obtained from the two methods. His conclusion was that the Gresens procedure was unnecessary in this case.

When the values are recalculated as gains and losses assuming aluminum constant (figure 42), they commonly exhibit the same trends as with the raw data. Assuming aluminum constant commonly exaggerates the trend present in the Dice diagrams. However, in the case of Si, the trend changes from a slight increase in the Dice diagrams to constant or to a slight loss (figure 18). Ni and Co change from constant trends to a slight decrease.

Plots of individual cored profiles (figures 43, 44, 45) exhibit similar trends as the mean values (figure 42), except for the lack of smoothing. The only differences are that, in hole 75 (figure 43), C and Ni are enriched and V is strongly depleted throughout the profile, and the Ba and Pb vary within the fresh rock. In core 67 (figure 45), the upper weathered zones are enriched in Ti and the lower zones in Ni, and in all three cases the lower zones are enriched with Mg, relative to the mean. Sr varies from hole to hole and As varies from sample to sample. U is enriched in the green zone of hole 67.

The geochemical trends fit well with the observed petrographic changes through the profile. Na_2O and CaO are strongly depleted throughout the profile as a consequence of leaching of elements following the early degradation of feldspar. MgO remains constant or increases in the green and red-greed zones as a result of the widespread formation of chlorite from biotite. In the red zone, MgO is depleted as the chlorite disappears. K_2O gradually decreases through the profile due to the slow degradation of alkali-feldspar. Local variations are due to the presence of illite in the lower zones and to illitization of kaolinite in the upper zones. Total iron is constant or only slightly depleted, except in the bleached zone where it is severely depleted. The oxidation state of the iron changes throughout the profile, but overall not much iron is lost or gained. The variable P_2O_5 profile is probably due to the local presence of apatite or the crandallite group minerals. TiO_2 is variable, but since its presence is probably due to trace amounts of heavy minerals (rutile, anatase), its distribution is not uniform. SiO_2 is constant or slightly depleted, indicating stability, except for minor surficial etching in the upper saprolite zones. Overall these profiles are consistent with a feldspar, biotite, quartz rock, which alters to a rock rich in illite and chlorite and then to one dominated by kaolinite and quartz.

Figure 46 presents the gain and loss data for hole 4, which consists partly of Mafic Mylonite. The alteration zone on top of the basement in hole 4 is anomalous in several respects. Si, P, Ca, Na, K, Pb, Ba, Ni, Co, Sr, Zn and U are enriched in the saprolite, whereas Mg, Fe, Mn and C are depleted. Ti is stable and As is variable. This profile varies considerably from the

Table 8. Trace element analyses for saprolite alteration (continued over page)

Analysis Number	Hole Number	Depth (m)	Alteration Type	Trace elements (ppm) Mn	Pb	Ba	V	Ni	Co	Sr	Zn	As	C	U
1	4	888.60	B	15	9	200	25	200	150	125	20	7	100	2
45	27	268.00	B	27	20	200	20	50	45	10	20	5	400	1
118	59	16.40	B	38	10	150	20	35	35	90	25	4	1000	1
60	33	133.40	B	3	20	75	20	15	30	410	10	3	200	3
113	57	20.90	B	8	10	50	20	20	30	100	10	4	100	1
154	75	154.60	B	10	25	50	20	30	30	355	10	6	200	3
53	31	81.00	B	6	50	75	20	50	25	330	10	11	100	3
96	46	113.30	B	6	30	50	20	55	50	250	15	13	100	2
116	58	33.80	B	11	45	80	30	25	30	630	10	5	100	1
142	72	192.80	B	8	10	75	20	10	20	110	10	2	100	2
91	45	110.70	R	10	25	60	20	25	60	75	10	4	100	1
65	35	131.90	R	132	20	50	20	25	30	75	25	3	100	1
122	63	10.10	R	53	20	380	40	25	30	125	20	3	100	3
126	63	23.80	R	44	15	250	90	40	25	90	10	3	2700	6
16	15	219.80	R	63	53	75	20	40	40	115	10	4	100	4
131	67	17.60	R	60	20	160	20	20	30	100	10	3	100	1
47	30	260.00	R	56	30	100	20	75	40	320	10	5	100	3
46	27	269.40	R	270	10	795	60	210	60	60	230	3	500	3
130	67	16.70	R	12	25	160	20	20	15	160	10	2	100	3
6	5	824.00	R	17	56	65	20	205	170	125	15	5	200	3
177	84	33.20	R	17	30	200	20	20	35	490	10	4	300	2
143	72	193.50	R	18	25	75	20	15	30	445	10	7	100	2
104	48	142.70	R	14	20	60	20	40	25	330	10	12	200	6
59	32	99.00	R	28	25	75	20	45	30	280	10	10	100	2
106	55	45.20	R	58	25	60	40	40	35	200	55	2	100	7
90	45	110.50	R	13	45	75	20	55	40	165	20	5	100	3
61	33	134.00	R	3	20	70	20	25	35	650	10	4	100	1
119	59	16.60	R	19	305	75	30	15	60	90	10	3	100	37
132	67	18.00	R	56	20	155	20	15	25	100	10	1	100	3
2	4	893.00	R	25	40	600	200	360	280	225	30	3	200	5
170	80	10.00	R	51	30	770	20	15	20	160	10	3	900	3
98	46	115.40	R	21	40	75	20	45	40	125	15	9	100	5
171	80	11.70	R	19	40	365	20	20	25	1265	15	3	100	1
155	75	156.40	R	285	30	250	60	45	35	50	120	1	100	2
175	83	16.30	R	13	25	50	20	15	25	490	10	3	100	1
99	47	88.00	R	24	10	70	70	195	25	70	65	2	200	3
54	31	81.40	R	38	25	75	20	40	30	200	15	11	100	1
85	41	88.30	R	17	20	50	20	35	20	110	15	11	100	2
114	57	21.40	R	116	55	80	40	25	30	300	10	5	100	2
97	46	113.40	R	79	15	75	25	15	25	125	15	15	7200	4
172	81	19.70	R	33	50	515	20	15	50	605	15	6	100	2
176	84	32.60	R	32	15	90	20	10	40	665	10	8	100	4
117	58	34.80	R	65	35	160	30	80	65	200	10	13	1000	4
86	41	92.40	R	8	25	50	20	45	20	70	10	3	100	1
103	48	136.60	R	27	40	60	20	15	20	300	10	30	100	4
56	31	94.50	RG	5	20	50	20	35	35	115	60	2	100	1
135	67	21.70	RG	18	30	100	50	30	35	40	15	2	100	3
156	75	161.60	RG	29	15	50	20	15	25	25	15	1	100	2
134	67	21.00	RG	53	15	240	50	30	30	125	45	4	100	3
49	30	265.30	RG	16	25	50	20	65	25	140	10	3	200	1
3	4	894.00	RG	96	20	150	50	255	110	75	180	1	500	9
133	67	19.70	RG	88	30	365	40	65	45	140	10	2	200	6
94	45	118.90	RG	36	40	50	20	75	40	75	20	2	100	3
174	81	27.00	RG	18	25	565	20	20	30	415	10	4	200	2
137	67	23.10	RG	34	15	200	60	25	40	25	15	2	100	4
158	75	169.40	RG	320	15	240	40	35	40	40	70	3	100	2
7	5	830.00	RG	18	34	55	20	165	30	100	30	1	500	4
105	48	147.20	RG	11	20	50	20	10	30	135	10	3	100	4
136	67	22.00	RG	22	15	150	40	20	15	75	10	3	200	4
173	81	20.30	RG	28	35	455	20	15	35	370	10	3	100	3
87	41	97.70	RG	18	20	50	20	35	20	345	15	6	100	1
79	39	173.10	RG	26	20	75	60	40	15	30	15	4	200	1

Table 8. (continued)

Analysis Number	Hole Number	Depth (m)	Alteration Type	Trace elements (ppm) Mn	Pb	Ba	V	Ni	Co	Sr	Zn	As	C	U
17	15	222.00	RG	26	17	70	20	80	30	90	10	6	100	1
110	56	40.40	RG	21	20	80	20	20	50	40	10	1	100	2
92	45	116.50	RG	26	30	140	20	45	55	230	35	8	100	4
68	35	139.40	RG	55	30	75	20	35	50	40	65	1	100	2
107	55	45.50	RG	133	40	150	90	25	45	235	120	2	100	6
4	4	896.80	G	66	19	750	200	160	50	115	90	3	300	33
138	67	23.60	G	100	35	820	40	30	40	50	45	3	100	22
80	39	182.40	G	11	20	75	20	40	15	110	15	4	100	1
48	30	268.90	G	220	20	230	75	75	35	50	130	1	200	5
82	39	188.70	G	71	40	75	20	60	50	165	15	2	100	2
88	41	100.00	G	25	25	50	20	70	30	115	35	3	200	1
144	72	195.20	G	106	20	75	20	10	40	150	50	1	100	3
145	72	197.40	G	95	20	75	20	25	40	125	50	1	400	2
8	5	831.00	G	44	22	50	20	100	50	25	10	2	300	10
157	75	167.50	G	101	20	100	60	45	45	10	40	1	100	3
9	5	832.40	G	45	29	355	20	100	75	60	15	5	100	6
120	59	33.90	G	112	20	445	50	20	45	50	35	1	100	8

B - Bleached Zone, R - Red Zone, RG - Red-Green Zone, G - Green Zone

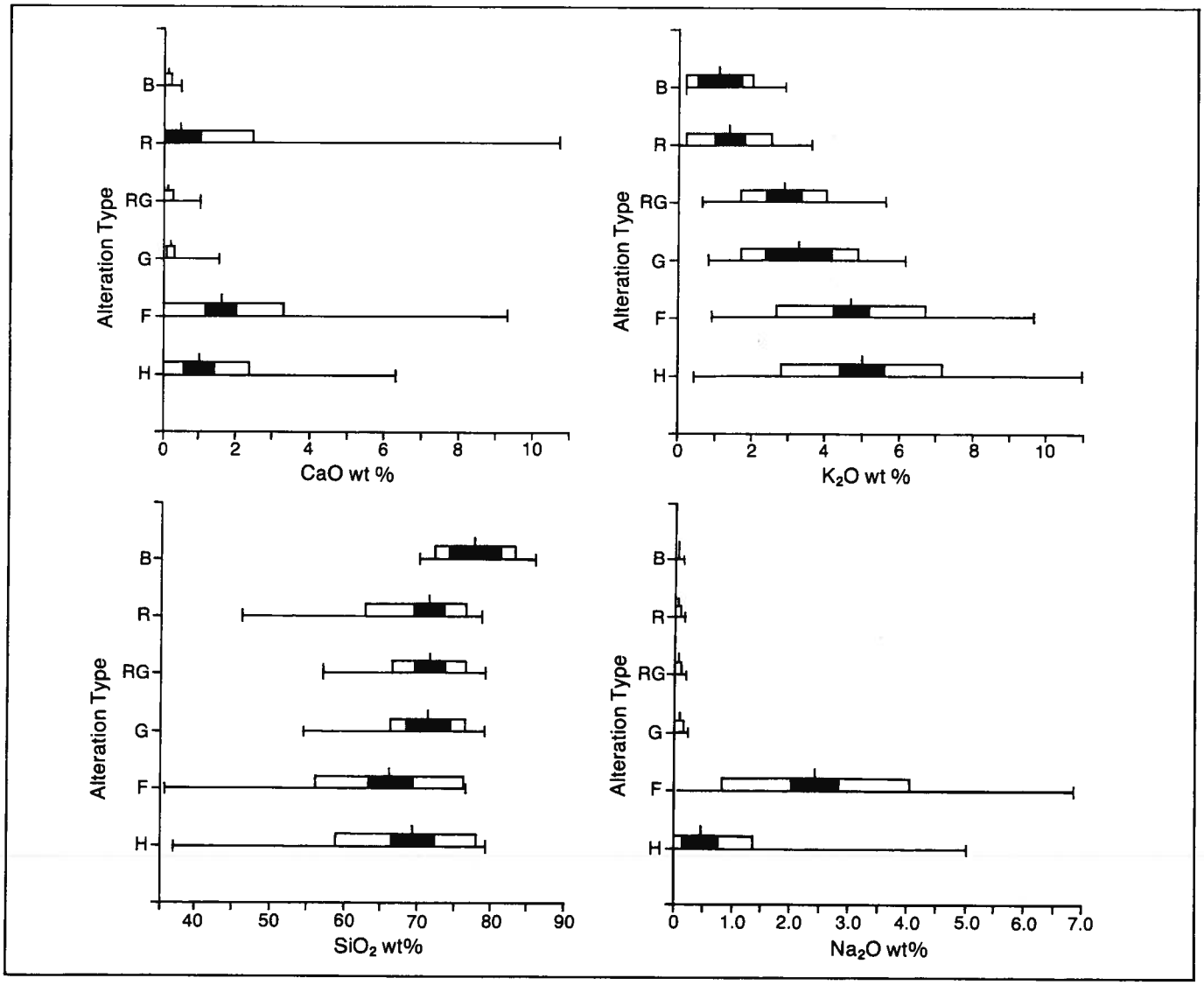

Figure 40. Dice diagrams of major element data for alteration type (continued on next page).

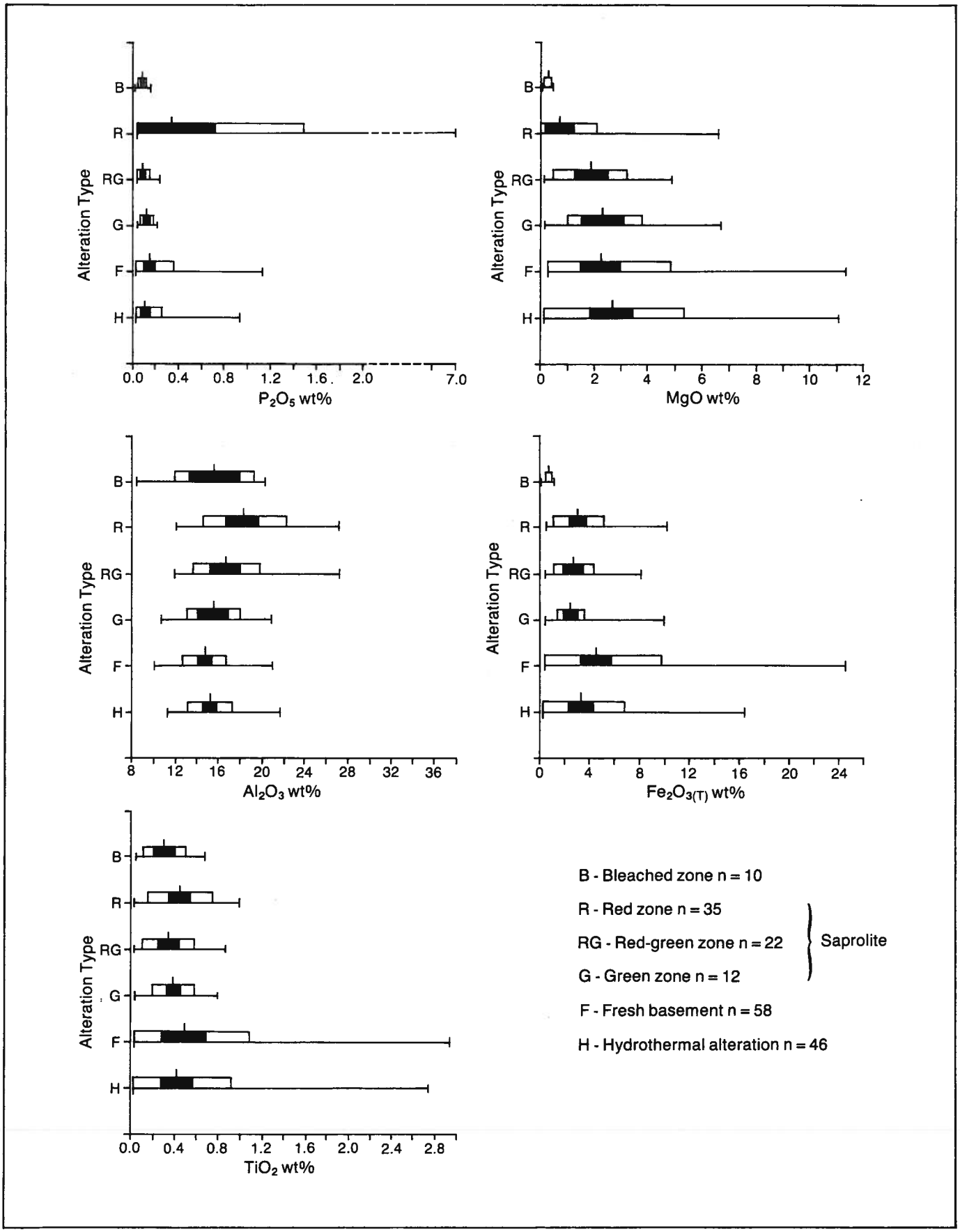

Figure 40. (continued)

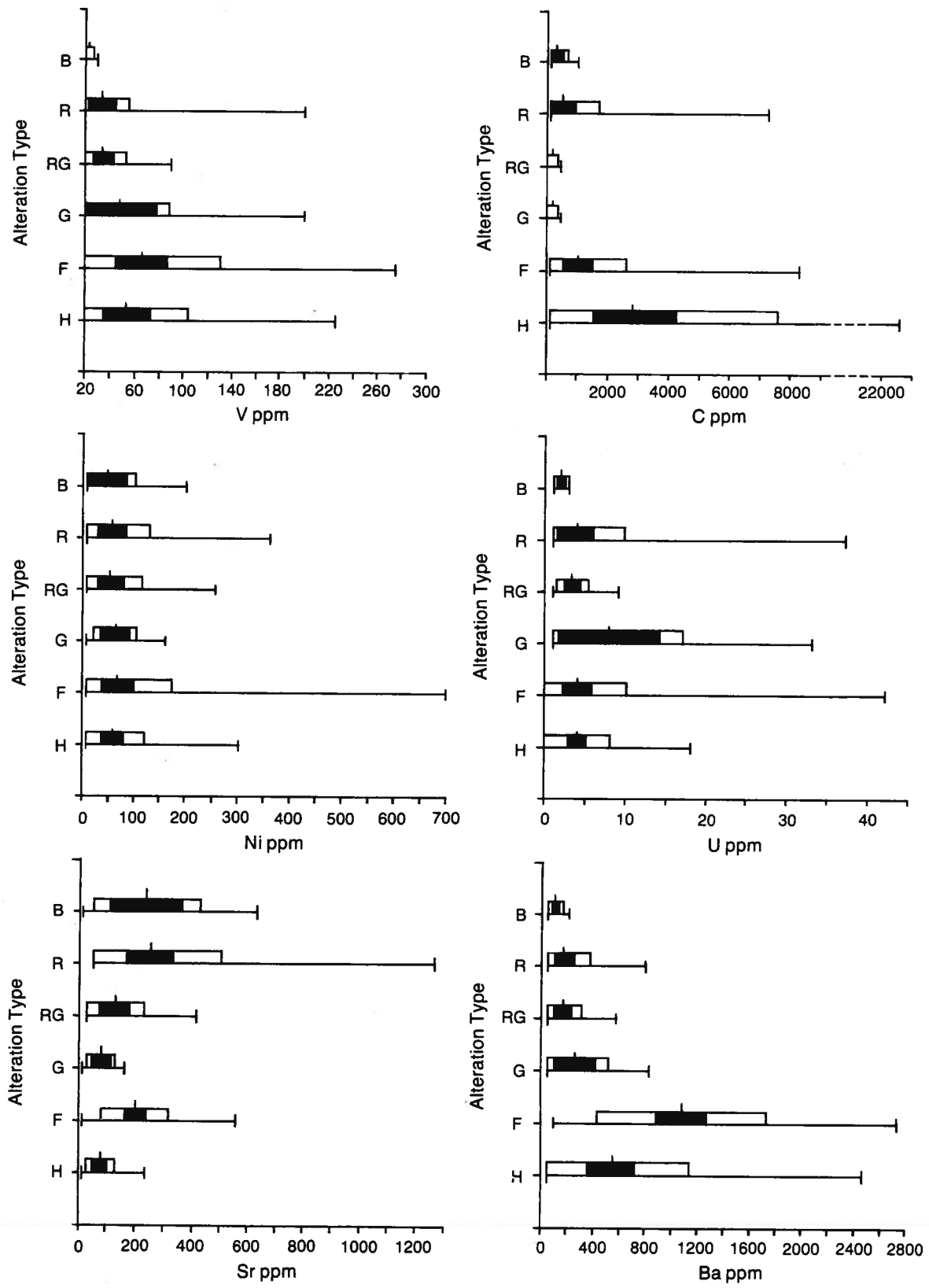

Figure 41. Dice diagrams of trace element data for alteration type (continued on next page).

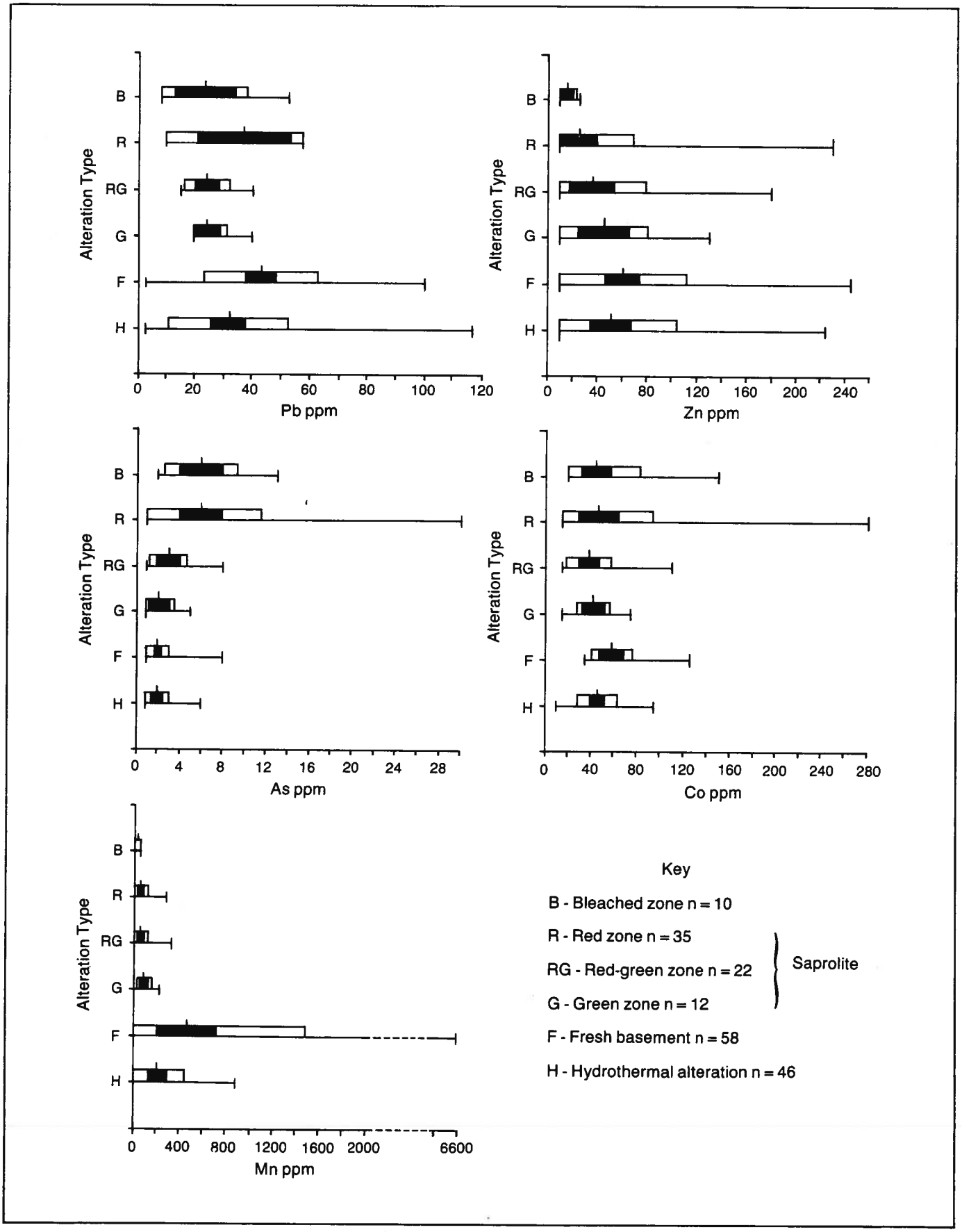

Figure 41. (continued)

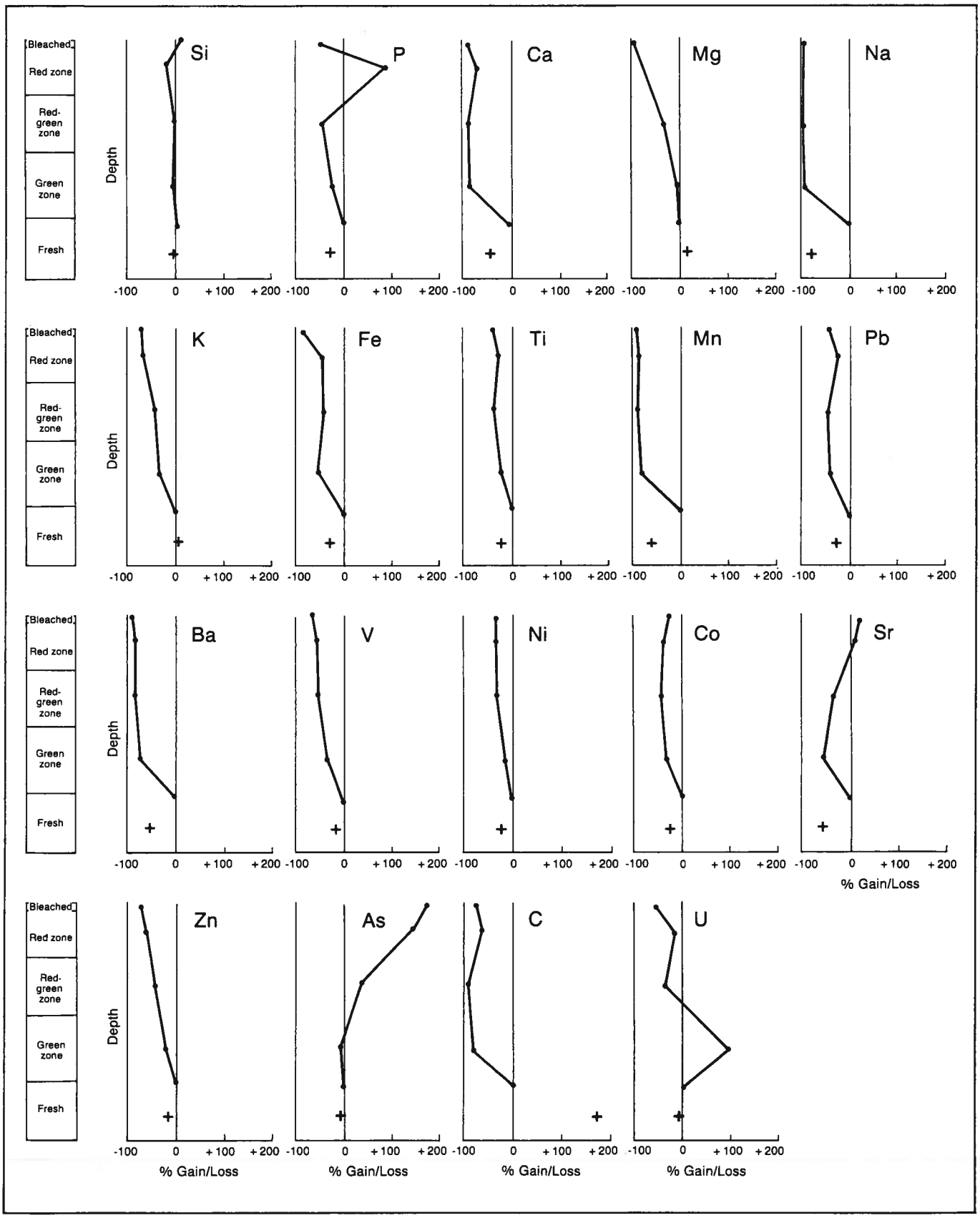

Figure 42. Percentage gain/loss of mean values for major and trace elements, assuming Al constant, in the saprolite profile; + – hydrothermal alteration n = 10 for bleached zone, n = 35 for red zone, n = 22 for red/green zone, n = 12 for green zone, n = 52* for fresh basement, n = 46 for hydrothermal alteration. *Only major fresh rock types having altered equivalents are considered here.

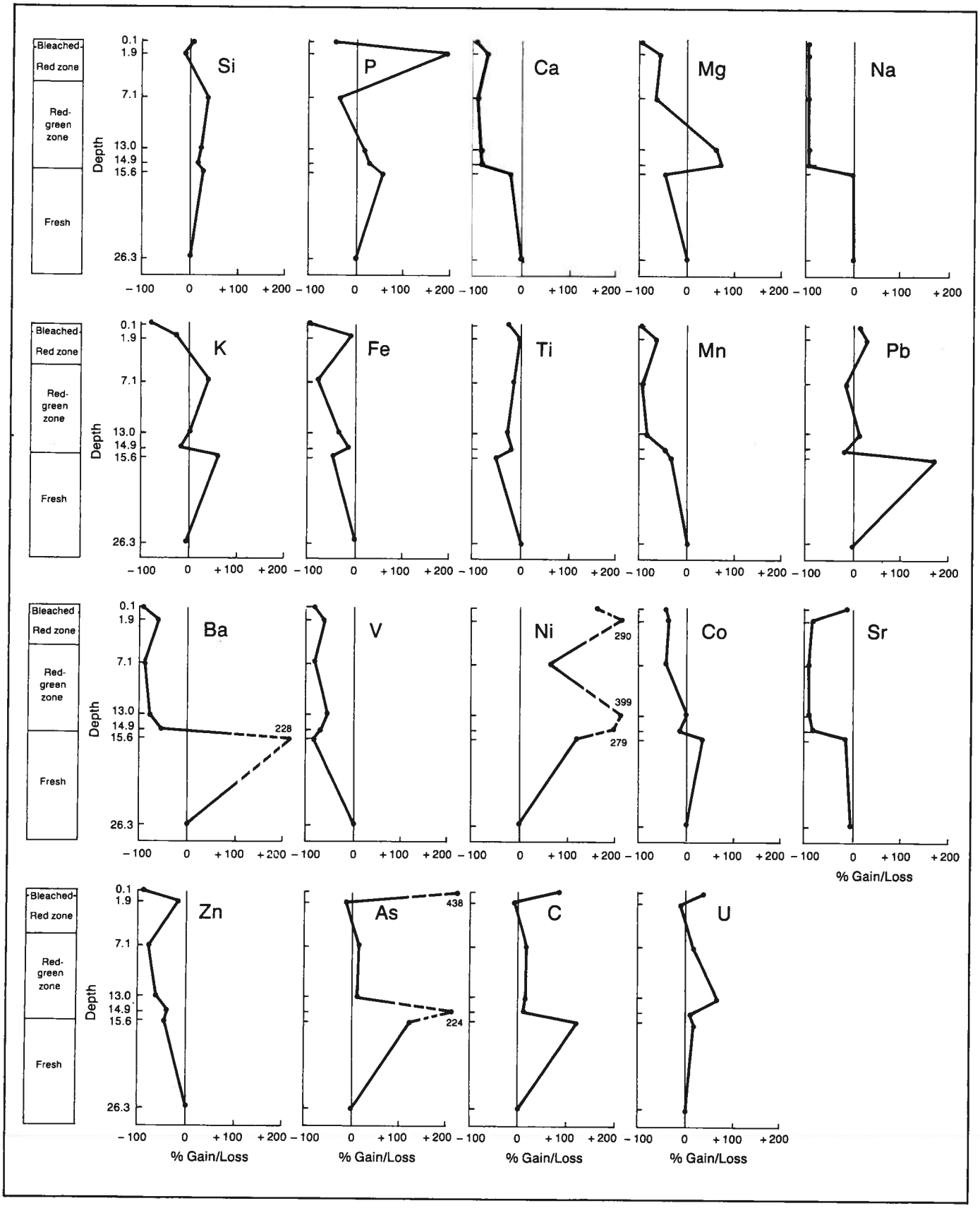

Figure 43. Percentage gain/loss of major and trace elements, assuming Al constant, in the saprolite profile in drill core 75. The saprolite is developed on Fishing Creek Granitoid.

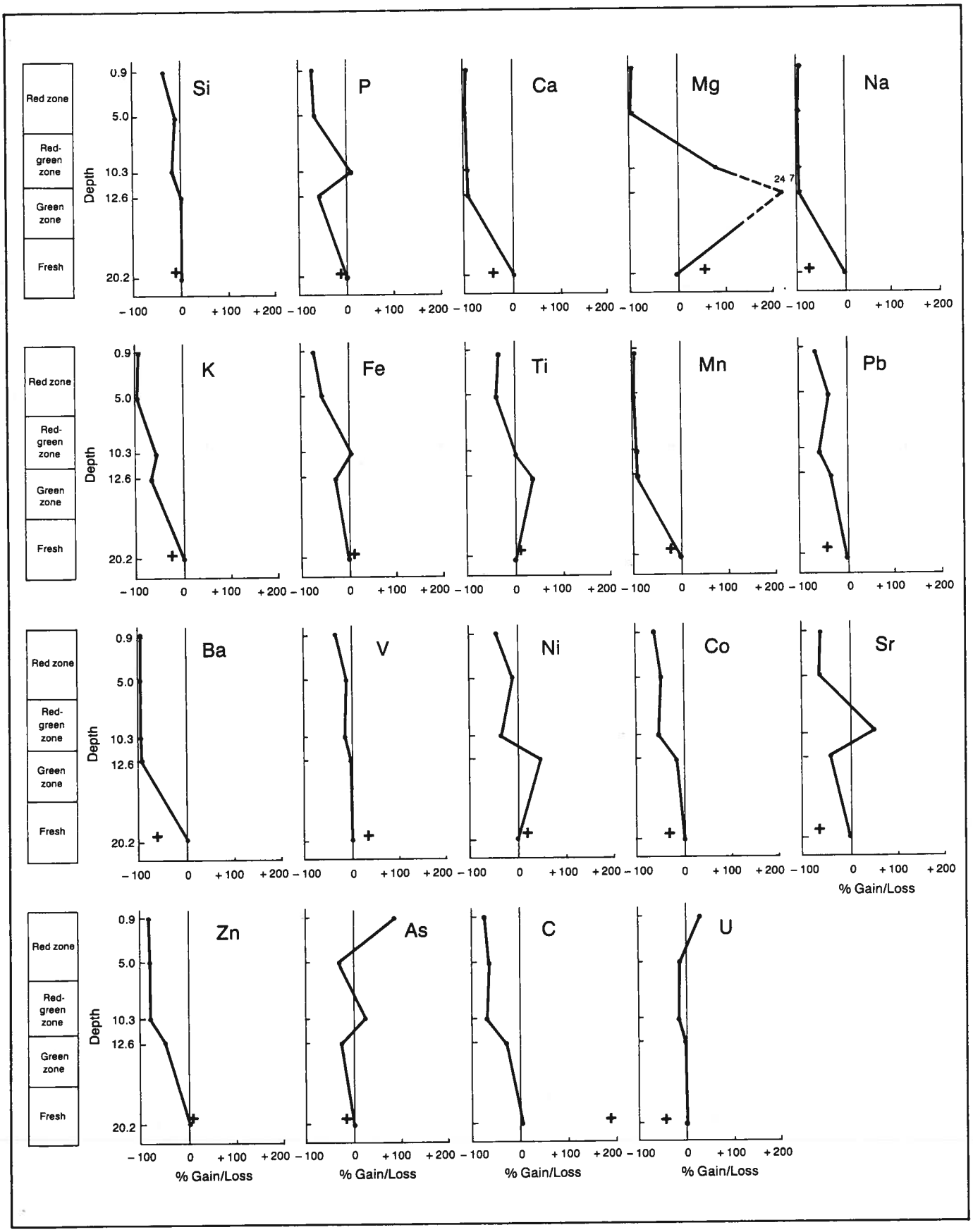

Figure 44. Percentage gain/loss of major and trace elements, assuming Al constant, in the saprolite profile in drill core 41. The saprolite is developed on Alkali Feldspar-Rich Granitoid.

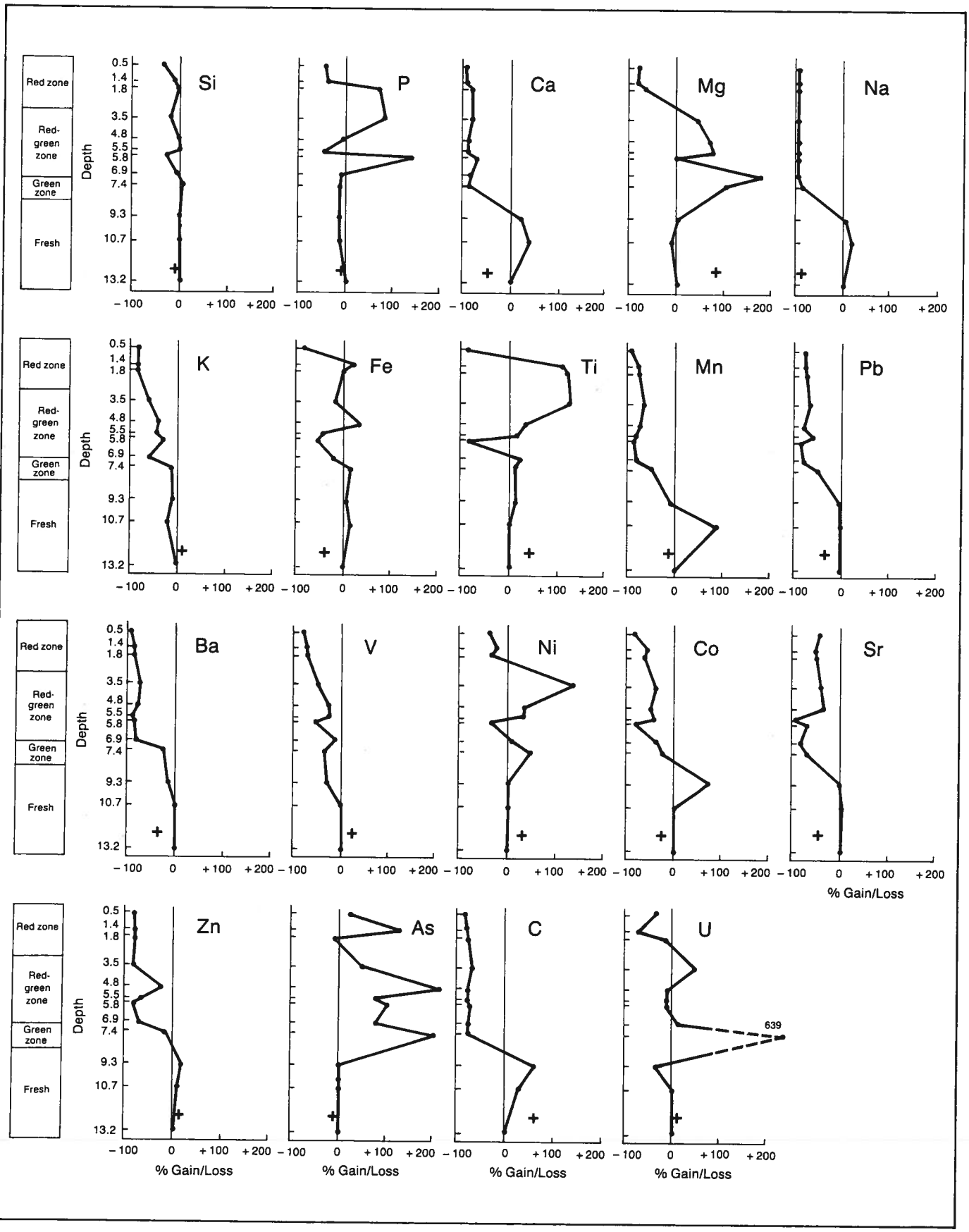

Figure 45. Percentage gain/loss of major and trace elements, assuming Al constant, in the saprolite profile in drill core 67. The saprolite is developed on Grey Foliated Granitoid.

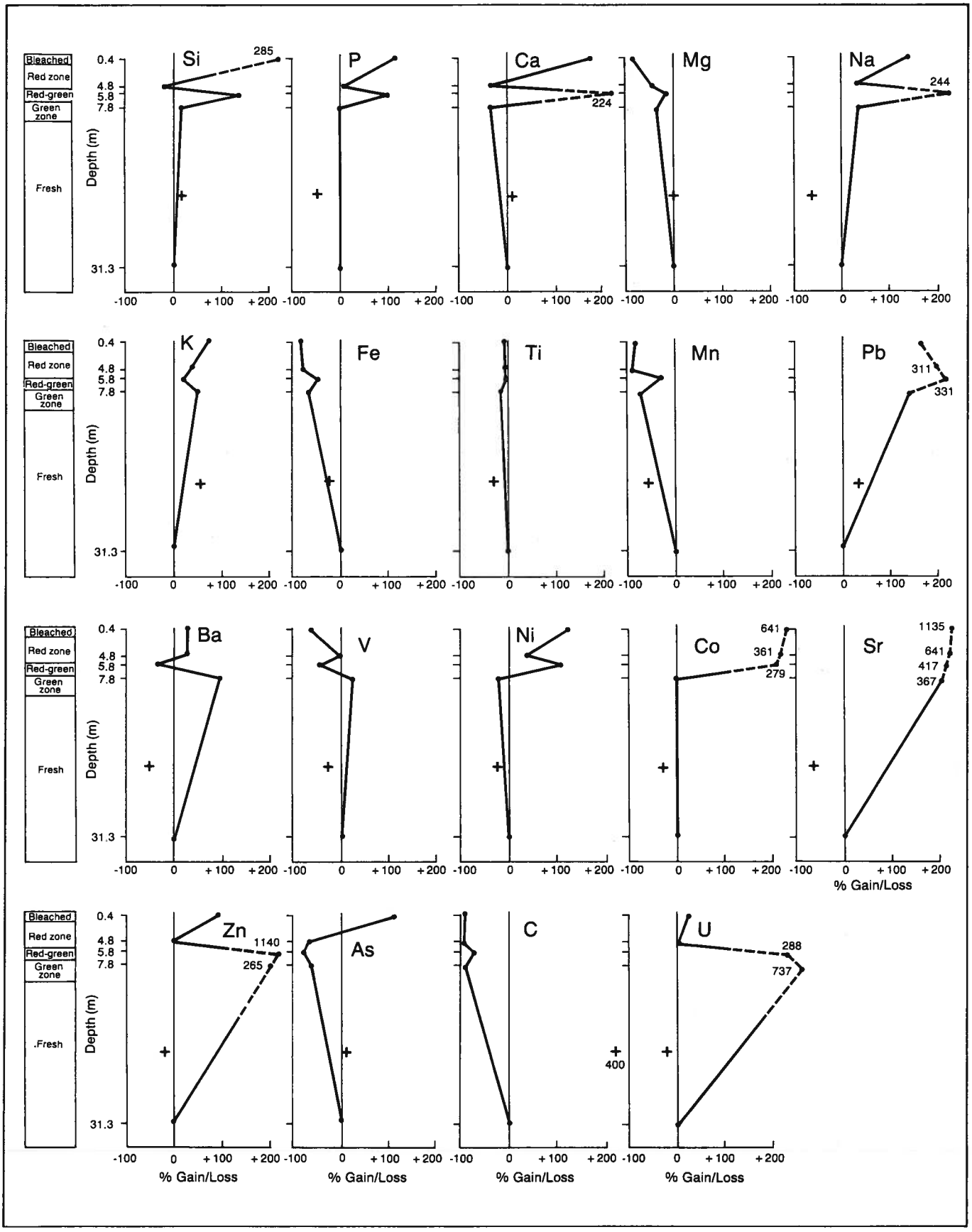

Figure 46. Percentage gain/loss of major and trace elements, assuming Al constant, in the saprolite profile in drill core 4. The saprolite is developed in part on Mafic Mylonite.

mean values and the individual granitoid profiles. Some of these differences can be explained by having a mafic parent rock type.

The depletion of MgO and total iron is more noticeable in hole 4, probably as a result of the fresh rock containing more ferromagnesian minerals than the granitoids. K_2O shows a slight gain in hole 4, probably due to the formation of illite. SiO_2 shows considerable gains, which may represent the late introduction of silica or the fact that the volume is not constant in this rock type and SiO_2 is enriched residually. The trends in hole 4 do not conform to the processes that formed the sub-Athabasca Group saprolite. This is in part due to a different parent rock type. However, it is also likely that later overprinting has concealed the original geochemistry.

Discussion

Several well-defined trends appear to be characteristic of the saprolite development on the granitoid rocks beneath the Athabasca Group. These are the severe depletion of Ca, Na, Mn, Ba and C in all saprolite zones and the minor depletion of Mg, K, Fe, Pb, V, Ni, Co, Sr and Zn, with the latter group tending to be more depleted in the higher zones. P and As vary between zones, and Si, Ti and U are stable. These trends are observed in individual profiles and in mean values for all the major rock types except the Mafic Mylonites. Local variation exists and is probably due to variation of a given element in the fresh rock, the perseverance of core-stones and fresh rock at high levels within the saprolite, or local hydrothermal overprinting.

The saprolite in Alberta is the product of a leaching process, which is consistent with it being the product of surficial weathering. No true soil textures are present in the Alberta saprolite, indicating that an upper soil horizon was not developed or was eroded off prior to deposition of the Athabasca Group. MacDonald (1980) stresses the similarity between the sub-Athabasca saprolite and parts of modern day lateritic soil horizons. However, the similarities are not so great that a direct comparison can be made. Probably the saprolite is the product of surficial weathering under conditions similar to those in which modern day laterites form. Differences could be due to the lack vegetation in the Helikian and to local topographic and climatic variations.

Overall, the results obtained in Alberta closely match those obtained in Saskatchewan by MacDonald (1980). The main difference is that he found K_2O to increase in the lower zones and to be depleted only in the red and white zones. In this study, that trend was only present in hole 75 of the Fishing Creek Granitoid. in MacDonald's study, MgO was found to increase in the lower zones, a trend present only in selected profiles in Alberta, and Ni and Co appear to be more stable in his samples. This close approximation to data obtained almost 400 km away confirms the regional aspect of sub-Athabasca Group weathering.

Broad similarities are also present between the above data and those presented in Fahrig and Loveridge (1981), although their data are not corrected for aluminum being constant. There are some similiarities to the data in Tremblay (1983), although his data are not extensive and the samples were taken close to ore mineralization.

The anomalous alteration present in hole 4 is partly due to rock types and, more importantly, to overprinting of the saprolite by later processes. These later processes served to enrich the rocks in a number of important elements and, thus, could be related to economic mineralization.

Hydrothermal alteration

Many of the cores examined have zones of alteration within the fresh basement rock or yellowish to white clay-rich alteration zones (figure 47) that may overprint saprolite zones. Commonly, these alteration zones can be directly related to fracturing. Hydrothermal alteration is characterized by sericitized plagioclase and fresh alkali feldspar (figure 48). This alteration appears to be unrelated to the saprolite weathering and probably occurred much later. The possibility exists that the hydrothermal alteration may be a regional expression of the alteration related to ore genesis; otherwise, it may be a basement expression of one of the diagenetic events present within the overlying sandstone. Zones of fracturing within the basement provided permeable pathways for the movement of hydrothermal fluids.

Geochemistry of the hydrothermal alteration

Tables 9 and 10 present the geochemical analyses of the hydrothermal alteration for major element oxides and trace elements. As with the saprolite data, the hydrothermal values have been recalculated as gains or losses assuming aluminum was immobile. These mean data are plotted as crosses on figure 42 for ease of comparison with the saprolite profile. On figures 44 to 46 the mean values for the appropriate rock type are plotted for comparison, because no hydrothermal alteration was sampled from the specific holes plotted. No hydrothermal alteration was sampled from the Fishing Creek Granitoid.

In general, the major elements are affected the same way by hydrothermal as by saprolite alteration. Si is immobile. P, Ca, Na, Fe and Ti are all depleted, but commonly not by as much as the saprolite samples. In some cases, the hydrothermal alteration is equivalent to green zone alteration in the saprolite. Mg and K show slight but opposite trends to the saprolite alteration.

Trends in the hydrothermal alteration in hole 67 from the Grey Foliated Granitoid and hole 41 from the Alkali

Figure 47. Pervasive hydrothermal alteration. Drill hole 39. Scale is in cm.

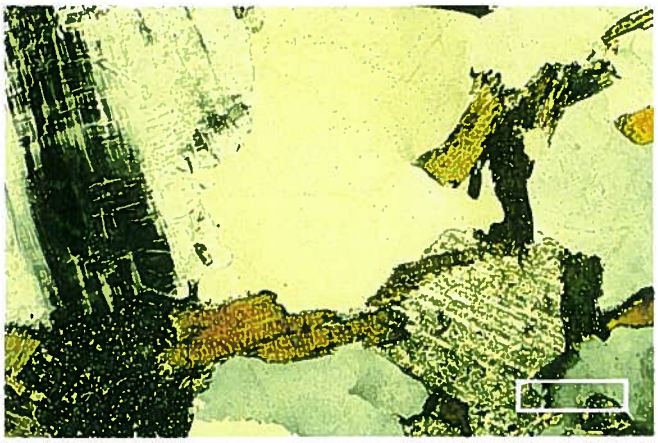

Figure 48. Fresh alkali feldspar and sericitized plagioclase. Zone of the hydrothermal alteration. Crossed nicols. JAW84-086-5.9. Scale bar is 0.5 mm long.

Feldspar-Rich Granitoid closely match the mean. Ti in hole 67 has an opposite trend, as do K, Fe and Ti in hole 41, although the differences are small. The variation in Ti probably represents variation in the fresh rock. In holes 67 and 41, the enrichment of Mg in the hydrothermally altered samples matches Mg enrichment in the green and lower red-green zones. In hole 4 from the Mafic Mylonite rocks, the hydrothermal alteration is very similar to the mean hydrothermal alteration, except for Ca, which shows opposite trends. However, with hole 4, the hydrothermal alteration trends do not match the saprolite trends for Si, P, Ca, Mg and Na.

As with the major elements, the average values for most of the trace elements show the same trends in the hydrothermally altered zones as for the saprolite, especially the green zone alteration. The exception is C, which is strongly enriched in the hydrothermal zones and strongly depleted in the saprolite. For holes 67 and 41, the trends match the mean except for V and Ni, although in both cases the Ni trends match the green zone alteration in each case. The similarity of the hydrothermal alteration to the green zone alteration is also observed in hole 4, where only Pb shows an opposite trend. However, as with the major elements, in many cases (Ba, Ni, Co, Sr, Zn, As, C and U) the hydrothermal trend in hole 4 does not match the saprolite.

Thus, for the trace and major elements, the hydrothermal alteration and the green zone alteration are similar. In hole 4, the hydrothermal alteration matches other hydrothermal alteration but not the green zone alteration in hole 4. This supports the idea that the saprolite alteration in hole 4 has been overprinted.

The bleached zone, which is locally present immediately below the unconformity, crosscuts the red zone alteration and thus formed later than the true saprolite. Thus, it may have a relationship to the superficially similar hydrothermal alteration. However, geochemical data in figures 42, 44, 45 and 46 show that there are some major differences between the hydrothermal alteration and the bleached zone. Figure 42 shows opposite trends for the two alteration types for MgO, K_2O, Sr, As and C, and major differences for CaO, $Fe_2O_3(T)$, Ba, V and Zn. In addition, figures 44, 45 and 46 show opposite trends, locally, for $Fe_2O_3(T)$, TiO_2, V, Ni, Zn, U, P_2O_5, Na_2O, Ba and Co. This strongly suggests that the bleached zone is not equivalent to

Table 9. Major element analyses for hydrothermal alteration

Analysis Number	Hole Number	Depth (m)	Alteration Type	Major elements (weight percent oxide) SiO_2	P_2O_5	CaO	MgO	Na_2O	K_2O	Al_2O_3	$Fe_2O_{3(T)}$*	TiO_2	LOI	Total Percent
13	13	96.9	H	66.55	0.03	2.07	1.94	0.13	8.70	13.04	2.73	0.38	2.8	98.37
14	13	101.5	H	58.32	0.05	0.09	2.09	0.53	10.86	15.69	7.01	0.76	2.5	97.90
18	15	230.0	H	77.90	0.11	0.16	1.58	0.17	5.88	13.04	0.54	0.06	2.5	101.94
21	18	74.1	H	66.02	0.18	1.64	1.53	0.52	4.26	16.63	4.29	0.85	5.1	101.02
22	18	78.1	H	70.83	0.05	0.41	1.36	0.74	8.16	14.46	1.82	0.29	2.2	100.32
23	19	26.5	H	37.13	0.06	3.43	10.79	0.22	3.06	15.21	16.52	0.87	8.1	95.39
24	19	28.0	H	74.58	0.05	1.96	1.64	0.03	6.18	11.34	0.53	0.03	3.4	99.74
25	19	32.2	H	46.87	0.10	4.34	8.96	0.15	2.05	16.63	10.30	1.55	9.1	100.05
34	20	30.1	H	74.15	0.06	0.17	0.91	0.21	7.68	14.08	0.30	0.02	2.4	99.98
36	20	60.7	H	57.14	0.06	0.28	3.98	0.11	5.10	17.01	6.44	0.71	5.0	95.83
52	30	290.8	H	66.98	0.11	0.19	3.04	0.15	6.96	14.65	2.93	0.38	3.0	98.39
55	31	93.6	H	72.87	0.06	0.08	0.45	0.01	4.02	14.46	0.72	0.08	2.4	95.15
58	31	110.7	H	73.83	0.04	0.21	1.59	0.14	5.70	12.47	1.07	0.13	2.7	97.88
62	33	157.8	H	77.15	0.03	0.09	0.22	0.05	3.36	12.00	0.64	0.08	2.0	95.62
63	33	181.1	H	71.48	0.04	0.73	0.69	1.44	5.76	14.08	0.43	0.02	2.0	96.67
66	35	135.0	H	70.41	0.10	0.02	0.06	0.00	0.41	17.67	1.39	0.01	6.4	96.47
67	35	138.2	H	70.19	0.04	0.05	1.61	0.00	1.42	15.50	0.49	0.02	4.8	94.12
71	36	55.9	H	63.24	0.14	0.51	3.10	0.05	6.96	14.65	4.65	0.51	3.1	96.91
73	38	36.2	H	68.16	0.07	1.47	2.26	0.11	5.04	15.03	3.58	0.36	4.2	100.28
74	38	54.8	H	49.86	0.22	4.27	8.13	0.02	3.90	15.03	8.22	0.74	9.3	99.69
75	38	56.2	H	63.24	0.04	1.88	1.36	5.00	6.36	18.81	2.46	0.19	3.4	102.74
77	38	57.5	H	71.90	0.25	0.80	1.03	1.16	5.34	13.51	4.36	0.87	2.3	101.52
81	39	185.4	H	77.68	0.05	0.03	0.17	0.06	1.94	16.25	0.93	0.08	4.4	101.59
83	39	207.0	H	76.93	0.10	0.10	0.72	0.07	4.32	16.16	1.34	0.12	2.6	102.46
84	39	214.3	H	75.76	0.19	0.29	1.78	0.09	3.78	15.40	0.89	0.16	3.2	101.54
93	45	117.8	H	76.93	0.07	0.12	2.67	0.03	2.64	15.50	0.62	0.02	3.9	102.50
100	47	95.4	H	51.79	0.94	1.61	10.96	0.05	7.80	15.21	7.65	1.19	3.6	100.80
108	55	54.6	H	69.76	0.08	0.19	3.49	0.07	2.82	18.05	1.40	0.02	4.9	100.78
111	56	40.6	H	75.33	0.07	0.21	3.49	0.10	2.64	16.63	0.87	0.04	4.6	103.98
123	63	18.6	H	75.22	0.08	0.13	0.90	0.05	4.56	16.73	0.83	0.33	2.8	101.63
124	63	24.4	H	59.81	0.08	0.67	5.23	0.05	4.14	21.26	3.65	0.31	6.7	101.90
127	65	28.1	H	70.19	0.16	0.21	0.81	0.02	2.15	17.10	4.43	0.61	4.8	100.48
128	66	27.8	H	75.65	0.07	0.12	1.06	0.69	5.88	14.93	1.70	0.14	2.5	102.74
146	74	66.8	H	56.92	0.19	0.80	3.00	0.11	9.00	15.12	4.79	0.57	3.9	94.40
148	74	74.7	H	47.72	0.22	0.90	3.98	0.05	7.26	15.88	10.94	2.74	7.3	96.99
164	78	22.1	H	63.34	0.06	3.01	2.51	0.02	4.50	15.59	1.19	0.50	6.8	97.52
165	78	35.9	H	77.68	0.05	0.10	0.41	0.04	3.42	12.57	0.89	0.01	2.2	97.37
166	79	18.1	H	72.65	0.05	0.32	0.53	2.39	4.74	13.99	0.90	0.10	1.4	97.07
168	79	30.1	H	71.26	0.05	1.05	1.93	0.02	3.84	14.36	2.16	0.13	2.5	97.30
169	79	30.1	H	67.95	0.07	1.01	0.91	0.56	7.26	13.80	0.71	0.06	4.0	96.33
179	87	11.9	H	74.04	0.07	0.88	1.15	0.02	3.54	12.76	1.43	0.04	3.3	97.23
181	87	24.6	H	69.44	0.07	0.87	1.89	0.08	6.06	14.08	1.76	0.21	3.5	97.96
183	93	206.8	H	58.85	0.23	0.40	5.15	0.27	4.38	16.25	8.51	1.37	5.6	101.01
184	93	207.9	H	49.97	0.14	6.30	6.72	0.36	6.06	14.84	2.93	0.47	12.4	100.19
185	93	214.9	H	73.62	0.05	0.29	0.70	2.90	4.50	13.80	2.27	0.18	1.2	99.51
186	93	239.4	H	53.18	0.02	0.18	3.10	1.61	5.04	21.64	7.36	0.95	4.6	97.68

*Iron is total iron calculated as Fe_2O_3, H - Hydrothermal Alteration

the hydrothermal alteration and is the product of a separate process.

Discussion

For many major and trace elements, the hydrothermal alteration in the basement closely approximates the green zone alteration of the saprolite. This does not necessarily imply a close relationship between the two types of alterations, because, in places, the hydrothermal alteration can be observed crosscutting the green zone. However, in some holes they look very similar, meaning that some samples taken as hydrothermal alteration may, in fact, be green zone alteration extending down into fresh rock, and some samples taken as green zone may really be hydrothermal overprinting. The main reason for the similarity is probably a similar mode of occurrence. Conditions in the lower weathering zones of the saprolite (perhaps beneath the water table) were probably very similar to conditions in deep permeability zones of the granitoids during the later history of the rock.

The presence in the rock of red zone alteration in hand specimens is a good indication of saprolite, rather than hydrothermal, alteration. The geochemical characteristics of the red zone are different from the hydrothermal alteration, although it is commonly a difference of degree, rather than opposite trends.

Table 10. Trace element analyses for hydrothermal alteration

Analysis Number	Hole Number	Depth (m)	Alteration Type	Trace elements (ppm) Mn	Pb	Ba	V	Ni	Co	Sr	Zn	As	C	U
13	13	96.90	H	158	13	855	50	120	45	75	60	6	1200	4
14	13	101.50	H	250	58	1160	175	115	90	170	80	2	500	7
18	15	230.00	H	23	55	240	20	100	95	65	25	2	200	4
21	18	74.10	H	127	70	750	50	60	45	75	105	3	3400	12
22	18	78.10	H	69	53	1120	20	80	80	115	35	2	900	3
23	19	26.50	H	900	20	280	180	200	70	75	175	4	6600	1
24	19	28.00	H	74	27	210	20	120	75	50	10	2	4100	0
25	19	32.20	H	525	39	295	130	190	30	110	130	4	7300	1
34	20	30.10	H	20	45	750	20	95	60	100	10	2	300	1
36	20	60.70	H	825	5	245	80	40	35	80	115	1	500	14
52	30	290.80	H	193	20	1300	20	50	60	75	35	1	200	4
55	31	93.60	H	13	25	50	20	55	60	75	15	2	100	1
58	31	110.70	H	32	25	90	20	30	35	165	20	2	200	1
62	33	157.80	H	4	5	75	20	35	40	50	20	3	200	1
63	33	181.10	H	49	45	100	20	50	60	65	10	2	600	1
66	35	135.00	H	144	10	50	20	60	30	25	20	4	100	1
67	35	138.20	H	6	30	50	20	20	50	25	10	1	100	0
71	36	55.90	H	480	50	940	80	75	55	65	85	2	800	3
73	38	36.20	H	57	60	220	25	60	30	50	35	2	5100	3
74	38	54.80	H	695	40	380	150	80	45	25	100	1	1360	2
75	38	56.20	H	168	20	1105	30	15	25	115	20	1	5700	3
77	38	57.50	H	70	50	1000	20	40	50	75	30	2	1700	3
81	39	185.40	H	59	20	50	20	40	45	115	15	4	100	1
83	39	207.00	H	11	10	50	20	20	40	235	20	1	100	1
84	39	214.30	H	13	20	100	20	65	45	65	25	1	300	6
93	45	117.80	H	8	10	50	20	60	55	50	10	5	100	2
100	47	95.40	H	650	20	2440	160	300	50	65	190	4	200	4
108	55	54.60	H	7	10	60	20	20	35	50	10	3	100	1
111	56	40.60	H	16	20	80	20	20	35	25	10	1	300	3
123	63	18.60	H	21	25	160	20	25	45	90	10	4	200	3
124	63	24.40	H	280	30	160	20	55	20	90	35	1	2100	18
127	65	28.10	H	105	30	420	40	25	30	200	60	2	100	3
128	66	27.80	H	117	45	900	20	50	50	100	20	1	100	5
146	74	66.80	H	151	15	1050	80	15	40	150	75	3	2200	1
148	74	74.70	H	345	15	405	200	55	25	115	85	2	1400	7
164	78	22.10	H	215	15	665	20	20	30	40	10	1	11000	10
165	78	35.90	H	16	20	160	20	20	40	110	10	1	200	1
166	79	18.10	H	63	45	1585	20	20	35	175	15	2	900	3
168	79	30.00	H	175	20	275	20	30	55	10	20	1	4300	2
169	79	30.10	H	89	115	2450	20	15	60	200	15	1	4000	2
179	87	11.90	H	81	25	115	20	25	40	25	20	1	16100	2
181	87	24.60	H	157	40	865	20	30	40	60	15	1	3000	10
183	93	206.80	H	460	40	160	225	30	40	10	225	3	8600	6
184	93	207.90	H	330	25	525	60	20	30	25	85	1	22600	5
185	93	214.90	H	300	55	825	20	10	50	125	35	1	600	4
186	93	239.40	H	810	15	200	175	30	10	40	125	2	200	3

H - Hydrothermal Alteration

Generally, it would be difficult to distinguish between green zone alteration and hydrothermal alteration. The exception to this appears to be with element C. In every case, the hydrothermal trend with C is moderate to strong enrichment, whereas the weathering profile is depleted throughout for that element. Tremblay (1982) suggests that Mg may also be an indicator, because it is enriched in the hydrothermal alteration and depleted in the saprolite. However, although this appears to be the case with the mean data, specific drill holes (67 and 41) show enrichment in Mg in the lower zones of the saprolite.

The bleached zone is geochemically different in many respects from the hydrothermal alteration. The hydrothermal alteration is due to fluids moving along fractures within the basement. The bleached zone is probably a result of the local interaction of fluids moving from the overlying sandstone, or along the unconformity, into the basement. The formation of the bleached zone may correspond to one of the reducing phases of the diagenetic history of the Athabasca Group (Wilson, 1985a).

In summary, four types of alteration are present: a regional surficial weathering profile; later hydrothermal

alteration similar to the lower zones of the weathering profile, but locally overprinted on it; an alteration of the mafic rocks around hole 4 with a geochemical character different from the first two types; and a local bleaching of the red zone, related to diagenesis of the sandstone.

Economic geology

The history of exploration in the Athabasca Basin of Alberta is outlined in Wilson (1985a). That publication also outlines the effect of the sandstone on exploration techniques. Since preparation of the work on the Athabasca Group, improved geophysical techniques have been successful in Saskatchewan at detecting deposits to a depth of 600 m. The effective depth of geophysics can be expected to increase further, and, consequently, the size of the area of interest beneath the edge of the Athabasca Group in Alberta would be greatly increased. Figure 49 shows the 600 m isopach for the Athabasca Group in Alberta. If this isopach is taken as the current cutoff for effective geophysical exploration, about 75 percent of the area underlain by the Athabasca Group in Alberta—or 6000 km² of land—is potentially attractive for exploration of unconformity-type uranium deposits. Consequently, regional knowledge of the basement geology beneath the Athabasca Group is essential in planning future exploration initiatives.

The Athabasca Group in Alberta is underlain by rocks of the Wylie Lake pluton (figure 22). No large areas of granite gneiss are present beneath the sandstone. However, to the south of the basin, areas of linear, high magnetic susceptibility may represent granite gneiss patches (figures 21 and 22). In addition, graphitic rocks are present very close to the edge of the Athabasca Group and probably occur beneath it. The regional structural trend beneath the Athabasca Group in Alberta is northwest/southeast. Future exploration will undoubtedly concentrate on finding linear, graphitic conductors in granite gneisses or mafic mylonites with this orientation. If the mafic mylonites are derived from metasediments or metavolcanics and are associated with faults, these areas would be excellent exploration targets.

Table 11 presents the analysis of major and trace elements for two samples of graphitic rock from drill hole 22 (figure 1). The basement at this locality lies beneath Devonian cover, but there is no evidence of Athabasca Group cover. Varied fresh basement rock types are present in the cluster of cores around drill hole 22, but the predominant type is Mafic Mylonite. No saprolite alteration is present in core 22. The analyses all fall within the range of fresh or hydrothermally altered basement.

When the analyses of the graphitic samples are compared to the values for the other rock types (figures 23 and 24), they show some interesting trends. For most of the analyzed elements (Si, P, Mg, Na, Fe, Ti, Mn, Pb, Ba, V, Ni, Sr, Zn, C), sample 40 plots with the Mafic Mylonite range, and sample 41 plots with the granitoids. Thus, sample 40 may be derived from a Mafic Mylonite, and 41 from a granitoid parent. The graphitic samples are not enriched in uranium, nor in any of the elements commonly associated with uranium ore genesis in Saskatchewan deposits.

Faulting is extensive beneath the southern part of the Athabasca Basin in Alberta (figure 22). Many of the faults may have been active after deposition of the Athabasca Group and would thus be prime exploration targets if they coincide with graphite zones or areas of granite gneiss.

Geochemical analyses of the basement indicate that the saprolite, bleaching, and hydrothermal alteration are all basically leaching processes and, therefore, not good mechanisms for the concentration of economically important mineralization. However, Sopuck, et al. (1983) state that "there is little or no distinction mineralogically or chemically between the less-intense hydrothermal alteration and the lower green ... layer of the paleoweathering profile." This "less intense

Table 11. Major and trace element analyses for samples of graphitic rock from drill hole 22

Analysis Number	Hole Number	Depth (m)	Alteration Type	Major elements (weight percent oxide) SiO_2	P_2O_5	CaO	MgO	Na_2O	K_2O	Al_2O_3	$Fe_2O_{3(T)}$*	TiO_2	LOI	Total Percent
40	22	106.0	GPH	54.36	0.07	1.16	6.64	0.01	3.06	16.35	9.94	0.81	10.6	103.00
40	22	101.2	GPH	72.55	0.06	1.55	2.11	0.01	2.88	10.87	2.36	0.05	4.6	97.04

Analysis Number	Hole Number	Depth (m)	Alteration Type	Trace elements (ppm) Mn	Pb	Ba	V	Ni	Co	Sr	Zn	As	C	U
40	22	106.00	GPH	965	20	200	220	110	50	25	140	1	4400	4
41	22	101.20	GPH	270	5	155	20	60	40	25	10	3	5800	1

*Iron is total iron calculated as Fe_2O_3, GPH - Graphitic Rock.

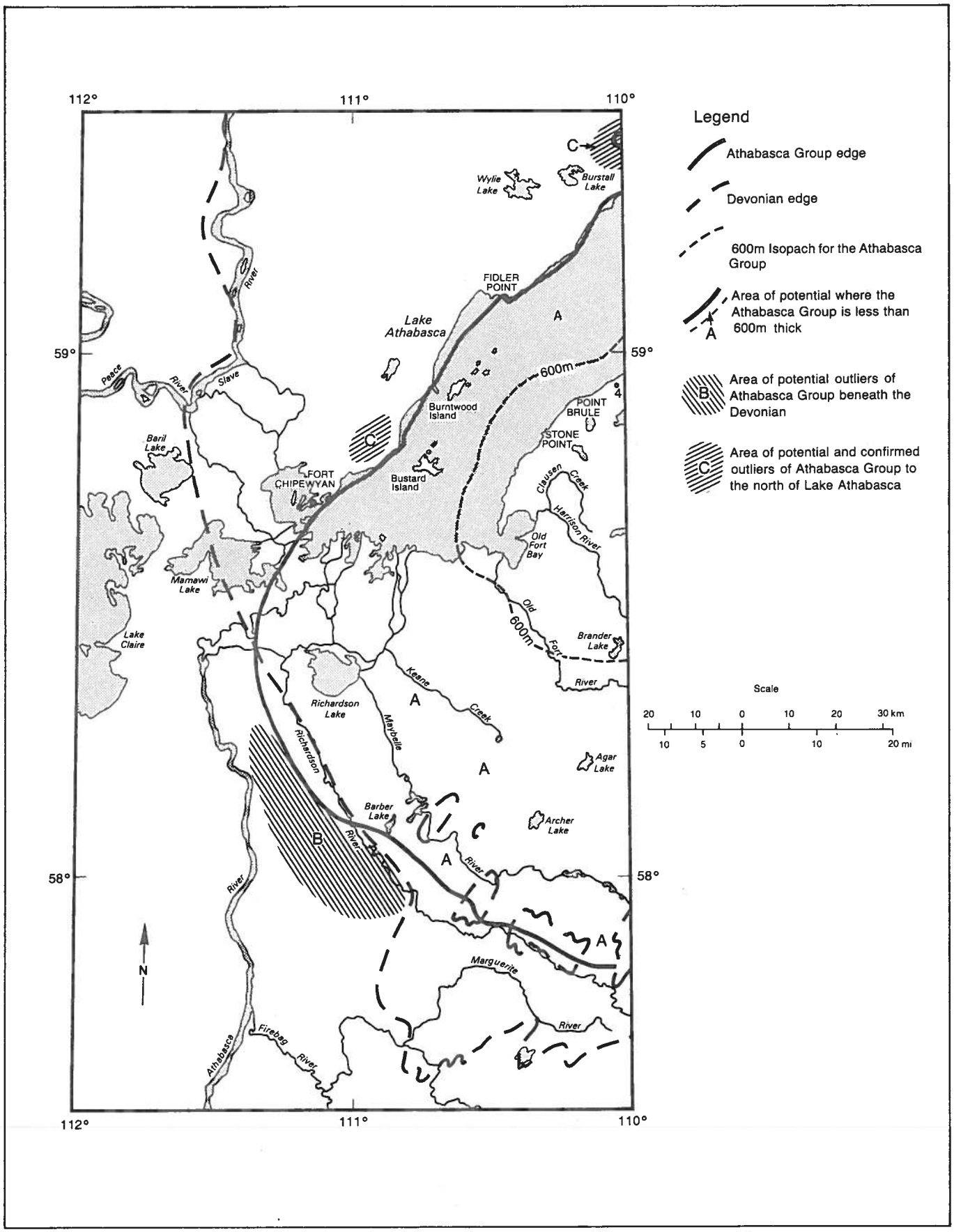

Figure 49. Areas favorable for uranium exploration (A,B,C) in the Athabasca Basin in Alberta (modified after Wilson, 1985a).

hydrothermal alteration" appears very similar to the hydrothermal alteration in this study. If it is directly related to more intense halos around deposits, then the regional hydrothermal alteration may be related to one phase of ore genesis. In this case, careful geochemical study of the hydrothermal alteration may indicate proximity to mineralization.

The fourth type of alteration is present in the Mafic Mylonites in hole 4. The rock in this hole is enriched in Si, P, K, Ca, Na, Pb, Ni, Ba, Co, Sr, Zn and U. Company lithologs (Nelson, 1978) contain assays that show uranium values up to 292 ppm, gold values of 0.08 oz/ton and enrichment in Ni, Co, Zn, Ag and As for holes 3 and 4. This enrichment shows similarity to enriched halos around known uranium deposits in Saskatchewan. In addition to these geochemical anomalies, a temperature increase of 22°C combined with very high gamma radiation levels was noticed near the base of one of the holes near hole 4 (W. Nelson, personal communication, 1980).

Tremblay (1982) suggests that the elements most commonly found with uranium in deposits in Saskatchewan are Pb, Ni, Co, As, V, Cu, Se, Te, Au and W. Near mineralized veins in the Carswell structure, there may be anomalies in Cu, Pb, Zn, As, Mo, Co, Au, Ni, V and Y, although not all elements are anomalous in each sample (Pagel and Svab, 1985). Ni, U, As, CO, V (Li, Mo, Ag, Cu, Zn) form small (<200 m) halos in the sandstone around the Key Lake and Midwest deposits in Saskatchewan (Sopuck et al., 1983). This similarity between geochemical halos around deposits in Saskatchewan and the alteration in hole 4 suggests that hole 4 may have been drilled into the halo of a uranium deposit. Unfortunately, in this area, depths to the unconformity range from 800 to 900 m, making additional exploration and any subsequent exploitation difficult. The role played in possible ore genesis by the Mafic Mylonites is not known, but if it proves to be important, other Mafic Mylonites beneath thinner Athabasca Group cover become economically interesting and considerably more accessible.

At the eastern end of the Athabasca Basin, there is a well-recognized association of uranium ore bodies with graphitic meta-pelite zones, faulting in the basement, and the unconformity (Tremblay, 1982). These conditions are present locally under the western end of the basin, and the association may be a suitable model to use in the search for undiscovered deposits. However, there are also many similarities with the geology at the Cluff Lake deposits where the ore bodies are associated with the unconformity, the contact between aluminous gneisses and granitoids, mylonite zones and faulting (Tona, et al., 1985). Locally, aluminous gneisses, garnetites and mylonites are present, suggesting that the Cluff Lake model may also be of use in the search for uranium in Alberta.

Summary

The basement rocks beneath the Athabasca Basin in Alberta are part of the Wylie Lake pluton, which is present in outcrop north of Lake Athabasca. Examination of fresh basement drill core has led to the subdivision of the Wylie Lake pluton into six major and several minor rock types. The major rock units consist of four granitoids and two mylonitic rocks. The granitoids are the Wylie Lake Granitoid and the Fishing Creek Granitoid, which are directly analagous to rock types present in outcrop, and the Grey Foliated Granitoid and the Alkali Feldspar-Rich Granitoid, which are alkali feldspar-enriched variations of the first two rock types and are probably also present in outcrop. The mylonitic rocks are subdivided into felsic and mafic types. The Felsic Mylonites are predominately derived from granitoid parent rocks and the Mafic Mylonites are derived from metasediments and metavolcanics. The minor rock types include amphibolite, pyroxenite, metasediments, minor mafic intrusions, aluminous gneiss and pegmatites.

Major and trace element geochemistry supports the above subdivision of the basement and indicates the different origin for the Mafic Mylonites. Geophysical data also support the broad subdivision and indicate the increased amount of tectonic activity and shearing in the south half of the Wylie Lake pluton. The mylonites and the south portion of the Wylie Lake Pluton are present in outcrop in the Marguerite River area.

On the basement surface beneath the Athabasca Group, a regionally developed saprolite is preserved. This surficial weathering zone formed prior to deposition of the Athabasca Group, perhaps over a much greater area than the present extent of the Athabasca Basin. The saprolite is developed in all rock types and commonly exhibits regionally correlative color zones. There are three color zones; an upper red, hematite-rich zone, a lower green, chlorite-rich zone, and an intermediate mixed red-green zone.

The saprolite is predominantly the result of leaching processes which can be related to mineralogical changes observed in thin section. Upward through the saprolite both plagioclase and alkali-feldspar degrade to clays. In the green zone, biotite is replaced by chlorite, which disappears upward as hematite becomes more prevalent. The mineralogy simplifies towards the top, with the red zone consisting of quartz in a groundmass of kaolinite and hematite dust and remnant biotites outlined in hematite.

Geochemical profiles for saprolite alteration in individual drill cores are similar for different rock types. This indicates the regional character of the saprolite. Locally, a thin bleached zone is present at the top of the red alteration zone. This crosscuts the saprolite alteration and is interpreted to be the result of the interaction of fluids from the overlying rocks with the basement.

Hydrothermal alteration is present throughout the

basement, commonly associated with fracture zones. The hydrothermal alteration is predominately white to paly yellowish green and crosscuts all zones of the saprolite. Geochemically, it is similar to the green zone of the saprolite except for carbon, which is strongly depleted in the saprolite and enriched in the hydrothermal alteration. The hydrothermal alteration has a geochemical signature distinct from the bleached zone.

The saprolite, hydrothermal alteration and bleached zones are all predominately products of a leaching process and do not appear to concentrate any economically important minerals. However, a fourth type of alteration is present in drill core 4. This alteration is associated with rock types that include Mafic Mylonites, and it overprints the saprolite alteration. Si, P, K, Ca, Na, Pb, Ni, Ba, Co, Sr, Zn and U are enriched in the alteration zone. This type of enrichment is similar to that present in geochemical halos around some unconformity-related uranium ore deposits in Saskatchewan, suggesting that drill hole 4 was drilled close to an economically interesting target.

The Athabasca Group is 800 m thick in the vicinity of drill hole 4. However, areas of Mafic Mylonites, possibly granite gneiss, post-Athabasca Group faulting, and graphitic basement rocks are present towards the south of the Wylie Lake pluton, where the Athabasca Group is less than 300 m thick. Where the above factors could be found in conjunction, they would present a very attractive target for uranium exploration. In addition, rocks similar to the aluminous gneisses and mylonites found within the Carswell structure are found locally, indicating that there may be uranium ore deposits in Alberta in a setting similar to the ones at Cluff Lake, Saskatchewan.

References

Ambrose, J.W. (1964): Exhumed paleoplains of the Precambrian Shield of North America; American Journal of Science, v.262, pp.817-857.

Armstrong, R.L. and Ramaekers, P. (1985): Sr isotopic study of Helikian sediments and diabase dikes in the Athabasca Basin, northern Saskatchewan; Canadian Journal of Earth Sciences, v.22, pp.399-407.

Ayres, D.E., Wray, E.M., Farstad, J. and Ibrahim, H. (1983): Geology of the Midwest Uranium Deposit; *in* Uranium Exploration in Athabasca Basin, Saskatchewan, Canada, E.M. Cameron (ed.); Geological Survey of Canada, Paper 82-11, pp.33-40.

Baadsgaard, H. and Godfrey, J.D. (1967): Geochronology of the Canadian Shield in northeastern Alberta, I. Andrew Lake area; Canadian Journal of Earth Sciences, v.4, pp.541-563.

—— (1972): Geochronology of the Canadian Shield in northeastern Alberta, II. Charles-Andrew-Colin Lakes area; Canadian Journal of Earth Sciences, v.9, pp.863-881.

Blaise, J.R. and Koning, E. (1985): Mineralogical and structural aspects of the Dominique-Peter uranium deposit; *in* The Carswell Structure Uranium Deposits, Saskatchewan, R. Laine, D. Alonso, and M. Svab (eds.); Geological Association of Canada, Special Paper 29, pp.139-151.

Burwash, R.A. and Culbert, R.R. (1976): Multivariate geochemical and mineral patterns in the Precambrian basement of Western Canada: Canadian Journal of Earth Sciences, v.13, pp.1-18.

Cameron, A.E. (1930): Report on progress on mineral explorations in the Precambrian; Alberta Research Council Report 25, Tenth Annual Report, 1929, pp.34-39.

Cameron, A.E. and Hicks, H.S. (1931): The Precambrian area of northeastern Alberta; Alberta Research Council Report 26, Eleventh Annual Report, 1930, pp.32-40.

Collins, G.A. and Swan, A.G. (1954): Preliminary report of geological field work, northeastern Alberta; Alberta Research Council, Mimeographed Circular No.18, 8 pages.

Dahlkamp, F.J. (1978): Geological Appraisal of the Key Lake U-Ni Deposits, northern Saskatchewan; Economic Geology, v.73, pp.1430-1449.

Day, L.W. (1975): Zircon geochronology of northeastern Alberta; M.Sc. Thesis, University of Alberta, 72 pages.

Duke, M.J.M. (1983): Geochemistry of the Exshaw Shale of Alberta - an application of neutron activation analysis and related methods; M.Sc. Thesis, University of Alberta, 186 pages.

Fahrig, W.F. and Loveridge, W.D. (1981): Rb-Sr isochron age of weathered pre-Athabasca Formation basement gneiss, northern Saskatchewan; *in* Rb-Sr and U-Pb isotopic age studies, Report 4; *in* Current Research, Part C, Geological Survey of Canada, Paper 81-1C, pp.127-129.

Fairbridge, R.W. and Finkl, C.W., Jr. (1980): Cratonic erosional unconformities and peneplains; Journal of Geology, v.88, pp.69-86.

Fortuna, P. (1979): Project 508 northeastern Alberta; Report on winter exploration 1979, v.1; Alberta Research Council, Quartz Mineral Open File 218-U-AF-146(1).

Fraser, J.A., Donaldson, J.A., Fahrig, W.F. and Tremblay, L.P. (1970): Helikian basins and geosynclines of the northwestern Canadian Shield; *in* Symposium on basins and geosynclines of the Canadian Shield, A.J. Baer (ed.); Geological

Survey of Canada, Paper 70-40, pp.213-238.

Gay, A.L. and Grandstaff, D.E. (1980): Chemistry and mineralogy of Precambrian paleosols at Elliot Lake, Ontario, Canada; Precambrian Research, v.12, pp.349-373.

Geological Survey of Canada (1964a): Fitzgerald, 74M. Aeromagnetic Map No. 7161G, Scale 1:253 440.

—— (1964b): Chipewyan, 74L. Aeromagnetic Map. No. 7159G, Scale 1:253 440.

—— (1964c): William River, 74K. Aeromagnetic Map No. 7019G, Scale 1:250 000.

—— (1966): Lloyd Lake, 74F. Aeromagnetic Map No. 7158G, Scale 1:250 000.

—— (1983): Bitumount, 74E. Aeromagnetic Map No. 7288G, Scale 1:250 000.

Gilboy, C.F. (1982): Sub-Athabasca basement geology project; *in* Summary of Investigations, 1982, Saskatchewan Geological Survey, Miscellaneous Report 82-4, pp.12-15.

—— (1983): Sub-Athabasca basement geology project; *in* Summary of Investigations, 1983, Saskatchewan Geological Survey, Miscellaneous Report 83-4, pp.28-31.

Godfrey, J.D. (1958a): Mineralization in the Andrew, Waugh and Johnson Lakes area, northeastern Alberta; Alberta Research Council, Report 58-4, 17 pages.

—— (1958b): Aerial photographic interpretation of Precambrian structures, north of Lake Athabasca; Alberta Research Council, Bulletin 1, 19 pages.

—— (1961): Geology of the Andrew Lake, north district, Alberta; Alberta Research Council, Report 58-3, 32 pages.

—— (1963): Geology of the Andrew Lake, south district, Alberta; Alberta Research Council, Report 61-2, 30 pages.

—— (1966): Geology of the Bayonet, Ashton, Potts and Charles Lake districts, Alberta; Alberta Research Council, Report 65-6, 45 pages.

—— (1970): Geology of the Marguerite River district, Alberta; Alberta Research Council map. Scale 1 in. to 1 mile.

—— (1980a): Geology of the Alexander-Wylie Lakes district, Alberta; Alberta Research Council, Earth Sciences Report 78-1, 26 pages.

—— (1980b): Geology of the Fort Chipewyan district, Alberta; Alberta Research Council, Earth Sciences Report 77-3, 20 pages.

—— (1984): The geology of the Ryan-Fletcher Lakes district, Alberta; Alberta Research Council, Earth Sciences Report 84-2, 28 pages.

—— (in press): Geology of the Bocquene-Turtle Lakes district, Alberta; Alberta Research Council, Earth Sciences Report 84-5.

Godfrey, J.D. and Langenberg, C.W. (1978): Metamorphism in the Canadian Shield of northeastern Alberta; *in* Metamorphism in the Canadian Shield, Geological Survey of Canada, Paper 78-10, pp.129-138.

—— (1986): Geology of the Fitzgerald, Tulip-Mercredi-Charles Lakes district, Alberta; Alberta Research Council, Earth Sciences Report 84-7, 32 pages.

—— (in press): Geology of the Myers-Daly Lakes district, Alberta; Alberta Research Council, Earth Sciences Report 84-6.

Godfrey, J.D. and Peikert, E.W. (1963): Geology of the St. Agnes Lake district, Alberta; Alberta Research Council, Report 62-1, 31 pages.

—— (1964): Geology of the Colin Lake district, Alberta; Alberta Research Council, Report 62-2, 28 pages.

Goff, S.P., Godfrey, J.D. and Holland, J.G. (1986): Petrology and geochemistry of the Canadian Shield of northeastern Alberta; Alberta Research Council, Bulletin 51, 60 pages.

Gresens, R.L. (1967): Composition-volume relationships of metasomatism; Chemical Geology, v.2, pp.47-65.

Harper C.T. (1979): Uranium metallogenic studies: Maurice Bay area, Geology and Mineraliation; *in* Summary of Investigations 1979, Saskatchewan Geological Survey, Miscellaneous Report 79-10, pp.96-106.

—— (1980): Uranium metallogenic studies: Cluff Lake area; *in* Summary of Investigations, 1980, Saskatchewan Geological Survey, Miscellaneous Report 80-4, pp.36-43.

Hicks, H.S. (1930): A petrographic study of Precambrian rocks in northeastern Alberta; M.Sc. Thesis, University of Alberta, 47 pages.

—— (1932): The geology of the Fitzgerald and northern portion of the Chipewyan map areas, northern Alberta, Canada; Ph.D. Thesis, University of Minnesota, 82 pages.

Hoeve, J. and Sibbald, T.I.I. (1976): The Rabbit Lake Uranium Deposit; *in* Uranium in Saskatchewn C.E. Dunn (ed.); Saskatchewan Geological Society, Special Publication No. 3, pp.331-354.

Jones, B. (1974): A biometrical analysis of *Atrypella foxi* N.Sp. from the Canadian arctic; Journal of Paleontology, v.48, pp.963-977.

Kerans, C., Ross, G.M., Donaldson, J.A. and Geldsetzer, H.J. (1981): Tectonism and depositional history of the Helikian Hornby Bay and Dismal Lakes Groups, District of MacKenzie; *in* Proterozoic Basins of Canada, F.H.A. Campbell (ed.); Geological Survey of Canada, Paper 81-10, pp.157-182.

Klewchuck, P. (1972): Mineralogy and petrology of some granitic rocks in the Canadian Shield north

of Fort Chipewyan, Alberta; M.Sc. Thesis, University of Calgary, 138 pages.

Koryakin, A.S. (1971): Results of a study of Proterozoic weathering crusts in Karelia; International Geology Review, v.13, pp.973-980.

Koster, F. and Baadsgaard,H. (1970): On the geology and geochronology of northwestern Saskatchewan I. Tazin Lake regions; Canadian Journal of Earth Sciences, v.7, pp.919-930.

Kuo, S.L. (1972): Uranium-lead geochronology of Kenoran rocks and minerals of the Charles Lake area, Alberta; M.Sc. Thesis, University of Alberta, 126 pages.

Laanela, H. (1977): Summary of report on exploration activities during 1975, 1976, 1977; Alberta Research Council, Quartz Mineral Open File 185-U-AF-115(2).

Langenberg, C.W. (1983): Polyphase deformation in the Canadian Shield of northeastern Alberta; Alberta Research Council, Bulletin 45, 33 pages.

Langenberg, C.W. and Nielsen, P.A. (1982): Polyphase metamorphism in the Canadian Shield of northeastern Alberta; Alberta Research Council, Bulletin 42, 80 pages.

Langenberg, C.W. and Ramsden, J. (1980): The geometry of folds in granitoid rocks of northeastern Alberta; Tectonophysics, v.66, pp.269-285.

LeCheminant, A.N., Ashton, K.E., Chiarenzelli, J.R., Donaldson, J.A., Best, M.A., Tella, S. and Thompson, D.L. (1983): Geology of Aberdeen Lake Map Area, District of Keewatin, Preliminary Report; *in* Current Research, Part A; Geological Survey of Canada, Paper 83-1A, pp.437-448.

Lewry, J.F., Sibbald, T.I.I. and Rees, C.J. (1978): Metamorphic patterns and their relation to tectonism and plutonism in the Churchill province in northern Saskatchewan; *in* Metamorphism in the Canadian Shield; Geological Survey of Canada, Paper 78-10, pp.139-154.

MacDonald, C.C. (1980): Mineralogy and geochemistry of a Precambrian Regolith in the Athabasca Basin; M.Sc. Thesis, University of Saskatchewan, 151 pages.

MacDonald, R. and Broughton, P. (1980): Geological map of Saskatchewan, Provisional edition, scale 1:1 000 000, Saskatchewan Mineral Resources.

Nelson, W.E. (1978): Report on the Lake Athabasca Joint Venture, Permits 219, 220, 221, 222, 223; Alberta Research Council, Quartz Mineral Open File 222-U-AF-150.

Nielsen, P.A., Langenberg, C.W., Baadsgaard, H. and Godfrey, J.D. (1981): Precambrian metamorphic conditions and crustal evolution, northeastern Alberta, Canada; Precambrian Research, v.16, pp.171-193.

Pagel, M. and Svab, M. (1985): Petrographic and geochemical variations within the Carswell Structure metamorphic core and their implications with respect to uranium mineralization; *in* The Carswell Structure Uranium Deposits, Saskatchewan, R. Laine, D. Alonso an M. Svab (eds.); Geological Association of Canada, Special Paper 29, pp.55-70.

Peikert, E.W. (1961): Petrological study of a group of porphyroblastic rocks in the Precambrian of northeastern Alberta; Ph.D. Thesis, University of Illinois, 151 pages.

—— (1963): Biotite variation as a guide to petrogenesis of granitic rocks in the Precambrian of northeastern Alberta; Journal of Petrology, v.4, pp.432-459.

Ramaekers, P. (1979): Stratigraphy of the Athabasca Basin; *in* Summary of Investigations, 1979, Saskatchewan Geological Survey, Miscellaneous Report 79-10, pp.154-160.

—— (1980): Stratigraphy and tectonic history of the Athabasca Group (Helikian) of northern Saskatchewan; *in* Summary of Investigations, 1980, Saskatchewan Geological Survey, Miscellaneous Report 80-4, pp.99-106.

Reiche, P. (1943): Graphic representation of chemical weathering; Journal of Sedimentary Petrology, v.13, pp.58-68.

Riley, G.C. (1960): Geology, Fort Fitzgerald, Alberta; Geological Survey of Canada Map 12-1960.

Ross, G.M. and Chiarenzelli, J.R. (1985): Paleoclimate significance of widespread proterozoic silceretes in the Bear and Churchill Provinces of the northwestern Canadian Shield; Journal of Sedimentary Petrology, v.55, pp.196-204.

Schau, M. and Henderson, J.B. (1983): Archean weathering at three localities on the Canadian Shield; Precambrian Research, v.20, pp.189-224.

Sokal, R.S. (1965): Statistical methods in systematics; Biological Review, v.40, pp.337-391.

Sopuck, V.J., deCarle, A., Wray, E.M., Cooper, B. (1983): Application of lithogeochemistry to the search for unconformity-type uranium deposits in the Athabasca Basin; *in* Uranium Exploration in the Athabasca Basin, Saskatchewan, Canada, Cameron, E.M. (ed.); Geological Survey of Canada, Paper 82-11, pp.191-205.

Sprenke, K.F., Wavra, C.S. and Godfrey, J.D. (1986): The geophysical expression of the Canadian Shield of northeastern Alberta; Alberta Research Council, Bulletin 52, 54 pages.

Stevens, R.D., Delabio, R.N. and Lachance, G.R. (1982): Age determinations and geological studies, K-Ar isotopic ages, Report 15; Geological Survey of Canada, Paper 81-2, pp.33-35.

Streckeisen, A. (1976): To each plutonic rock its pro-

per name; Earth Science Reviews, v.12, pp.1-33.

Tona, F., Alonso, D. and Svab, M. (1985): Geology and mineralization of the Carswell structure - a general approach; *in* The Carswell Structure Uranium Deposits, Saskatchewan, R. Laine, D. Alonso and M. Svab (eds.); Geological Association of Canada, Special Paper 29, pp.1-18.

Tremblay, L.P. (1982): Geology of the uranium deposits related to the sub-Athabasca unconformity, Saskatchewan; Geological Survey of Canada, Paper 81-20, 56 pages.

—— (1983): Some chemical aspects of the regolithic and hydrothermal alterations associated with uranium mineralization in the Athabasca Basin, Saskatchewan; *in* Current Research Part A, Geological Survey of Canada, Paper 83-1A, pp.1-14.

Wallis, R.H. (1970): A geological interpretation of gravity and magnetic data, northwest Saskatchewan; Canadian Journal of Earth Sciences, v.7, pp.858-868.

Wallis, R.H., Saracoglu, N., Brummer, J.J., Golightly, J.P. (1983): Geology of the McClean uranium deposits; *in* Uranium Exploration in Athabasca Basin, Saskatchewan, Canada, Cameron, E.M. (ed.); Geological Survey of Canada, Paper 82-11, pp.71-110.

Watanabe, R.Y. (1961): Geology of the Waugh Lake metasedimentary complex, northeastern Alberta; M.Sc. Thesis, University of Alberta, 89 pages.

—— (1965): Petrology of cataclastic rocks of northeastern Alberta; Ph.D. Thesis, University of Alberta, 219 pages.

Wilson, J.A. (1985a): Geology of the Athabasca Group in Alberta; Alberta Research Council, Bulletin 49, 78 pages.

—— (1985b): Geology of the basement beneath and around the Athabasca Basin in Alberta, NTS74L and parts of 74M and E; Alberta Research Council, Open File Map 85-10.

—— (1985c): Crandallite group minerals in the Helikian Athabasca Group in Alberta, Canada; Canadian Journal of Earth Sciences, v.22, pp.637-641.

Yule, J.W. and Swanson, G.A. (1969): A rapid method for decomposition and the analysis of silicates and carbonates by Atomic Absorption Spectroscopy; Atomic Absorption Newsletter, v.8, pp.30-31.

Appendix A

Plots of major element concentration against a modification of the Larsen Index (MLI)([SiO_2 + K_2O – CaO – MgO]/3 after Goff et al., 1986) for drill core samples.

Key

● - Fishing Creek Granitoid
o - Grey Foliated Granitoid
+ - Alkali Feldspar-Rich Granitoid
x - Wylie Lake Granitoid
M - Mafic Mylonites
F - Felsic Mylonites
S - Metasedimentary rocks.

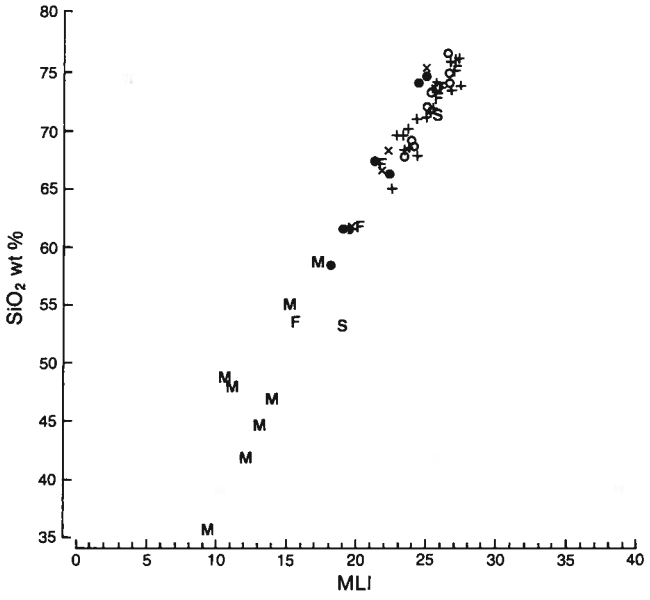

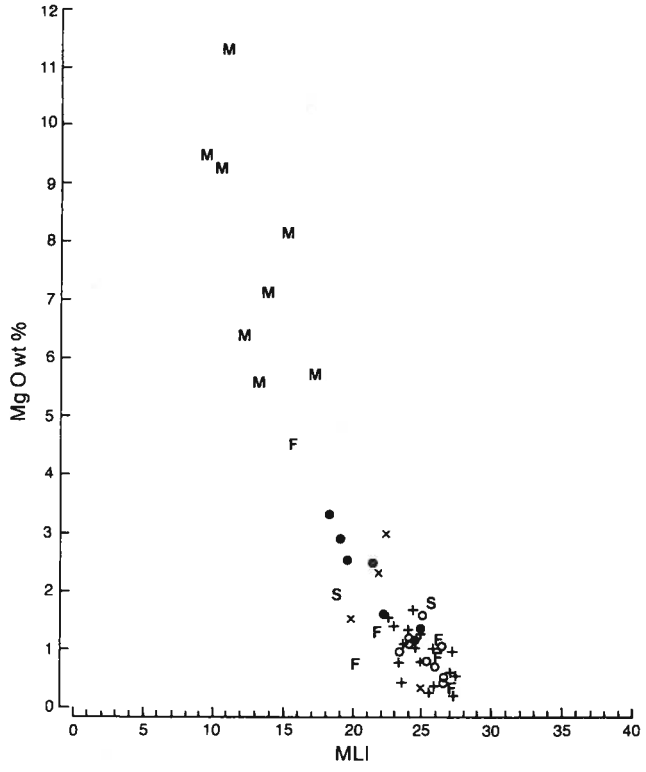

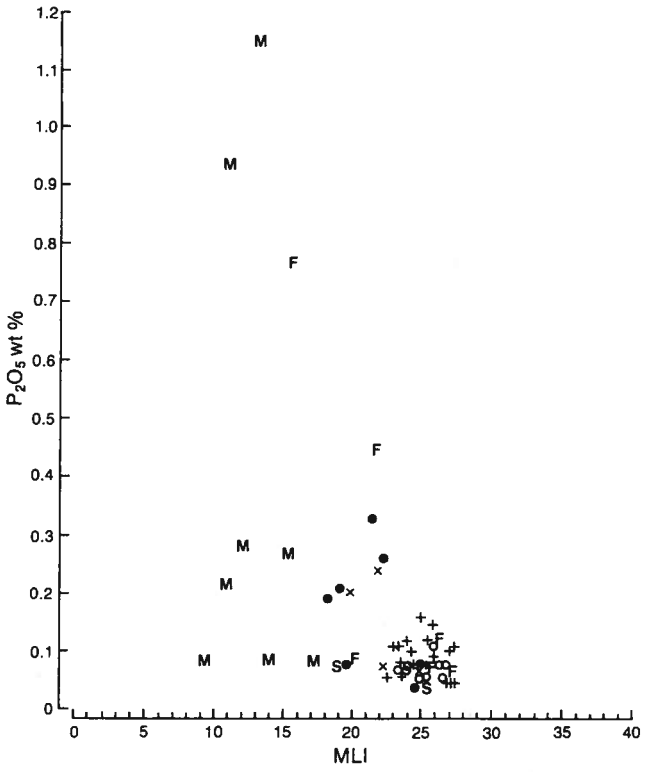

Appendix A (continued)

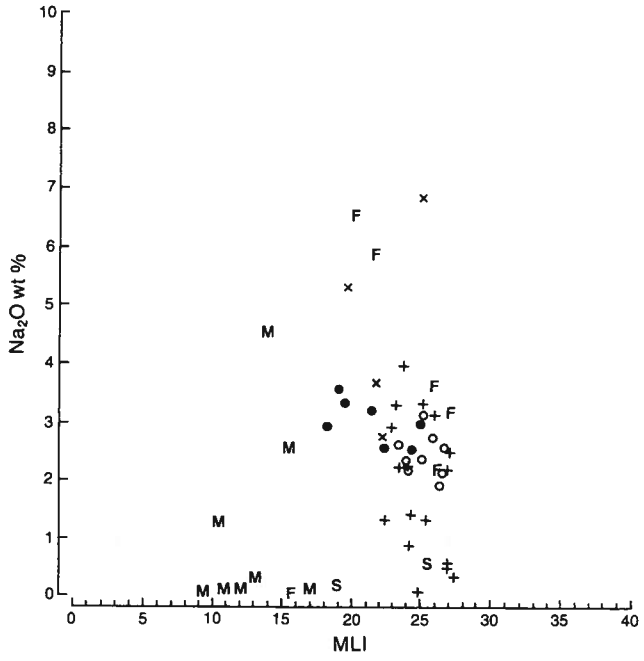

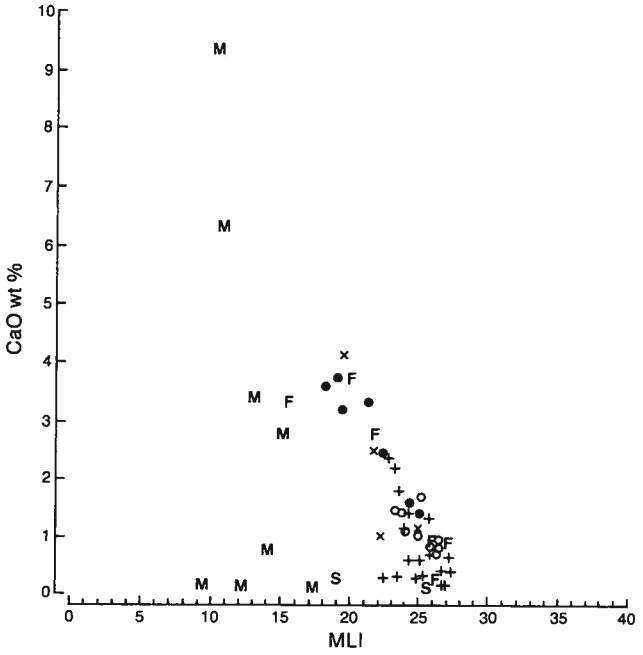

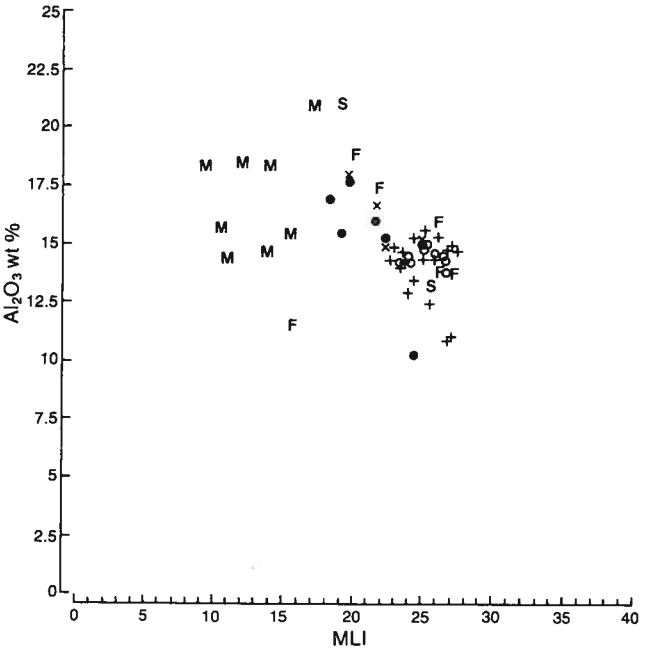

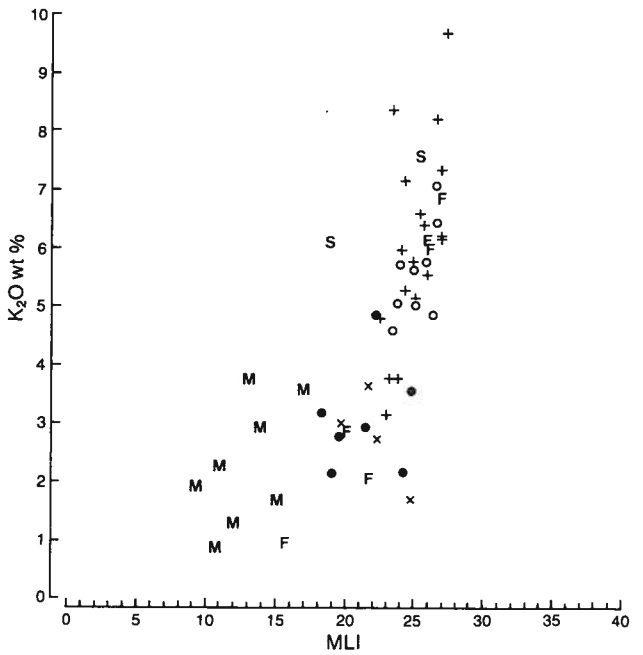

Appendix A (continued)

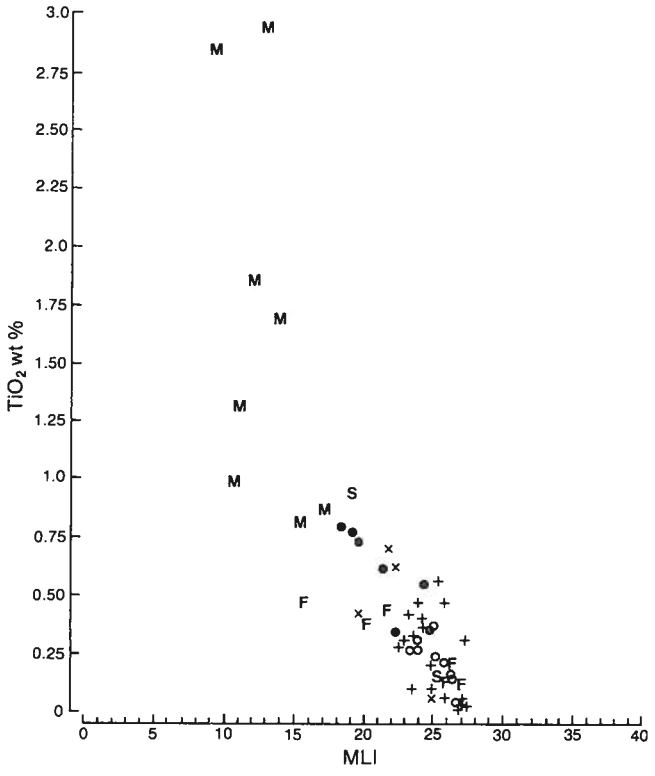

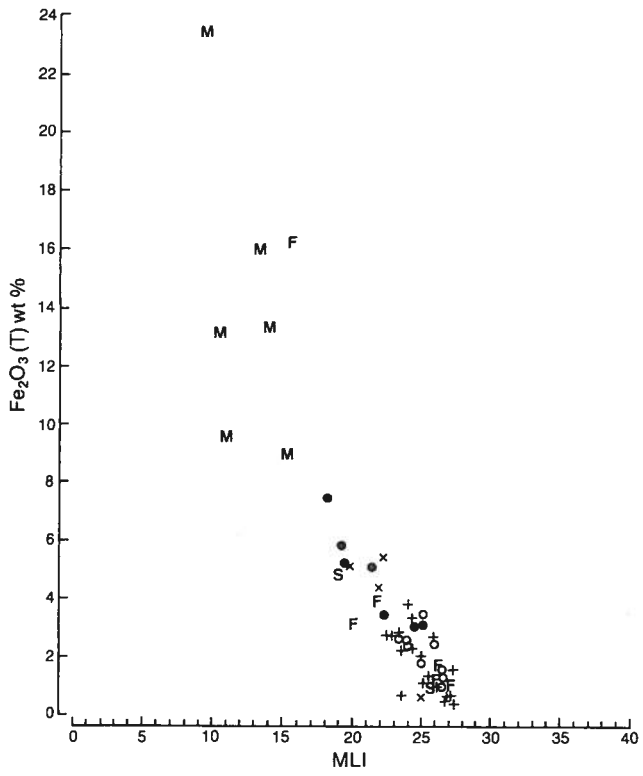

Appendix B

Plots of major element concentrations against a modification of the Larsen Index (MLI)([SiO_2 + K_2O – CaO – MgO]/3 after Goff et al., 1986) for Marguerite River area standard samples. Key as in Appendix A.

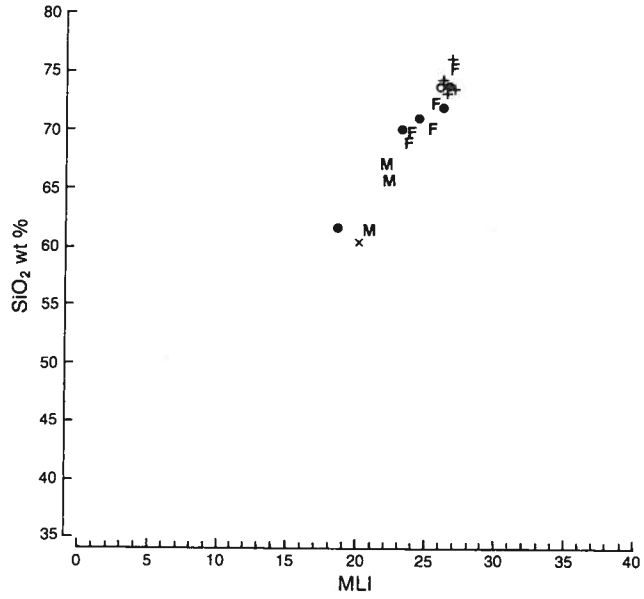

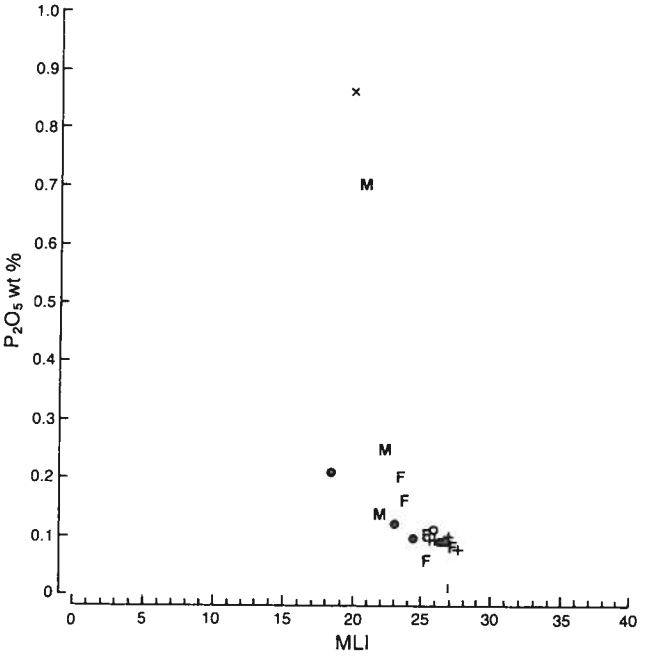

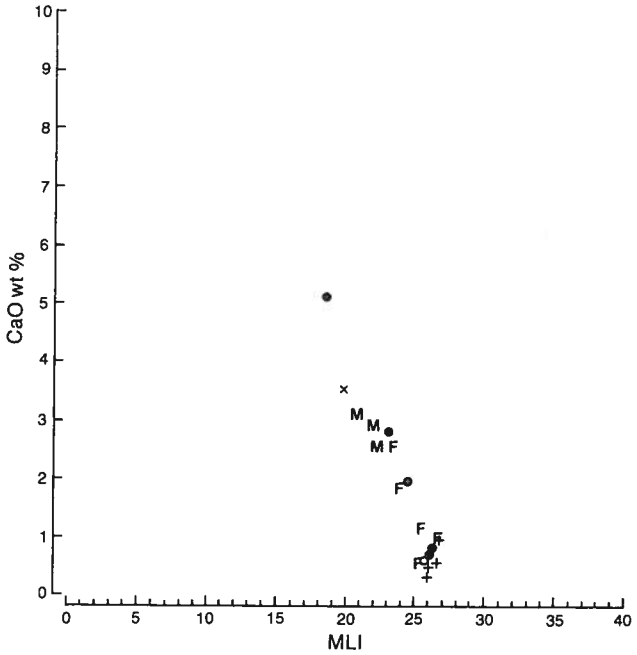

Appendix B (continued)

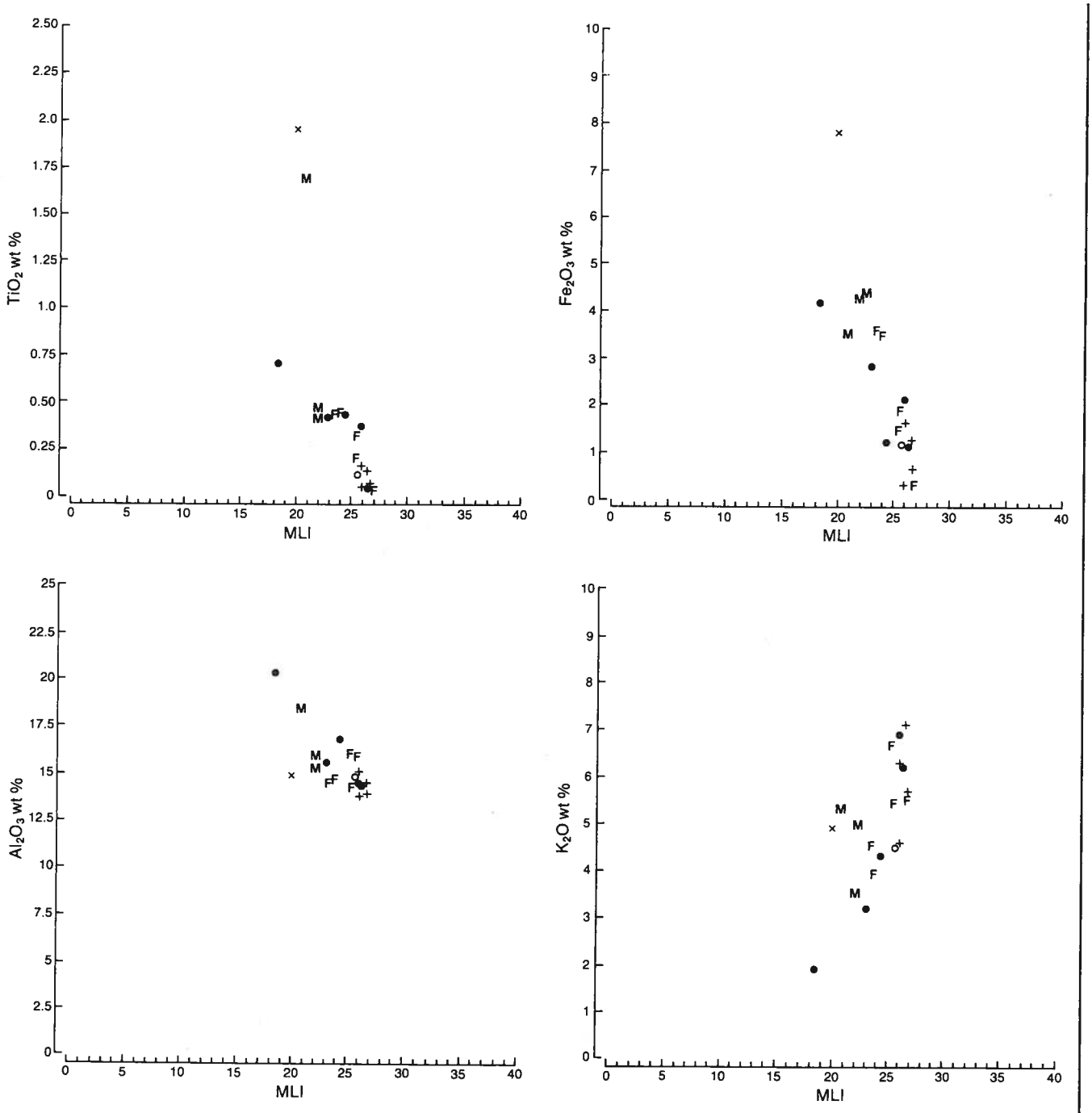

Appendix B (continued)